Aus dem Bereich Theoretische Medizin und Biowissenschaften
der Medizinischen Fakultät der Universität des Saarlandes,
Homburg/Saar

Numerical Modeling and Experimental Validation of Involuntary Attentional Capture and Long–Term Habituation by the example of Tinnitus Aurium

Dissertation zur Erlangung des Doktorgrades
der Naturwissenschaften (Dr. rer. nat.)
an der Medizinischen Fakultät
der Universität des Saarlandes
2015

vorgelegt von:
Dipl.-Biol. Lars Haab, M.Sc.
geboren am 04. Januar 1977 in Ottweiler/Saar

Dekan: Prof. Dr. med. Michael D. Menger

Referent: Prof. Dr. rer. nat. Dr. rer. med. Daniel J. Strauss

Korreferent: Prof. Dr. rer. nat. Andreas Keller

Tag der mündlichen Prüfung: 28.04.2016

There is nothing more deceptive than an obvious fact.

Sir Arthur Ignatius Conan Doyle

Dedicated to Anita, my beloved family and my friends for their love, support, help and for standing by me.

Eidesstattliche Erklärung

Hiermit erkläre ich an Eides statt, dass ich die vorliegende Arbeit ohne unzulässige Hilfe Dritter und ohne Benutzung anderer als der angegebenen Hilfsmittel angefertigt habe. Die aus Quellen direkt oder indirekt übernommenen Daten und Konzepte sind unter Angabe der Quelle gekennzeichnet. Bei der Auswahl und Auswertung folgenden Materials haben mir die nachstehend aufgeführten Personen in der jeweils beschriebenen Weise unentgeldlich/entgeltlich geholfen:

- Alle in der Danksagung des Dissertationsmanuskripts erwähnten Personen haben mir in der dort beschriebenen Weise unentgeltlich geholfen.

Weitere Personen waren an der inhaltlichen und materiellen Erstellung der vorliegenden Arbeit nicht beteiligt. Insbesondere habe ich nicht die entgeltliche Hilfe von Vermittlungs– bzw. Beratungsdiensten (Promotionsberater/innen oder anderer Personen) in Anspruch genommen. Außer den Angegebenen hat niemand von mir unmittelbar oder mittelbar geldwerte Leistungen für Arbeiten erhalten, die im Zusammenhang mit dem Inhalt der vorgelegten Dissertation stehen.

Die Arbeit wurde bisher weder im Inland noch im Ausland in gleicher oder ähnlicher Form in einem anderen Verfahren zur Erlangung eines Doktorgrades einer anderen Prüfungsbehörde vorgelegt.

In versichere an Eides statt, dass ich nach nach bestem Wissen die Wahrheit gesagt und nichts verschwiegen habe.

Vor Aufnahme der vorstehenden Versicherung an Eides statt wurde ich über die Bedeutung einer eidesstattlichen Versicherung und die strafrechtlichen Folgen einer unrichtigen oder unvollständigen eidesstattlichen Versicherung belehrt.

St. Ingbert, den 21.07.2015

Dipl.-Biol. Lars Haab, M.Sc.

List of Abbreviations

A	Amygdala
AEP	Auditory evoked potential
Ag/AgCl	Silver/Silver-chloride
ALR	Auditory late response
AN	Auditory nerve
AP	Action potential
BDI	Beck depression inventory
CA1	Cornu Ammonis 1
CA3	Cornu Ammonis 3
CeA	Central nucleus of the amygdala
CNIC	Central nucleus of the inferior colliculus
CoV	Coefficient of variation
DCN	Dorsal cochlear nucleus
EEG	Electroencephalography
EPSP	Excitatory post synaptic potential
ERC	Entorhinal cortex
ERP	Event related potential
FD	Fascia dentata
FIR	Finite impulse response
FR	Formatio reticularis
FS	Fast spiking interneurons
GABA	Gamma aminobutyric acid
GAD	Glutamic acid decarboxylase
HCN	Hyperpolarization activated cyclic nucleotide gated cation channel
HL	Hearing level
HRSD	Hammilton depression rating score
IEG	Immediate early gene
IPSP	Inhibitory post synaptic potential
ISI	Inter stimulus interval

LFP	Local field potential
LTP	Long term plasticity
MEG	Magnetencephalography
MF	Mossy fibres
MFB	Medial forebrain bundle
MGB	Medial geniculate body
MRI	Magnet resonance imaging
MSDB	Medial septum diagonal band of Broca
NAc	Nucleus accumbens
NEST	Notched environmental sounds therapy
NT	Neurotransmitter
OLM	Stratum oriens lacunosum moleculare
pe	Peak equivalent
PfC	Prefrontal cortex
PP	Perforant pathway
PSP	Postsynaptic potential
PTA	Pure tone average
Pyr	Pyramidal cell
RN	Raphe nuclei
RR	Response reliability
RS	Regular spiking interneurons
SC	Schaeffer collaterals
SG	Spiral ganglion
SPL	Sound pressure level
SSTC	Sweep to sweep time scale coherence
STDP	Spike timing dependent plasticity
STP	Short term plasticity
TF	Tinnitus Fragebogen
TMNM	Tailor-made notched Music (therapy)
TRN	Thalamic reticular nucleus
TRT	Tinnitus retraining therapy
WPSS	Wavelet phase synchronization stability

Contents

1 Abstract and Motivation

Zusammenfassung: Obwohl in den letzten Jahrzehnten große Datenmengen über die Entstehung und Chronifizierung von Tinnitus Aurium aufgezeichnet und gesammelt wurden, sind die grundlegenden neuronalen Mechanismen dieser akustischen Phantomwahrnehmung weitgehend ungeklärt. Grundsätzlicher Konsens besteht jedoch darin, dass ausgehend von einer peripher–akustischen Ursache, die Chronifizierung der Symptome durch eine sukkzessive Zentralisierung bedingt ist. Die Begründung einer Exazerbation des Tinnitus wird in einem breiten Feld diskutiert. Einerseits wird die Ausschüttung von Dynorphinen durch Stress– und Angstreaktionen als Ursächlich angeommen, andererseits steht aber auch die unilaterale Veränderung sensorischer Verarbeitung im Verdacht die progressive Dekompensation zu begünstigen.

Diese Dissertation thematisiert ein funktionales Modell für die Entstehung und für die pathologische Chronifizierung von Tinnitus. Dieses Modell basiert auf experimentellen Daten und quantitativer Modellierung der Mechanismen neuronaler Verarbeitung. Wir stellen eine physiologisches, schnell reagierendes neuronales System zur Diskussion, welches Phantomwahrnehmungen nach einem sensorischen Trauma auslösen kann. Intrinsische Kompensationsmechanismen reagieren auf unterdrückte sensorische Reizzufuhr und können durch eine Hochregulierung der neuronalen Spontanfeuerrate für sich alleine genommen schon ausreichend sein um ein Perzept auszulösen. Das dynamische Verhalten neuronaler Verschaltungen mit einer lateralen Komponente kann die Häufigkeitsrate von Tinnitus sowie dessen sensorische Charakteristiken erklären. Die Aktivität solcher neuronalen Netze zeigt ein Selbstordnungsbestreben abhängig von den synaptischen Eigenschaften und der neuronalen Verschaltungsarchitektur. In der Folge einer Hyperaktivität nach sensorischer Deprivation kann sich so ein Muster synchroner Nervenaktivität aus-

bilden. Diese Synchronisierung kann kompetitive Vorteile im Fall multisensorischer Rivalität mit sich bringen. In der Folge erhöht sich die Wahrscheinlichkeit einer hierarchisch höheren, bewussten Verarbeitung. Jedoch ist ein zweigleisiger Ansatz zur Aufklärung der Tinnitus Pathogenese notwendig um den subjektiven Einfluss der akustischen Phantomwahrnehmung auf den Patienten zu erfassen. Die Fähigkeit den Tinnitus zu bewältigen ist mit nachweislich mit der Aufmerksamkeitsbindung an den Tinnitus Ton verknüpft. Unsere Vorarbeiten konnten eine Korrelation aufzeigen zwischen dem Grad der Dekompensation und der individuellen Aufmerksamkeitsleistung des Patienten. Hierarchische top–down Projektionsbahnen können somit zusätzlich die neuronale Synchronisierung erhöhen und in der Folge die Wahrscheinlichkeit einer bewussten Wahrnehmung des pathologisch veränderten Aktivitätsmusters erhöhen. Um diese veränderte Aufmerksamkeitsleistung funktionell beschreiben zu können wurde ein Modell erarbeitet, welches die Valenz eingehender sensorischer Information bewertet. Das Modell beschreibt die initiale Aufmerksamkeitsbindung an den Tinnitus durch eine Verknüpfung von Modellen thalamo–kortikaler Feedbackschleifen als Steuerungszentrum der Aufmerksamkeitslenkung und von limbischen Arealen, welche Motivation und emotionale Reaktion auf den Stimulus steuern.

Schlüsselworte: Tinnitus & Numerische Modellierung & Hierarchische sensorische Verarbeitung & Habituation & Kognitive Dysfunktion

Abstract: Although a vast amount of data on origin and chronification of tinnitus aurium was collected in the last decades, the neural mechanisms underlying the course of these acoustical hallucinations are still elusive. However, there is convergence to a peripheral origin and subsequent central transition into chronicity of the disease. Yet the reasons for the exacerbation of tinnitus are widely discussed in research and therapeutic communities. On one hand the elevated release of dynorphins in stress and fear reactions could be the cause for a progressive decompensation. On the other hand, unilateral shifts in the neuronal processing of stimuli could promote the tinnitus exacerbation.

This dissertation presents a functional model of tinnitus onset and the pathological chronification of tinnitus, based on available experimental data and on quantitative modeling of neural processing mechanisms. We propose a physiological, fast reacting neural mechanism, foundational for the occurrence of phantom perceptions in response to a peripheral sensory trauma. Intrinsic peripheral compensation mechanisms respond to deprived sensory input by an upregulation of neural spontaneous activity which might be sufficient to generate a percept. The dynamic behaviour of neural networks with lateral components, being highly susceptible to synaptic properties and pathway architecture, could explain the incidence rate of tinnitus and the characteristics of the perceived sensory event. Neural network activity tends to self–organizing behaviour, expressing synchronous firing across a population as the spontaneous activity increases due to sensory deprivation. This might result in a competitive advantage in perceptual rivalry, i.e., an increased probability of hierarchically higher, conscious processing. Yet a double–traced approach to tinnitus pathogenesis is necessary to explain the subjective impact of the hallucinations on the patient. The ability to cope with tinnitus is most likely connected to the attention paid to the tinnitus tone. Preliminary studies in our lab demonstrated a correlation of the degree of tinnitus decompensation and free attentional resources. Hierarchical top—down projections thus can further promote synchrony and increase the probability of conscious processing of the pathologically altered neuronal activity underlying the acoustical hallucination. For a functional description of this altered attention guidance, I implemented a modeling framework for the appraisal of incoming sensory information. This model delineates the initial tie down of attention by connecting the thalamo—cortical feedback system, as governing structure of attention allocation, to limbic areas, responsible for emotional and motivational reaction to a perceptual event.

Keywords: Tinnitus & Numerical Modeling & Hierarchical stimulus processing & Habituation & Cognitive Dysfunction

Motivation: Homeostatic plastic processes in the early stages of the auditory pathway elevate the spontaneous neural activity in tinnitus aurium in a compensatory reaction to acute hearing loss. These plastic changes can emerge as short–term plastic effects directly after an acoustic insult and can induce long lasting changes in neural information transmission. Yet hyperactivity alone can not be an explanation for the emergence of the tinnitus percept.

The increase of the spontaneous firing rate can be considered as a physiological compensation process in response to a notch like hearing loss and the related deafferentiation of higher levels of sensory processing. This phenomenon is yet not sufficient to explain why the tinnitus percept arises not with every hearing loss, nor can it illuminate the mechanisms underlying the tinnitus exacerbation (decompensation). Moreover the discrepancy of subjectively perceived tinnitus intensity and objective loudness measures in masking studies is not explicable on the base of an increased spontaneous firing rate.

The sections 2.2 and 3.1, introduce a computer simulation of self—organizing patterns in relation to increased neural response reliability and spiking coherence following a noisy impulse input. This increased spiking coherence can be considered as a base for synchronous activity across a neural population, which in turn might be sufficient to activate cortical neurons, generating a percept in consequence. These sections outline a possible neural origin of the tinnitus phantom perception and will be discussed in section 5.1 based upon the modeling results in section 4.1.

A notch—like peripheral hearing deficit and the resulting neural hyperactivity is not necessarily sufficient to generate a persistent tinnitus as not all hearing impaired patients automatically develop enduring phantom perceptions. We hypothesize a physiological mechanism underlying the tinnitus symptoms. Along this line of arguing, the pathogenic chronification of auditory phantom perceptions may thus originate in brain areas responsible for attention guidance, as well as in brain areas only indirectly involved in auditory information processing, which nevertheless influence the allocation of attentional resources and the plastic reorganization in the auditory system [141; 94].

Dysfunctional circuitries for evaluating the importance of a stimulus might lead to pathologic attention binding as we observe it in tinnitus. Moreover the co–activation of limbic and sensory areas can lead to a consolidation of sensory synapses. This plastic reinforcement of thalamo–cortical circuitry hints also towards a learned focal point of attentional resource allocation. Along this line of arguing the plastic effects in the thalamocortical system reinforce the peripheral intrinsic self–organization as described above. In the sections 2.3, 3.1 and 4.1 I thus implement and experimentally test a numerical modeling explanation for the tinnitus exacerbation and chronification. The model includes hierarchical stages of the sensory pathway that allow for a regulation of attention by means of thalamocortical gain adaptation, as well as extrasensory areas in the amygdalo–hippocampal complex for the appraisal of the stimulus valence.

Contributions of this work:

1. First description of objective attention and habituation correlates in the Electroencephalogram (EEG) of tinnitus sufferers. The experimental validation of our working hypothesis demonstrated a strong correlation of the subjective distress level, free attention resources and the ability to habituate to insignificant stimuli.

2. Multiscale–modeling approach to dysfunctional stimulus valence appraisal in the regulation of attention allocation. The model is based on the up/down regulation of thalamo–cortical gains by a amgygdalo–hippocampal comparator module.

3. Computational analysis of the transition of unstructured peripheral hyperactivity to a coherent perceptual stream.

4. Experimental validation of habituation correlates in (1.) and modeling predictions in (2.)

Contents of this PhD–Thesis were published in: [184; 182; 180; 183; 21; 57; 181; 54; 55; 56; 53; 49; 52; 150; 51]

2 Introduction

2.1 General Introduction

Despite decades of research, the neural mechanisms underlying the pathogenesis and chronification of tinnitus aurium are still not entirely understood. Tinnitus is a common symptomatic, affecting about 10 to 15% of the population in western societies. Moreover 98% of healthy subjects suffer from tinnitus—like symptoms when deprived of auditory stimuli, e.g., in a sound—proof chamber. This suggests an underlying physiological mechanism causing auditory sensations during absence of an external sound source. Steven Grossberg proposed a mechanism by which hallucinations arise from mechanisms of learning, attention and volition [46]. Translating Grossbergs results to a hypothetical homeostatic compensatory mechanism, notch—like hearing deficits are sufficient for experiencing auditory hallucinations, while the chronification of tinnitus should be attributed to attentional amplification and reorganization processes. Additionally in tinnitus sufferers the auditory sensation is accompanied by the inability to habituate to this endogenous sound. This disability might originate from a coactivation of brain areas that are only indirectly involved in cognitive processing. Tinnitus is heterogeneous in its sensory characteristics, ranging from pure tones to complex sounds, and its individual impact on the patients quality of life. Subjective testing by standardized questionnaires like, Goebel and Hillers tinnitus questionnaire (TF) [45] or the tinnitus handicap inventory (THI) [122] allows for a binned classification of the patients distress–level. According to Goebel and Hiller's TF, which has established as a gold–standard in German–speaking regions, tinnitus sufferers can be classified into four grades of severity. Grade I and II (compensated) patients cope well with their tinnitus, while type III and IV (decompensated) patients, which account for about 3% of the po-

pulation, suffer from severe social restrictions and co—morbidities like depression or insomnia. In clinical self–assessment those patients often report a subjective tinnitus loudness which is comparable to a high-–intensity noise exposure (like, e.g., jackhammers). However masking studies to assess the objective tinnitus loudness, resulted in a objective loudness of approximately 10—20dB above the individual hearing threshold [133]. This divergence of subjective load and objectively measurable loudness, as well as the patients' inability to habituate to this phantom sound, could be explained by an increased attentional binding to the tinnitus tone [180].

In 1958, Donald Broadbent [18] presented a limited—capacity model of attention. Although this all—or—nothing scheme of an attentional bottleneck was an early subject to a number of revisions, e.g., [178; 30; 76], due to explanatory gaps, the limited capacity of simultaneous sensory processing still remains a valid hypothesis of attentional resource allocation [91; 92]. Along this line of arguing, healthy subjects should be able to allocate more attentional resources to a target stimulus than patients with increased attentional binding to their tinnitus tone. We discuss this hypothesis and experimental support in [171] and in section 2.3.2.

The discrepancy of the ability to habituate towards sounds between tinnitus sufferers and healthy subjects respectively vanishes if the healthy subjects are presented with aversive acoustic stimuli [110]. This calls for a subjective weighting of sensory information and the resulting allocation of higher processing resources and thus for an attention management by brain regions responsible for the appraisal of stimulus valence. In the context of this work, we refer to exogenous weighting due to the physical properties of the stimulus and endogenous weighting due to the subjective impact of the stimulus respectively, as defined by Albert Bregman [15]. See also sections 2.3.1 and 2.3.2 for further details.

2.1.1 Tinnitus: Definition

The term tinnitus derives from the latin verb tinnire, meaning "ringing". Despite the name, it commonly describes the perception of a multitude of acoustic spectra (ringing, hissing or buzzing, etc.) in the absence of a corresponding external sound source, often accompanied by a measurable hearing loss. Though the origin of objective phantom sounds can lie in vascular disorders, such as malformations of the carotid artery or the jugular vascular systems, or in myocloni of the middle–ear mus-

culature [8], in the absolute majority of cases tinnitus is subjective and probably multicausal, involving band–limited sensory deprivation (hearing loss) and over-shooting reactions in subsequent hierarchical stages of auditory processing. Møller defines this subjective form of tinnitus [116]:

> "Subjective tinnitus is a broad group of sensations that are caused by abnormal neural activity in the nervous system that is not elicited by sound activation of sensory cells in the cochlea."

> **Møller et al. 2011 Textbook of Tinnitus**

We thus can discriminate two classes of tinnitus. The first–mentioned objective form of tinnitus is audible also to the attending physician and often allows for a surgical intervention. The latter, subjective form of tinnitus, is audible only to the patient and the aim of treatment is to assist the patient in managing his condition routinely. This dissertation only addresses the subjective form of tinnitus aurium, trying to shed a bit of light onto its still elusive origin.

Tinnitus is a highly heterogenous symptom with respect to its sensory characteristics, ranging from pure tones to complex sounds, its etiology and comorbidities, as well as its impact on the patients daily routine and its response to therapeutic interventions [185].

Additionally the tinnitus symptomatic shows high spontaneous recovery rates in the acute condition. The acute tinnitus can last from only a few minutes to weeks after the acoustic trauma. Spontaneous recovery is expected in more than 75% of the tinnitus sufferers. A chronic tinnitus that lasts for more than 2 years is considered permanent and manifests significantly reduced chances to alleviate the symptoms by therapeutic intervention. Some cases report a gradual exacerbation over the course of several years, causing a compensated tinnitus patient to develop a decompensated, bothersome tinnitus.

2.1.2 Tinnitus: Epidemiology and economic impact

The prevalence of tinnitus ranges between 10–15% of the population of western industrial societies. The incidence of chronic bothersome tinnitus increases with advancing age, reaching its peak around the ageband of 65 to 80 years [67]. Yet

advancing trends in mobile and ubiquitous access to music programmes distort this age–relationship. Recent studies report a high incidence of hearing–related symptoms, such as tinnitus, in adolescents due to music consumption at potentially hazardous loudness levels [187]. Males show significantly higher risk to contract tinnitus. This difference might be connected to personal circumstances, such as a higher likelihood of loud noise exposure in males [67].

Hearing loss, arising from occupational or recreational noise exposure, age or oto-toxic agents, can be considered a main cause of tinnitus. Additionally the exacerbation of tinnitus corresponds to the individual stress level. Tinnitus has also a number of common comorbidities, such as sleep disorders, depression, hyperacusis or increased tension in neck muscles and/or the muscles of mastication. These concomitant symptoms often lead to severe psychosocial and psychosomatic cuts with major health economic effects:

The prescription of rheologica, such as Dusodril, Natil or Trental, caused expenses of more than 51 mio. Euros in Germany in 1999. The average duration of administration was 9.6 years. Moreover the symptoms caused by concomitant or follow–up disorders impair the patients working capacity (ca. 4% of affected persons) and/or could cause addictions to the administered medications (e.g., antidepressant drugs, ca. 24% of affected persons) with respective follow–up costs [39].

In the US the retirement pensions for military personal with trauma induced tinnitus sum up to 2 bil. US$. This budget is expected to reach 3 bil. US$ in 2015.

2.1.3 Diagnosis

The heterogenous characteristics of tinnitus require differentiated and tailor–made therapeutic concepts, which imply a precise and individual diagnosis. Yet state of the art in diagnostics is a characterization of the tinnitus in wide classes of individual distress levels. In addition this coarse classification is based on subjective methods, such as self–assessment methods conducted by the patient:

Questionnaires: During the last years the demand of accurate diagnostic tools for individualized tinnitus treatment gradually increased. Nine different psychometric instruments for the estimation of the patients degree of decompensation with clinical relevance have emerged by now. All of these tools are questionnaires for a

subjective self–assessment. In German–speaking countries the Tinnitus–Fragebogen (TF) by Goebel and Hiller [45] has established a gold standard. The TF is a direct adaptation of the questionnaire by Hallam et al [59]. Goebel and Hiller presented a study of quality management in the tinnitus diagnostics and treatment in which they evaluate the psychometric quality of all established questionnaires [44]. More than half of those diagnostic tools exhibit severe shortcomings in their psychometric grading and thus they are only of limited value in the anamnesis and the design of an individual therapeutic approach. But also the high graded questionnaires have deficits in comparability due to severe differences in their factor structure in the anamnesis. The majority of those psychometric instruments include, besides cognitive deficits, also the psychologic and psychosocial burden of the individual patient. Consequently those questionnaires monitor possible concomitant morbidities with an independent pathogenesis, resulting in a distortion of the test scores.

New studies, e.g., by Robinson et al [145], show a high correlation coefficient of multiple tinnitus questionnaires with the Hamilton depression rating scale (HRSD) and the Beck Depression Inventory (BDI), both established instruments in clinic routine for the assessment of depressive disorders. Besides those issues the medical practitioner also has to consider the patients form on the day during the self–assessment. The usage of questionnaires for the evaluation of therapeutic success and –quality could also lead to a distortion of the scoring due to treatment– and placebo–effects. The sustainability of the therapy approach thus cannot be guaranteed.

Objective diagnostic tools: Objective diagnostic tools for the categorization of the patients' distress level are lacking in clinical routine. Scientific approaches demonstrated the feasibility of individual distress assessment by objective markers in the EEG. Preliminary works of our research group demonstrated the usability of attention and habituation correlates in ALRs (Auditory late response) [64; 171] for the classification of subjective distress levels, see also sections 2.3.3 and 3.2.1. Recent studies by Dirk de Ridder identify an electroencephalographic correlate of the subjectively perceived tinnitus loudness [26]. This loudness correlate is based on nested gamma–theta oscillations in the AC (Auditory cortex) and the parahippocampal area. Both methodologies could find application in the tinnitus diagnostic support in the future.

2.1.4 Therapy approaches

Tinnitus Retraining Therapy (TRT): The TRT is based on a neuropsychologic model by P. Jastreboff [74]. According to this hypothesis, tinnitus can be blocked from conscious perception for a significant reduction of the patients distress. The TRT focusses on plastic learning effects to lessen the individual impact of the tinnitus tone. In a cooperation of medical practitioners and psychologists, the goal of the TRT is to achieve a habituation to the tinnitus by practicing coping strategies. The therapy thus does not aim at a cure for tinnitus but for an improvement of every–day life quality. The TRT is a long–term therapy; its duration ranges from 12 to 24 months. Conceptually the TRT consists of a four pillar concept: Counseling (rather the central element of the TRT), psychological supervision, relaxation techniques and the provision of aiding devices, such as hearing aids or noiser/masker devices. All those intervention techniques aim to impart the patients knowledge about the mechanisms underlying the tinnitus to encourage the patient to reassess the tinnitus tone and reduce the fear of the tinnitus tone and its psychosocial outcome.

Medication: The earliest approaches to cure tinnitus involved the administration of medication. The phantom noise was medicated with intravenous injection of glucocorticoids, local anaesthetics or rheologica. Up to now, no drug could achieve a higher rate of therapeutic success than a placebo [34]. Direct interventions in the neurotransmitter balance were futile. Only the administration of intracranial (via coroidal artery) sedatives, e.g., Amobarbital, had a significant higher rate of success compared to a placebo, but only on a short time–scale and at the cost of severe side effects. Although this medication is not suitable for clinical routine, it hints towards a direct link between the attention focus on the tinnitus tone and the activity of functional structures in the hippocampal–amygdaloid complex [28]. We introduce and evaluate an amygdaloid–hippocampal contribution to the tinnitus perception in the subsections 2.3.6 and 2.3.7.

Music therapy and acoustic stimulation: The music therapy intervention uses the embedding of the tinnitus tone in a musically controllable hearing process. For every patient the medical practitioners create a unique sound scheme, matched to their tinnitus tones. This sound scheme can be used actively (singing, making music) or receptively (passive listening and relaxation). The therapy aims to give the patient active control of the tinnitus tone. Additionally the tailored acous-

tic stimulation should reactivate the pathologic deficient brain areas, leading to a normalization of dysfunctional neurodynamics [3]

Another form of acoustic invention is the tailor–made notched music therapy (TMNM) by Okamoto et al. [130]. This therapy is based on the idea of utilizing the lateral inhibition in the hearing path to reduce hyperactivity–induced synchronization of neural ensembles. Centered on the individual tinnitus frequency, a specific frequency band (1 octave) is blocked from a wideband stimulus. The reduction of hyperactivity in the blocked frequency band can reduce the perceived tinnitus loudness. Pantev et al. specify that this targeted plastic reorganization benefits from an active and attentive processing of the acoustic stimulus. They intentionally use music for its appetitive effect. Music, in contrast to notched broad band noise, carries a meaning and is likely to bind attention and elicit positive emotions. Please refer to sections 2.3.9 and 2.3.3 for additional information.

Neurofeedback: Established neurofeedback interventions monitor the spontaneous activity in the EEG to derive a correlate of the tinnitus–related distress. The analysis of the ratio of Delta–band power and Alpha–band power (Tau–Delta feedback) is frequently used. This measure is commonly utilized to quantify the patients state of relaxation or vigilance. Cyclic recurring comorbidities, like insomnia, yet have a significant influence on the patients vigilance. The classic neurofeedback is thus strongly dependent from the patients form on the day. The feedback is routinely given visually, which results in a distortion of the Tau–Delta ratio caused by the Berger Effect [31]. In the scientific community additional neurofeedback therapies have been tested using magnetencephalography (MEG) or magnetic resonance imaging (MRI) [60; 75]. Though those techniques provide a more substantiated therapeutic intervention the astronomical costs of device acquisition and maintainance prohibit the use of these therapy approaches on a daily routine.

2.1.5 Bioelectromagnetism

Physiological background: Nerve cells communicate in most cases by a serial process of electrical and chemical signal transduction. Pure electrical cell to cell connections (gap–junctions) exist but are far outnumbered by electro–chemical synapses.

Fluctuations of the axonal membrane voltage, defined as voltage gradient between inner and outer membrane surface, elicit traveling action potentials (AP) by a change of ion channel conductances. The transition of ion channels from open state to closed state (and vice versa) triggers an intense but short–duration swing of the membrane voltage from a subthreshold resting state (-50 to -80 mV) to an impulse–like active state (up to +100 mV). This AP in turn activates adjacent ion channels where another AP is generated and so on. Upon reaching the nerve presynaptic terminal the information transfer is switched to chemical transduction by cell specific neurotransmitters. Neurotransmitters (NT) exist in a variety of chemical compounds (>100) [138] and can be classified into small–molecule NTs (rapid synaptic processes) and neuropeptides (lasting synaptic processes). All NTs can be additionally grouped according to their reaction mechanism, which involves its endo–synthesis, its postsynaptic receptor specificity and its rapid removal from the synaptic cleft. The most prevalent NT is Glutamate in excitatory- and Gamma–Aminobutyric Acid (GABA) in inhibitory neurons.

At the postsynaptic membrane the NT binds to receptors and triggers in a primary or second–messenger reaction the opening of ion channels. The ion flux changes the membrane voltage of the postsynaptic neuron, generating a postsynaptic potential (PSP), which can be excitatory (EPSP) or inhibitory (IPSP). As every neuron receives simultaneously both excitatory and inhibitory input from 1000 up to 100.000 synapses the PSP is integrated as sum potential at the axon hillock. Upon crossing a voltage threshold the Axon hillock triggers an AP.

Electroencephalography (EEG): Although the sum of every transmembranic ion current constitutes the extracellular field, slow synaptic activity is the dominant contributor to local field potential (LFP) of a neural patch. The most simple description of the field produced by active neurons is the superposition of point sources, embedded in an pure Ohmic, spheric volume conductor:

Let σ be the conductivity of the embedding tissue; I_j is a current current source in the distance of $|r - r_j|$ to the recording electrode. So $V(r)$ is given by

$$V(r) = \frac{1}{4\pi\sigma} \sum_j \frac{I_j}{|r - r_j|}. \qquad (2.1.1)$$

A pyramidal neurons dendritic arbor can be seen as Ohmic conductance in an isolating membrane, driven by thousands of excitatory and inhibitory synaptic connections. Due to the spatially separated ionic fluxes and return currents the neuron forms an instantaneous electric dipole moment with its displacement vector along to the spatial distribution of local sinks and sources. The field, originating from this dipole decays in a volume conductor with $1/r^2$. Buzsaki et al. review the influence of several additional contributors to local field fluctuations, such as fast APs, Ca^{2+} driven spikes and neuron glia interactions [22]. These secondary contributors are not necessarily counterbalanced by return currents an thus can form electric monopoles [29]. The field distortion by monopole effects is less pronounced than it is in the case of the synaptic dipole, but the monopole field effects decay only with $1/r$.

The EEG is mainly a spatiotemporally blurred integration of the activity of a large set of neurons arranged in parallel, whose local field fluctuations superimpose. The magnitude of EEG fluctuation thus largely depends on the simultaneous activation of the neural dendritic arbors (i.e., synchronization of the pyramidal cells). The summation of individual dipoles yet is impeded by the cortex folds, as the displacement vector of the pyramidal cell dipole is oriented perpendicular to the cortex surface. The summation of a set of dipoles is equivalent to a single dipole moment with a displacement vector equal to the average orientation of the individual dipoles (equivalent current dipole) [104]. The EEG recording is distorted additionally by Ohmic and capacitive influences of the skull and tissue inhomogeneities of the volume conductor. The skull thus frequency specific attenuates the potentials generated by the source components, acting as a low–pass filter [128].

The EEG response to a series of specific stimuli can be recorded on the basis of a stimulus–locked trigger. This stimulus response is termed "event–related or evoked potential (ERP)" or is more precisely named according to its modality and latency. (e.g., "auditory late response (ALR)"). Common clinic practice is the averaging of

a series of single responses to emphasize diagnostically relevant signal components. This method is justified as single event–related potentials triggered by the same stimulus, are similar to each other in terms of their latencies and general morphologies. Averaging thus can increase the signal–to–noise ratio as noise events add up destructively, while the signal of interest sums up constructively. Yet the drawback of this methodology is a loss of temporal precision and the inability to monitor trends of morphology variance over the duration of the experiment. In the signal–processing context of this work we focus almost exclusively on methodologies to process single–trial responses to optimize the extraction of relevant trends in ERP feature changes.

2.2 Tinnitus in the peripheral hearing path

2.2.1 Peripheral origin

In the majority of cases tinnitus is associated with a peripheral high—frequency hearing loss. The population of high–risk—groups for hearing loss due to noise exposure or age [66], has in consequence a higher prevalence for tinnitus. According to literature the percentage of tinnitus associated with hearing loss is in the range of 85—95% of the cases [112; 6; 125; 123]. Tinnitus can also occur in normal hearing subjects, but is in most of these cases characterized by a significantly lower degree of severity compared to tinnitus sufferers with hearing loss [156; 26]. A recent study by Schaette et al. [159] additionally demonstrates a reduced amplitude of the wave I potential in brainstem audiometry of tinnitus sufferers with a normal audiogram. The wave I potential is the direct correlate of auditory nerve fibre activity. This reduction hints towards a "hidden hearing loss" (i.e., it is not visible in the conventional audiogram) as the neural response magnitude is renormalized or even exaggerated [48] within subsequent processing stages, indicating a firing—adaptation in high–level processing. Moreover studies demonstrate that auditory deafferentations can exist without hearing loss [26]. These results also indicate a peripheral origin of the acoustic phantom perception. Experimental support for this hypothesis was provided by Weisz et al., who demonstrated an increased tone detection threshold in high—intensity background noise in tinnitus sufferers with normal audiograms [190; 35]. This phenomenon of phantom perceptions in response to peripheral deafferentiation is not strictly related to the auditory pathway, but appears also in a number of comparable symptomatologies [27], such as phantom (limb) pain or Charles Bonnet syndrome due to macular degeneration [73]. All these symptomatologies have in common a hyperactivity/hyperexcitability of the deafferentiated midbrain neurons, demonstrated, e.g., by an increased metabolism rate [1; 20; 36].

Mulders et al. recently presented experimental results on the relationship between hair cell loss, auditory thresholds and spontaneous activity in the central nucleus of the inferior colliculus (CNIC) in guinea pigs [118]. This spontaneous activity is restricted to frequencies specifically related to bands with peripheral hearing loss [119] after acoustic trauma. The authors could assess an increase of spontaneous neural

activity in the CNIC in frequencies less than one octave in distance to the frequency of the acoustic trauma with a maximum slightly above the exposure frequency. The persistent spontaneous firing frequency of CNIC neurons in the tonotopic range of the noise frequency increased from approximately 2 Hz in sham controls to more than 15 Hz in animals with severe acoustic trauma [118]. Backing up these results, Schaette et al presented in 2006 a computational model of the increase of spontaneous neural activity due to homeostatic plasticity [158]. According to this model a homeostatic mechanism controls the range of neural firing rates. The detrimental effect in Tinnitus thus might occur due to a reduction of the ratio between spontaneous activity and mean firing rate. This abnormal gain in the auditory pathway was also described by Melcher et al. [113] and Yang et al. [195]. The increased neural activity might be sufficient to activate cortical neurons and to generate a percept, yet is not sufficient to explain course and interpersonal variability of the tinnitus pathogenesis [124]. Attentional top—down mechanisms must be able to further boost the activity of subcortical neuron populations in the sensory pathway. A number of authors proved the modulation of bottom-–up sensory processing by top—down mechanisms [174; 135]. Short ranged corticofugal top—down effects, i.e., to the thalamic cores, can be subsumed under the term of attentional focus and will be addressed separately in chapter 2.3.3.

2.2.2 The auditory nerve (AN)

The inner hair cells build synaptic connections to the bipolar cells of the spiral ganglion (SG), whose axonal projections maintain the cochlea's tonotopic structure. About 90–95 percent of those projections are type I fibres that innervate inner hair cells, whereas the type II fibres that innervate the outer hair cells constitute only 5 to 10 percent of the auditory nerve. The cells have individual response thresholds, depending on intensity and frequency of the stimulation. The stimulus frequency with the lowest response threshold is called characteristic frequency. The axons of the SG bipolar cells form the auditory nerve, which is part of the paired vestibulocochlear nerve. Combined with the vestibular nerve, it forms the 8th cranial nerve. Both nerves share a common envelope of conjunctive tissue. The vestibulocochlear nerve enters the brain stem at the lower down of the pons. At this point the auditory nerve detaches from the common projection and innervates the cochlear nucleus complex [201].

Most type I fibres of the AN show spontaneous activity in absence of an adequate stimulus. The neurons with the highest spontaneous AP rates (20–50 Hz) usually have the lowest response threshold at its characteristic frequency and vice versa [157]. Above this threshold the neural response rate shows a sigmoidal behaviour, growing (almost) linear with increasing intensity until reaching a plateau for high stimulus intensities. This dynamic range can span 20–40 dB(SPL). Higher sound intensities lead to the recruitment of neighboring fibres upon exceeding their threshold for non–characteristic frequencies (off–resonance threshold) [146].

2.2.3 The dorsal cochlear nucleus (DCN)

Anatomy and physiology: The DCN is the dorsal subdivision of the first nuclei in the hearing pathway and receives direct input from the auditory nerve. It is a laminated structure, but the actual number of distinct laminar structures might vary across different species [149], likely due to phylogenetic changes in the DCN cytoarchitecture. Commonly literature refers to three distinct layers for primate mammals: (a) The molecular layer is a cerebellum–like structure of parallel axonal fibres, projecting from granule cells in the fusiform layer, and of GABAergic stellate cells. This DCN–layer integrates multimodal sensory information, such as somatosensory feedback of the head position. (b) The fusiform layer, containing glutamatergic fusiform (also called pyramidal) principal neurons, glutamatergic granule cells, glutamatergic unipolar cells, glycinergic cartwheel interneurons and GABAergic Golgi cells. The fusiform cells receive auditory and non–auditory input to apical and basal dendrites respectively, and directly project to the Inferior Colliculus (IC) [9]. (c) The deep layer consists of glutamatergic giant cells and of glycinergic tuberculoventral cells. The giant cells also receive input from the AN and send projections to the IC [129].

In the numerical description of the DCN activity we focus on the fusiform layer, which shows elevated spontaneous activity in response to an acoustic trauma with behavioural evidence of a tinnitus pecept [9]. See section 3.1.2 for a detailed description of the model.

The role of the DCN in tinnitus: In the early 1980s studies brought evidence that tinnitus is apparently no cochlear malfunctioning, but has its origin in higher stages of the auditory pathway. Dissections of the auditory nerve did not necessarily

mute the tinnitus tone [69]. Depending on Literature source, the surgical section of the AN failed to bring amelioration in 40–80 percent of the treated patients. Even worse, tinnitus can develop as a result of eighth nerve dysfunction, either by surgical section treatment, vascular compression or acoustic neuroma. Postulating an auditory origin of the tinnitus percept, these results match with the model of peripheral hyperactivity by Schaette et al. [158] (see subsection 2.2.2) and the progressive centralization of hyperactivity, as described by Mulders et al. [120].

Animal studies (predominantly in non–primate mammals) demonstrate a hyperactivity in the DCN principal neurons in response to excessive noise exposure or treatment with tinnitus–inducing agents, e.g., cisplatin [78]. These acoustic insults produce a wide range of plastic changes in the DCN, such as Axonal fibre degeneration, axonal sprouting or changes in neurotransmitter release and reuptake [77]. We hypothesize that short term plastic effects initiate the tinnitus, as the symptoms develop within a narrow time–window after noise exposure [57]. This noise induced hyperactivity bears strong similarities to stimulus–driven activity as both exhibit a related tonotopic profile. Animal studies demonstrate a strong relationship of increased DCN activity and the strength of behavioural evidence for tinnitus [77].

Electrical stimulation of the DCN caused changes in the tinnitus loudness perception in patients with auditory brainstem implants after vestibular Schwannoma removal. 8 out of 10 subjects reported a volume change in their tinnitus perception; 7 patients gave account of a loudness reduction, 1 subject reported an increase of tinnitus intensity ([77] and references within).

As the molecular layer of the DCN integrates sensory information from different modalities, the DCN hyperactivity might also be an explanation for the phenomenon of "somatic tinnitus". A number of tinnitus patients reported a change in their tinnitus perception when they voluntary change the tonus of the neck– or masticatory muscles. These patient case reports are reinforced by studies that demonstrate a change in DCN spontaneous activity following a stimulation of the innervation of the head–neck musculature [80], especially of the 2nd cervical nerve or the trigeminal nerve. An analogue explanation could serve as illustration of the "gaze–evoked" tinnitus.

Plastic changes in neural DCN activity are mirrored in alterations in the subjective tinnitus perception. Changes in tinnitus pitch and loudness over time are common

among chronic tinnitus patients. In the DCN, the level of hyperactivity and its location along the tonotopic axis shift over time [79]. Equivalently short–term plastic effects in the DCN, such as spike timing dependent plasticity (STDP) in DCN neurons, might provide an explanation for the residual inhibition in masking experiments.

2.2.4 Descending pathways in sensory perception

The auditory pathway is controlled by a number of descending fibres forming multiple feedback–loop systems. These top–down pathways have various functions, such as the protection of the cochlea from sudden high–intensity sounds (stapedius reflex) or the improvement of subcortical signal properties in terms of stimulus competition (e.g., corticothalamic loops - see also section 2.3.3) [173]. These feedback systems can be classified according to origin and length of their projections. The olivocochlear system has a prominent role among the feedback loops of non–cortical origin. It governs reflexes to protect the cochlear from high sound intensities and can modulate AN responses by targeting outer hair cells. Top–down projections originating from the cortex target every hierarchical level of the auditory pathway [127]. Every level's response, from the cochlear to the thalamic cores, can be adjusted by corticofugal top–down projections [135]. This corticofugal system is able to modify the response of subcortical neurons, so the neurons tuning curves to frequency content, amplitude and spatial characteristics of the stimulus can be shifted for an improvement and adjustment of input to the sensory cortex.

In fear conditioning the corticofugal projections, along with limbic areas, play a key role in tone–specific plastic changes [173]. This reorganization process could be a neural correlate of an attention focus on a particular tonal percept, as e.g., in tinnitus. In fact similar plastic changes in limbic and defined areas of the auditory cortex were revealed by C–Fos and Arg3.1 staining in an animal tinnitus model [188]. In healthy subjects the perception of behaviourally insignificant stimuli is attenuated over the number of repetitive stimulations. This effect can also be attributed to corticofugal pathways to sensory and extrasensory areas of stimulus processing [42; 183; 53]. These corticofugal projections appear not only in the auditory domain but are a multimodal mechanism, shared e.g., by the visual and somatosensory modality across a wide range of mammal species.

2.3 Tinnitus in prosencephalic structures

2.3.1 Auditory scene analysis and stream segregation

In natural–world situations individual sounds overlap in their spectral components. Their temporal characteristics, such as onset and timbre, as well as their frequency components, are interlaced. Natural sounds and speech normally exhibit a $1/f$ characteristic in their power spectrum, representing a dominance of low–frequency amplitude modulations [167]. The probability density function of sound intensities exhibits an almost symmetric Gaussian–like distribution of logarithmic amplitudes (in decibel, relating to the mean intensity) that tends to be blurred on both sides. Both, the AN model and the model for the generation of ALRs, use consequently a Gaussian function as input signal. The dynamic range of a stimulus is defined by its 90th percentile–range, where speech has the broadest dynamic range (up to 50 dB) and white noise has the narrowest dynamic range (about 20 dB).

For a listener the separation of sound sources in their acoustic environment is difficult as the pressure wave detected by their ears is a sum of all pressure waves from all concurrent sound sources. This acoustic conglomerate has to be segregated into single source representations by heuristic processes. These primitive grouping mechanisms can be described by the Gestalt principles of sensory processing. A Gestalt is formed by a set of simple rules, such as proximity, similarity, common fate, continuity and so on. In a simple example of acoustic continuity, human speech carries different fundamental frequencies for individual speakers which can be separated and grouped by the common spacing of their harmonics. The grouping is thus justified by regularities in the respective sound sources. This mapping of the acoustic environment into a set of sound sources is called auditory scene analysis [15]. Every information content produced by a single source (or a set of conjunct sources, such as organ–pipes) is referred to as stream. The streaming of acoustic information determines the perception of pitch, timbre, loudness and spatial position.

A more complex form of information grouping is schema–driven. These schemes contain previous knowledge of signal classes. Schema–driven perception matches a set of closed forms against perceptual templates, that change with personal experience. Richard Gregory's Dalmatian is an descriptive illustration of visual template

matching. Although the image consists only of black spots the observer can recognize the shape of a Dalmatian. The spots are cleverly arranged to resemble lighting and shading of a familiar scene, thus the brain tries to match the perceived pattern to already known templates [160]. There is evidence that these pattern templates are learned and change during childhood and adolescence. Considering the picture "Message d'Amour des Dauphins" by Sandro del Prete, the entire perception of the drawing is dominated by individual experience. Whereas adults see a couple in embrace, children who are not familiar with such scenes will only see a school of dolphins. The schema–driven template which is grouping the basic shapes to form the superimposed picture of a couple is not working for infants.

In this work, the tinnitus tone is dealt as information stream, as it integrates the activity of several neural projections into a functional percept. Though the tinnitus tone has no physical correlate in the sensory environment, the pattern matching mechanisms of auditory stream segregation apply. This stream formation puts the tinnitus tone in sensory rivalry with concurrent acoustic streams. The following sections shed a light on universal mechanisms that cause the tinnitus to occupy such a prominent position in the conscious perception of tinnitus sufferers. Focussed attention is likely to enhance the perceived intensity (subjective loudness) and dysfunctional valence assessment is likely to prevent a habituation to the tinnitus stream.

2.3.2 Attention

Definition: Attention can be seen as a filter mechanism that promotes the processing of relevant information while it simultaneously suppresses insignificant stimuli. As introduced in section 2.3.1, the natural acoustic environment is build up of numerous concurrent streams of auditory information. The multitude of streams does not carry behaviourally relevant content, while other streams might contain crucial information. In order to select the most relevant stream for higher processing, each stream must be assigned a quality depending on stimulus–saliency and motivation. The stimulus driven orienting of attention, referred to as exogenous attention, depends on physical properties of the stimulus, e.g., intensity. The more abrupt the changes in the stimulus properties (also the sudden appearance of a sound source), the higher is the probability of attention capture. This stimulus–driven orienting

is short lasting until signaling behaviourally relevant information. Complementing this reflexive orienting, goal–driven or endogenous attention allows for a voluntary switch of attention from one stream to another.

Apart from the orienting reaction of attention, either voluntary or towards sufficiently salient stimuli, the concept of attention includes active searching and the filtering of irrelevant sensory streams. In the description of attention mechanisms in the tinnitus symptomatic, active search plays only a minor role. The main focus of this work thus lies on the orienting reaction, as measure for involuntary capture of attention by the tinnitus and on the filtering, as model for the dysfunctional habituation towards the tinnitus tone.

Although attention and conscious perception are closely related, they can be separated into two distinct conceptual processes. Experiments to inattentional– or change blindness, e.g., by Daniel Simons ("Gorillas in our midst" or "The door study" [164; 165]) suggest that everything that is not attended will not be perceived consciously. Yet studies to divided attention and to the cocktail party phenomenon (reorienting to salient clues) demonstrate that inattentional but conscious processing of sensory events is also possible. This effect can at least partly be attributed to the stimulus saliency.

The following item list exemplary highlights predominantly phenomenological attention models in a non–judgemental way to draft a framework and limits for our computational models of attentive stimulus processing:

Bottleneck–models of attention:

- Donald Broadbent: In 1958 Broadbent postulated an all–or–nothing scheme of attention, described as attentional bottleneck. Only attended information streams pass this bottleneck and are subject of a higher conscious processing; whereas streams that are unattended will be completely blocked ("filtered"), never reaching consciousness.

  In modeling terms Broadbents model is a single stage filtering process: Incoming sensory information is stored in a register and checked for physical properties such as intensity, duration and time course (i.e., stream segregation). The attended stream, indicated by specific physical characteristics, is allowed for higher processing. During the transition of the attended in-

formation from sensory storage via semantic processing to working memory the stream occupies the entire bandwidth of the attentional bottleneck; thus preventing concurrent streams from entering higher processing levels and protecting the attended stream from an eventual interference during semantic processing [18].

This early–selection model yet cannot explain key aspects of the allocation of attention resources. Independent from their physical properties, messages with high subjective relevance, such as names or nowadays ringtones of mobile devices, are sometimes (about 33%) able to avoid filtering and reach high–level processing stages. This effect was described as cocktail–party phenomenon [23; 117; 192; 148].

- Anne Treisman: In an auditory shadowing experiment, Anne Treisman demonstrated that mechanisms of selective attention attenuate the unattended stream rather than blocking this information. During the simultaneous presentation of two channels in a selective listening task, the content of the unattended stream is almost completely tuned out; the information content is seemingly not conferred to contextual levels of the processing hierarchy. Yet occasionally this filtering can be penetrated by words from the rejected channel that have a high transition probability, especially if the transition probability in the attended stream is violated. Earlier studies, e.g., [23; 117], also demonstrate the contextual processing of subjectively significant keywords (the persons own name) from rejected streams. In [178] Anne Treisman offers two possible model explanations for this phenomenon. She introduced a hierarchical double–stage filter model with a low–level filter for physical stimulus properties and a hierarchically higher filter for semantic processing. But instead of deploying an impermeable attentional filter, the rejected stream will be attenuated. Both streams reach a dictionary unit in which the threshold for higher processing is set upon a probability distribution of semantic transition. Additionally this dictionary unit stores a number of keywords with an intrinsic low threshold value. The unattended stream has, by definition, a significantly higher threshold for the activation of dictionary units, unless its semantic content matches one of the low–threshold keywords. In consequence the attenuation filter can be contextually shifted to either attended or rejected stream.

Alternatively the semantic content of the rejected stream could be stored in a memory register and processed occasionally. The pattern–matching with the keywords of the dictionary unit thus could elicits an attention–shift to the rejected stream. This "serial" processing of semantic content can be considered an early outlook for the model of probabilistic stream selection.

- Deutsch & Deutsch: Diana and J. Anthony Deutsch took a different point of view on the data of Anne Treisman. They reinterpreted the model in a way that makes the dual–stage filtering redundant. Instead of implementing a low–level filter for physical stimulus properties, they introduce a selective threshold modulation of the higher–level dictionary units. This discriminatory system weights the stimulus valence according to the stimulus attributes. The selective mechanism of attention transfers this weighting to other units with which they are grouped, while suppressing the outputs of rivaling discriminatory units. Whereas in Treismans attention model only the suprathreshold (high weighting) units are activated, in Deutsch & Deutschs model the stimulus valence of the attended stream is mapped onto all discriminatory units in parallel, de facto saving a filter level by introducing a "late–selection" model.

The crucial question whether early– or late–selection attention models approximate the biological truth is still debated in recent literature (see [109] and references within). However, the magnitude of attentional modulation seems to increase within subsequent hierarchical levels in stimulus processing [96]. In computational neural–network models for visual selection, a top–down influence can be achieved by implementing gain functions to improve the processing of given target features, e.g., a certain color. This feature mapping can increase target discrimination if the feature gradients in the original image are not sufficiently salient [191]. In these models the top–down modulation affects early feature detection, whereas in our model the attentional modulation affects the neural representation on a more abstract level.

Probablistic stream selection and attention load: Without addressing the problem of early– and late–selection theories, Trenado and Strauss introduce a probabilistic model of attentional resource allocation [179]. Every concurrent stream is evaluated on the base of a bottom–up weighting due to its physical properties (e.g., intensity) and of a top–down weighting due to its matching to consolidated sensory templates. These templates can be seen as simple Gestalt forms or more

refined, learnt schemes (see exemplary schemes in section 2.3.1). Both weightings, exogenous (from the outside: physical properties) and endogenous (from the inside: template matching), are summed up for a total weighting. In a decision circuit the stream with the highest weighting has the highest probability to be selected for higher–level processing; followed by the next lower weighting and so on. See figure 2.1 for a simple illustration of this probabilistic attention model.
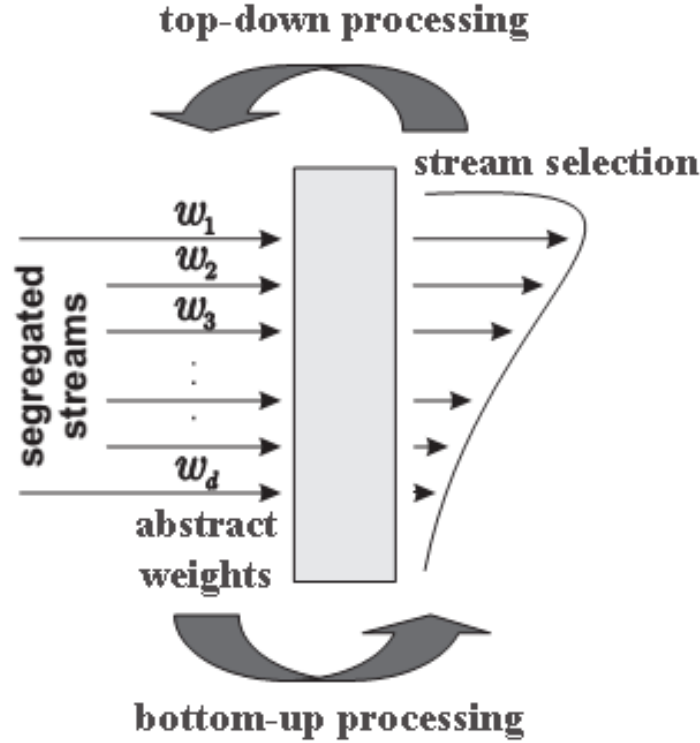

Figure 2.1: Conceptual illustration of a probabilistic stream selection model. The stream are labeled and sorted according to their exogenous and endogenous weight total. The probability distribution (indicated by the curve) on the right side of the decision circuit reflects the chances of every single stream to be selected for higher–level processing.

The effect of endogenous weighting yet requires a more detailed analysis of the streams information content. Thus the question arises how wide is the endogenous "spotlight of attention" (bandwidth of the attentional bottleneck) and how the initial attention onset is generated. We discuss the register shift of information and the factor of vigilance in section 5.2.

2.3.3 Bottleneck–filtering by spiking regularity and thalamocortical loop gain modulation

When addressing the problem of the generation of endogenous and exogenous weights the mechanisms of neural information transfer have to be taken into account. Exemplary, the thalamus is a relay node for almost all types of sensory stimuli, connecting hierarchically superior areas of stimulus processing and sensor–side functional elements. Surprisingly only about 15% of the synapses onto cortical layer IV spiny neurons originate from thalamocortical projections [10]. This sparseness of parallel input fibres indicates, that excitation by the specific thalamic nuclei is weak and requires an additional mechanism of amplification for suitable signal transduction [105]. Sakmann et al. could demonstrate in 2006 that a temporal amplification mechanism exists in the animal model of whisker movement PSPs (Post synaptic potentials) in the barrel cortex of rats. The authors confirmed the low efficacy of thalamocortical synapses, but could substantiate a near—synchronous pattern of APs among the majority of the converging inputs in the case of strong sensory stimulation [19].

Coherent neural activity may not only be the key concept of perceptual binding, requiring concerted neural activity to integrate the converging sensory input into a single percept [166]. Moreover coherent signals might also facilitate stimulus selection as already addressed in section 2.3.2 with the introduction of exogenous weights. Advantage in perceptual rivalry is tightly linked to gamma-–band synchronization [41]. Fries et al. stated in 2005 a top–down "entraining mechanism" in stimulus processing, utilizing subthreshold oscillations to give preference to a selected sensory input stream over competing input streams [40]. This effect is the neural analogon to the endogenous weight in 2.3.2. Börgers and Kopell gave additional support for this hypothesis in 2008, presenting an *in–silico* model linking gamma activity and selectivity. A coherent input in the gamma—band can effectively inhibit less coherent competing inputs via $GABA_A$ mediated inhibitory interneurons [16; 17]. Cortical top-–down projections to thalamic areas and even to hierarchically lower stages of sensory processing might promote synchrony in excess of the self-–organization dynamics (as discussed later in section 5.1) by a reduction of initial phase noise [5; 102].

2.3.4 Habituation

Habituation is best known from the attenuation of the gill and syphon withdrawal reflex in Aplysia californica in response to repetitive stimulation. The definition of habituation originates from an article of William Thorpe [176] in 1944:

> "We may, therefore, define habituation as an activity of the central nervous system whereby innate responses to mild shock and warning stimuli wane as the stimuli continue for a long period without unfavourable results."

William H. Thorpe, 1944, Some Problems of Animal Learning

This effect appears even without reinforcement learning and thus needs to be differentiated from Pavlovian conditioning. Yet a progressive attenuation of behaviour may reflect side–effects such as sensory adaptation or fatigue. To delimit the habituation from these unspecific effects, habituation is defined as:

- **Stimulus specific:** The behavioural response attenuation is limited to a specific stimulus. The probability to evoke an already habituated reaction by a deviant stimulus increases with its dissimilarity. This dishabituation effect allows for a differentiation from fatigue and sensory adaptation. In a physiologically fatigued organism all behavioural responses are attenuated equally, while in habituation a deviant stimulus is able to elicit the respective behavioural response in full strength (sensitization).

  We examine this dishabituation effect as delineation to fatigue effects in a visual stimulus–exchange paradigm. Please refer to section 3.2.2.1 for a detailed description of materials and methods.

- **Reaction specific:** The habituation of a behavioural reaction to a specific stimulus does not implicate a general attenuation of all reactions to the given stimulus.

One could argue that the absence of "unfavourable results" in the definition of Thorpe is an expectation violation and thus could be explained by Pavlovian conditioning, yet the restriction of habituation to possibly tenuous stimuli, as in the

definition of Thorpe, can be extended to all stimuli with no or little subjective relevance.

In the context of this work long–term habituation [121; 140] is defined as a process of attention–drift, away from an irrelevant target–stimulus over time during repetitive stimulus presentation. The behavioural response to the stimulus is an orienting reaction followed by a potential sustainment of attention. Every link of this attentional chain of orienting reaction, attention sustainment, habituation and dishabituation bears unique correlates in late evoked responses, that can be utilized to quantify these behavioural responses. See section 3.2.1 for a detailed methodology outline.

2.3.5 Intermodal effect of emotion–tinged stimuli on the allocation of attentional resources

Studies on the serial processing of attended objects show that the required time for a visual search paradigm increases with the number of distractors. We discuss this effect in the context of our probabilistic attention model in section 5.2. Surprisingly the time to find a given object can be shortened significantly by presenting emotionally tinged targets, with the most consistent time reduction for fear–related stimuli (see [32] and references within). This mechanism is also in effect when using target cues: highly valent stimuli or cues are likely to increase the attentive performance in every sensory modality. The question whether this pre–attentive evaluation of the stimulus valence is inherently integrated in every single sensory pathway can be addressed by a spatial orienting task with multimodal target cues. Subjects react faster to targets presented on the same side as an emotional cue, regardless of the clue's modality (emotional facial expressions, thread words) [32].

Imaging studies demonstrate the activation of distinct brain areas for emotional processing (i.e., the limbic areas) even before high–order sensory processing. In face processing, the first valence–dependent cortical MEG correlates appear as early as 120 ms poststimulus, whereas the characteristic face–related response is the N170 component (at 170 ms) of the VEP (see also section 3.2.2.1). There is a "short–cut" to the activation of the limbic system in every sensory modality which is an extrasensory pathway originating from early sensory processing stages. Studies

demonstrated the activation of the amygdala for subliminal fear–related stimuli across different modalities and for emotional stimuli in the neglected hemifield of subjects with visual extinction [32; 99]. This modality unspecific pre–attentive evaluation is likely to influence attentional capture and further sensory processing, as outlined in section 2.3.2 as it seems to play a major role for the modeling of extrasensory stimulus processing.

2.3.6 Limbic contributions to Tinnitus and cortico–thalamic modulation

Artificial elicitation of tinnitus in the animal model by salicylate injection or acoustic trauma induces region specific increase of the immediate-–early genes (IEGs) c-–fos and arg3.1 [188]. These plasticity markers feature a significant level increase in the central amygdala (CeA) and primary auditory cortex layers II, III, IV and VI [100]. Whereat the increase of limbic plasticity markers is most likely attributed to (sensory) stress [188]. Fundamental studies on CeA activation by electrical stimulation suggest a modulation of cortical activity (suppression of cortical delta activity) by cholinergic afferent fibers [81; 108]. The cortical layer IV forms the primary target of vMGB (ventral medial geniculate body) projections to the AC, whereas the corticofugal projections to specific thalamus nuclei and the thalamic reticular nucleus (TRN) origin from layer VI. The plastic changes described above thus directly influence the cortico-–thalamic—feedback loops, which are deemed to govern the facilitation of higher cognitive processing resources, i.e., attention [25; 111; 199; 86]. Layers II and III are primary afferent target and efferent source respectively for cortico–cortical projections. We can only hypothesize an involvement in the cortico—limbic interactions via Entorhinal Cortex (ERC) and Prefrontal Cortex (PfC). Cortical hyperactivity was attributed to diminished intracortical inhibition by a number of authors [139; 193; 97; 175] but the plastic changes demonstrated in [108] only affect excitatory pyramidal neurons. Moreover this study suggests that these cortical plastic changes cannot be attributed solely to thalamic projections but also to other afferent areas in the limbic system.

2.3.7 The role of the hippocampus in attention resource allocation

As the attentional binding to a sudden phantom noise, e.g., after an acoustic trauma is very quick [177]. It cannot be correlated with plastic changes in the thalamocortical pathway. This plasticity might be responsible for tinnitus decompensation, but a more primitive mechanism must be responsible for the early attentional binding [28]. Yi et al. [196] proved that only selectively attended events were able to consolidate memory traces, which hints towards a fundamental connection of attention and memory formation and retrieval. Moreover animal studies showed an unsettled investigative behaviour in rodents with hippocampal lesions, comparable to exploration in entirely new environments [143; 43; 85]. An attentional habituation towards the orienting reaction might be considered as loss of attention. Novelty thus seems to serve as its own quality for focussing attention and the conduction of behavioural schemes. Honey et al. provided additional evidence that a spatial representation still exists in rats with hippocampal lesions, by showing spatial preference behaviour in lesioned animals [68]. These results indicate for a modulation of stimulus intensity or perceptual saliency due to hippocampal activity. Many authors suggested a role of the hippocampus in the allocation of attentional resources in the form of a comparator of actual sensory stimulation and already preprocessed memory [115; 169; 152; 47; 186; 153]. The detection of novel events might thus be an important function of the hippocampus, leading to a reallocation of attentional processes and investigative behaviour. Sato et al. [154; 155; 194] proposed the formation of a cognitive map by theta—phase coding in the projections of ERC to hippocampal CA3. This map provides a dynamic prediction of the egocentric representation of the sensory environment and might also serve as a detector of deviants, representing novel events in the respective space. We address this model in the framework of the theta—guided attention hypothesis [186] and provide the implementation of a model on attentional guidance by a hippocampal comparator [53]. In a recent study, Zikopolous and Barbas highlighted the convergence of emotional and attentional pathways in the thalamic reticular nucleus (TRN) [200]. The importance of TRN as attentional gating structure was already demonstrated by a number of publications [25; 111; 199; 86].

2.3.8 Numerical modeling of neurons and neuron populations

Conductance based neuron models: Conductance based models were introduced by Hodgkin and Huxley in 1953 [65]. They are based on equivalent circuit models of small membrane patch of neural cells. The membrane lipid bilayer is simulated by a capacity c_m, with a leakage current given by a voltage source V_L and a fixed conductance g_L. The voltage gated ion channels are represented analogously by voltage sources $V_{K,Na}$ and associated controllable conductances $g_{K,Na}$. The net transmembrane current is thus given by $I_m(t) = I_c + I_{ionic}$, where $I_c = c_m \frac{dV_m(t)}{dt}$. V_m is the membrane voltage [168]. Hodgkin and Huxley introduced three gating variables m, n and $h \in [0,1]$ to reproduce the opening-/closing probability of voltage gated ion channels. The transmembrane current is given by:

$$I_m = c_m \frac{dV_m}{dt} + g_K n^4 (V_m - V_K) + g_{Na} m^3 h (V_m - V_{Na}) + g_L (V_m - V_L), \quad (2.3.2)$$

where m, n and h are subject to voltage dependent changes and are described by three ordinary differential equations.

As this model has a high computational demand, a number of simplified models have been introduced to simulate large numbers of neurons in parallel. Notable simplifications of this model are the FitzHugh–Nagumo model [72] and the NeuroMime model used for our DCN model. See section 3.1.2 and [107].

Formal spiking models: Formal spiking models are a drastic reduction of the dimensionality of conductance based models. The neural spiking reproduction by the Hodgkin–Huxley model can be emulated by a single variable threshold equation [87].

A well–established formal spiking model is the leaky integrate and fire model. This model integrates the input currents $I_i(t)$ until the membrane voltage V crosses a given threshold value θ. The cell membrane is represented by a parallel circuit of a membrane capacitance c and an Ohmic resistance R, expressed by the membrane time constant τ_m. The input $I(t)$ to the model yields:

$$\tau_m \frac{dV}{dt} = -V(t) + RI(t) \quad (2.3.3)$$

The morphology of the spike is omitted; instead the membrane voltage V is set to an afterspike value $V_r < \theta$ (reset potential) if V exceeds the spiking threshold θ. The points in time, where $V \geq \theta$, form a point process which can be analyzed for, e.g., synchronization patterns.

In this work we use the Izhikevich simple spiking neuron model, which is another prominent example of a formal spiking model. Izhikevich uses bifurcation methodologies to reduce the 4–dimensional Hodgkin Huxley neuron model to a 2D system of ordinary differential equations with a spike reset after V_m exceeds a predefined threshold value. The equations were fitted to the spike initiation dynamics of a cortical neuron to ensure biological plausibility [71]. For a detailed description of the Izhikevich neuron model see also section 3.1.3.

Neural–field models: As the neurons, their synaptic connections and the neuro-modulatory effects in a functional element of a processing structure in the brain are by far too numerous to be mapped in a computational model, the need arises to find a simplified yet biologically plausible model for the dynamic behaviour of neural populations. These tissue level models describe mean state variables (neural mass) such as, e.g., firing rate in a continuous approximation of the imbedding medium. Generally those models are described by spatio–temporal dynamics of a scalar field $\xi(r,t)$, $r \in \mathbb{R}^3$ and $t \in \mathbb{R}_{>0}$, where r represents the spatial component and t the temporal component. We can describe this spatio–temporal dynamics by the convolution of a connectivity function $W(r)$ and a function S governing the neural state variable. For a description of the population firing rate, typical applications are a Heaviside step function or a sigmoidal function. Starting from a resting state ξ_{rest} the generic model is given by:

$$\frac{d\xi(r,t)}{dt} = -\xi_{rest} + \int_{\mathbb{R}^3} W(r - r')S[\xi(r',t)]\ dr' \qquad (2.3.4)$$

More elaborate versions of these models include the propagation velocity c in the form of a temporal delay, leading to the following general change in the expression of $S[\xi(r', t - \frac{|r-r'|}{c})]$. In the model utilized for the simulation of evoked responses the propagation of the field of spikes is given by a second order wave equation with a decaying spatial connectivity function $W(r - r') = \frac{1}{2\sigma}exp(\frac{-|r-r'|}{\sigma})$, where σ represents the spatial decay. A general one–dimensional form is given by:

$$\left(\frac{\delta^2}{\delta t^2} + 2\omega_0 \frac{\delta}{\delta t} + (\omega_0^2 - \sigma^2 \Delta) \right) \xi(r,t) \;=\; (\omega_0^2 + \omega_0 \frac{\delta}{\delta t}) \; \rho(r,t), \qquad (2.3.5)$$

where $\omega_0 = c/\sigma$ and Δ is the Laplacian operator. $\rho(r,t)$ is given by

$$\rho(r,t) \;=\; S[a\xi(r,t) + \xi_s(r,t)]. \qquad (2.3.6)$$

Here a represents a general scaling factor and $\xi_s(r,t)$ additional input to the model from neighboring populations [179].

2.3.9 Notched acoustic stimulation as therapeutic intervention in tinnitus

In 1999 Pantev et al. used MEG measurements to monitor rapid plastic effects in response to sensory deafferentation at the cortical level. The functional deafferentation was achieved by filtering a narrow frequency band, centered at 1 kHz, of an acoustic stimulus. Subjects were instructed to listen to this "notched" music for three hours. After listening to the modified sound stimulus, the MEG field–strength of the N1m component was smaller for a 1 kHz stimulus, compared to the pre–experimental condition. This effect did not emerge for a control stimulus at 500 Hz [132]. The authors attribute this effect to rapid changes in the frequency tuning of cortical neurons, although they could not exclude plastic changes in subcortical nuclei. Such plastic effects in the peripheral hearing path were found in animal cochlear lesion models.

Okamoto and Pantev used in 2010 the suppression of neural activity in the bandwidth of the the notched frequencies in a therapeutical approach to reduce the subjective tinnitus loudness. The patients were instructed to listen to custom notched music. One octave, centered on the individual tinnitus frequency, was removed from the music spectrum. They report a significant reduction of tinnitus loudness in the target group in comparison to a "placebo" treated control group [130]. Okamoto attributes this treatment effect to cortical neurons, which expand their characteristic frequency range as they amplify their synaptic contacts to neighboring neurons. This re–wiring of thalamo–cortical input might cause tonotopic maps to fuse.

The patients in Okamoto's study were listening to their preferred music. The authors claim that enjoyable music is strongly connected to attention processes. Referring to the work of Robert Zatorre, Okamoto and Pantev argue that the described anxiolytic effect [197] originates from an activation of the reward system and the release of dopamine in the Nucleus Accumbens (NAc) [14] as driving force of cortical plastic reorganization [130]. So the reversal of maladaptive plastic effects of tinnitus must be credited to both, the notch effect and the promotion of plastic reorganization by a pleasurable acoustic stimulation This unspecific activation of limbic structures can be seen as unfocused analogue to the psychological intervention of the TRT (section 2.1.4).

Referring to our own experimental study utilizing notched environmental sounds, we discuss the necessity of tailored particularly enjoyable music stimulation in section 5.4.

3 Materials and Methods

3.1 Tinnitus in the peripheral hearing path

3.1.1 Auditory nerve model

The aforementioned increase in spontaneous activity in the periphery of the auditory pathway can be attributed to the brain's drive to maintain the homeostasis of a mean population firing rate. A lesion in the input to the AN momentarily reduces the mean firing rate of the AN, without affecting the dynamic range of response rates. Plastic changes in top–down neurons, e.g., from the Dorsal Cochlear Nucleus, subsequently restore the mean firing to a targeted level [157].

Schaette [157] addresses the question of hyperactivity and homeostatic plasticity effects in a computational model, which quantifies the response of AN fibers and the activity of downstream (top–down) projections [127]. As we can assume that the intensity distribution of natural sounds is Gaussian with mean μ and the standard deviation σ on average we can approximate the population firing rate of the AN as unified response function $f(I)$ over all frequencies:

$$f(I) = \begin{cases} f_{spont} \text{ for } I < I_\Theta \\ f_{spont} + (f_{max} - f_{spont})\frac{\int_{I_\Theta}^{I} p_I(I)dI}{1 - p_{spont}} \text{ for } I \geq I_\Theta \end{cases} \tag{3.1.1}$$

with

$$p_I(I) = \frac{1}{\sqrt{2\pi\sigma_I^2}} \, exp\left(-\frac{(I - \mu_I)^2}{2\sigma_I^2}\right) \tag{3.1.2}$$

and

$$p_{spont} = \int_{-\infty}^{\Theta} p_I(I)dI \tag{3.1.3}$$

We consider a likewise loss of inner– and outer hair cells, in which change the intensity–dependent firing frequency is modeled by the introduction of an impairment–factor $H_i \in [0,1]$, yielding $f' = H_i f_{min,max}$. To maintain a homeostatic effect, the decreased firing rate is compensated by additional input from downstream neurons (see equations 3.1.4 and 3.1.5). These downstream neuron are modeled as firing rate units which receive variable input f from the AN and a constant additional top–down input f_{td} originating from hierarchically higher areas of auditory processing. The sum of both inputs is weighted using a gain factor g and a response threshold Θ. The top–down influence in terms of a firing rate is given by:

$$r = R(f + f_{add}) = \begin{cases} r_{max} \tanh\left(\frac{g(f+f_{td})-\Theta}{r_{max}}\right) & \text{for } g(f + f_{td}) \geq \Theta \\ 0 \text{ otherwise} \end{cases} \tag{3.1.4}$$

with r_{max} is the maximum firing frequency of the top–down neuron. For the healthy condition the gain factor g is set to 1 The threshold value Θ is set f_{td}. Spontaneous firing and maximum firing rate are thus described by

$$r_{sp} = R(f_{sp} + f_{td}) \quad \text{and} \quad r_{max} = R(f_{max} + ftd) \tag{3.1.5}$$

So the model simulates firing rates of AN fibres, which are used as input signal in the model of the dorsal cochlear nucleus in the following section.

3.1.2 Model of the Dorsal Cochlear Nucleus

Neuron model: The implementation of the DCN model is based on the conceptual circuitry by Hancock et al [61], while actual neuronal dynamic behavior is described by the NeuroMime model by McGregor [107] and its utilization by Zheng [198]. Except for the non–specific afferents all neurons are modeled using the NeuroMime

model. The NeuroMime equivalent circuit is set up from a membrane capacity C_m and a resting conductance G, representing leaking currents. The transmembrane potassium current is modeled by a variable potassium–channel conductance g_K and the potassium reversal potential E_K.

The excitatory and inhibitory synaptic influence onto the membrane potential V_m is modeled by parallel branches with the reversal potentials E_{Ex} and E_{In} respectively and variable conductances g_{Ex} and g_{In}. Figure 3.1 illustrates the equivalent circuit of the NeuroMime model.
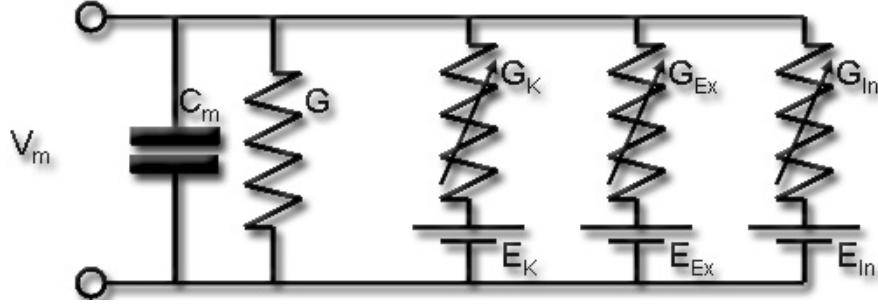
Figure 3.1: Equivalent circuit model of the NeuroMime by McGregor. V_m denotes the membrane potential, G is the resting conductance, characterizing leaking currents. E_K and G_K indicate the potassium reversal potential and the variable potassium conductance. Synaptic inputs are modeled by parallel branches with the reversal potentials E_{Ex} and E_{In} for excitatory and inhibitory terminals respectively and the variable conductances G_{Ex} and G_{In}

This equivalent circuit can be described by the following equations:

$$\tau_m \frac{dV_m}{dt} = -V_m - g_K(V_m - E_K) - g_{Ex}(V_m - E_{Ex}) - g_{In}(V_m - E_{In}) \quad (3.1.6)$$

$$\tau_k \frac{dg_k}{dt} = -g_K + b_K S \quad (3.1.7)$$

$$S = \begin{cases} 0, \ V_m \ < \ \theta; \\ 1, \ V_m \ \geq \ \theta \end{cases} \quad (3.1.8)$$

$$g_x = \frac{G_x}{G} \ \mid \ x \in \{K, Ex, In\} \quad (3.1.9)$$

In the simulation we omit a detailed depiction of the action potential. As given

in Eq. 3.1.8 the spike detection variable S is set to 1 if V_m crosses the threshold value θ, thus the voltage dependent changes in the conductances during the AP are neglected; the description of neural activity is in the form of a temporospatial point process (with space corresponding to a gradient of characteristic frequencies). The refractory period is simulated by an increase of the potassium conductance G_K.

Conceptual circuitry: The DCN model is set–up from 800 isofrequency–channels from 1.25 Hz up to 20 kHz in steps of 0.005 octaves. Every channel contains a set of three neurons with two independent input sources. The model simulates Type IV neurons, associated with DCN fusiform and/or giant cells, in the following referred to as principal cells (P). Those neurons respond best to broadband noise. The vertical inhibitory interneurons are of type II (I2). Contrary to the P cells, those neurons respond strongly to a tone stimulation at their characteristic frequency, but respond weakly to pure tone stimuli. The wideband inhibitory interneurons (W) receive inputs over a wide frequency band (magnitude of 3 octaves) and inhibit both P and I2 neurons to wideband stimuli. Fig. 3.2 illustrates the excitatory and inhibitory connections underlying the DCN model.
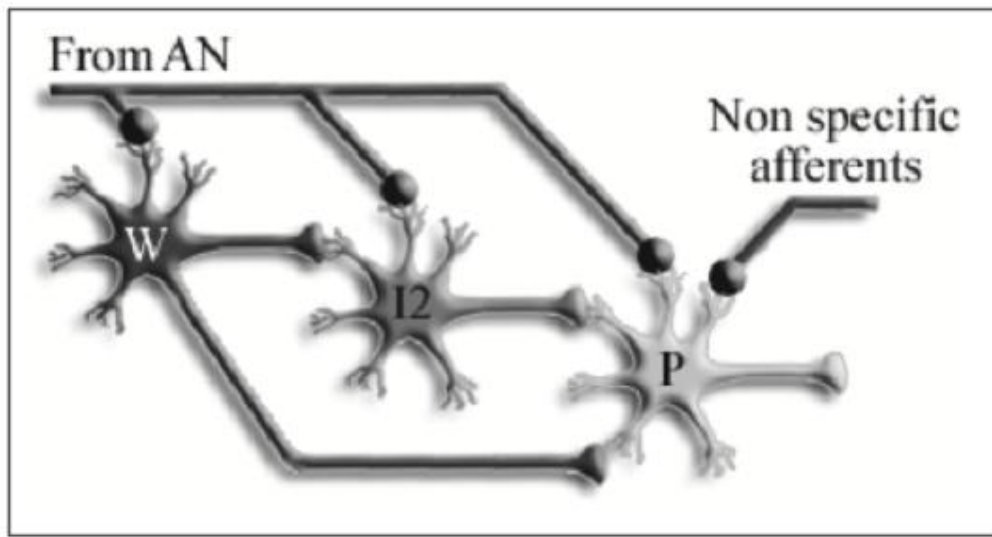

Figure 3.2: Conceptual circuitry of a single DCN channel. Principal cells (fusiform and giant cells) are labeled with P, I2 denotes inhibitory interneurons of type II. Wideband inhibition is labeled W. Additionally the cells receive input from the auditory nerve (AN) and non–specific excitatory afferents. Inhibitory synapses have cone–shaped illustrations, excitatory synapses are depicted spherical. The non–specific afferent projections are introduced to maintain spontaneous activity in the principal cells even after cochlear ablation.

The non–specific afferent projections to DCN principal cells are introduced for modeling convenience. The DCN principal cells maintain spontaneous activity even after cochlear ablation. As the source of this spontaneous activity is still vague [88], the modeling implementation is done by the introduction of a Poissonian process.

3.1.3 Ascending lateral inhibition networks

For modeling purposes we describe the spontaneous and evoked activity of the prior models by a Poisson point process, in which each point represents one action potential. This simplification of neural group activity is admissible, as no relevant information is conveyed by the shape of individual action potentials [134; 134; 12].

Glutamic acid decarboxylase (GAD) staining shows GABAergic inhibitory and glutamatergic excitatory crosstalk in higher ascending projections of the auditory pathway. The GABAergic projections might serve as contrast enhancers between channels and to promote information transmission through a specific band [114].

To simulate excitatory and inhibitory projections ascending in parallel to higher processing stages we set up a lattice structure of 800 excitatory projections, interconnected by inhibitory interneurons. The synaptic strength and width of the lateral inhibition is given by a symmetric truncated Gaussian: $X \sim N(\mu, \sigma^2)$ is a normal distribution, defining the range of inhibitory interneurons.

The simulated network is based on regular spiking Izhikevich–type neurons [71]. The individual neurons thus follow coupled differential equations, where V represents the membrane potential and u is a recovery variable. Parameter a alters the temporal scale of the recovery parameter u, while parameter b influences the sensitivity of u to subthreshold fluctuations in the membrane potential. c and d define the after–spike reset. I_{input} is a sum input of the antecedent DCN model and the weighted lateral inhibition from neighboring units activated in parallel:

$$\frac{dV}{dt} = 0.04V^2 + 5V + 140 - u + I_{input} \qquad (3.1.10)$$

$$\frac{du}{dt} = a(bV - u), \qquad (3.1.11)$$

with a reset condition

$$\text{if } V \geq 30 \begin{cases} V \leftarrow c \\ u \leftarrow u + d \end{cases}, \qquad (3.1.12)$$

Simulation of a notched acoustic stimulation: In this *in–silico* experiment we analyze the neural response reliability of our combined model in answer to peripheral hyperactivity. For a high frequency tinnitus, simulated by increased spontaneous activity in a narrow band of the tonotopic frequency representation, we monitor the neural response reliability, conveyed by the coefficient of variation.

Additionally we monitor the neural mean firing rate of a "pathologic" hyperactive model responding to an arbitrary stimulus and compare the results to the models' response to a notched stimulus. We collected data from a series of notch–bandwidths ranging from 0.7 to 1 octave centered around a virtual 3 kHz "tinnitus tone". Additionally we stepwise exaggerated the frequency bands neighboring the notch. The mean firing rate is tested against the respective spontaneous activity.

3.2 Tinnitus in prosencephalic structures

3.2.1 Quantification of attention– and habituation correlates from electroenzephalographic data

Auditory evoked responses: Auditory evoked potentials (AEP) origin from activity within the auditory system in reaction to an acoustic stimulation. The AEP can be grouped, according to their latency, in early, middle and late evoked responses. The individual signal components can be allocated to specific areas of the auditory pathway [58]. The quantification of attention and habituation relies on the late response component of AEPs (i.e., ALR), in a time range from 50 up to 250 ms as envelope of the N1–P2 complex. In 1973 Hillyard could already demonstrate a dependency of the N1–P2 peak–to–peak amplitude and the subjects attentional expenditure [64]. The higher the attentional effort, the larger is the peak–to–peak amplitude difference and vice versa.

The characteristic wave form of the N1–P2 component presumably arises from the auditory cortices [58] and gives account of cognitive processes [84] and the feedback interaction with hierarchically lower areas of sensory processing, i.e., the thalamic cores [183; 53]. Fig. 3.3 illustrates the characteristic wave forms of an averaged ALR in terms of voltage fluctuations over time; the waves are named according to their polarity (vs. vertex reference) and their order of occurrence or their latency respectively.
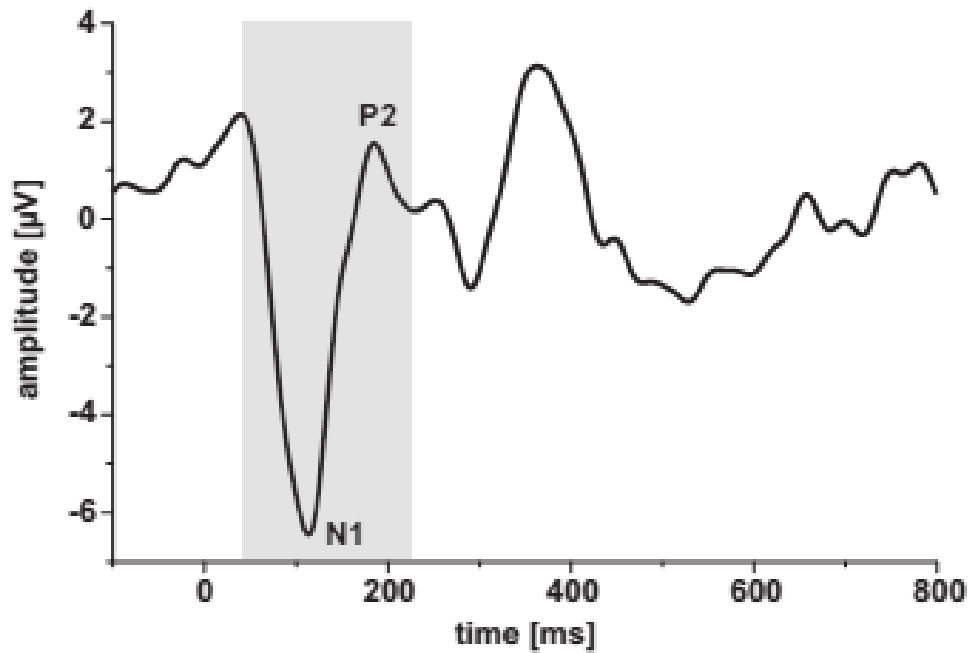

Figure 3.3: Characteristic wave forms of the averaged auditory late response as voltage fluctuations (in μV) over time. The N1–P2 complex is indicated by a light grey background and respective text labels.

As the examination of the averaged ALR results in a loss of temporal information in terms of amplitude dynamics, we focus on the processing of a series of single–sweep ALRs, which are individual responses to subsequent acoustic stimuli. Those single–sweep, or single–trial, responses can be mapped topographically and examined for the temporal dynamics of prominent traces, e.g., by the analysis of instantaneous phase changes. Fig. 3.4 illustrates topographic maps of single sweeps for states of focussed attention and for unattended stimuli. The image plots a series of single–trial responses over time, while the amplitude is color coded.
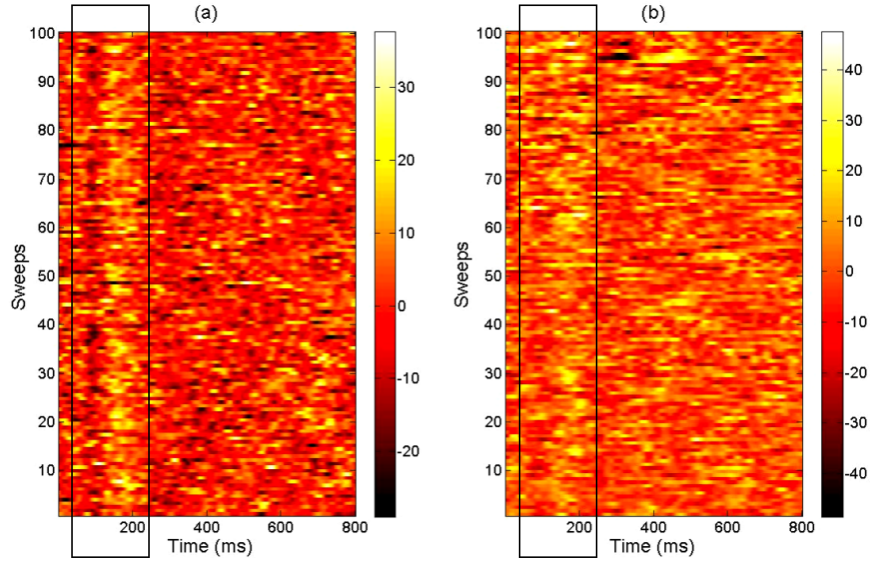
Figure 3.4: Topographic mapping of single–sweep responses. Depicted is a series of single–sweeps over time (samples); amplitude is coded by a color gradient, where dark, red colors indicate low Amplitudes (negative wave polarity) and light, yellow and white colors indicate high amplitudes (positive wave polarity). The N1–P2 complex is visible as vertical trace in the range of 100–200 ms. (a): Attended stimulus. The N1–P2 trace (black envelope) is clearly discernible in this map. (b): Unattended stimulus. The N1–P2 trace is more blurred.

Instantaneous phase stability measure: The peak–to–peak amplitude increase in the N1–P2 complex of the averaged signal in the case of attention can be interpreted to origin from a decrease of instantaneous phase jitter in the single–sweep responses. We defined a wavelet phase stability measure (WPSS) [103; 172] to monitor those attention correlates: The synchronization stability $\Gamma_{a,b}$ of a sequence χ of M ALR sweeps $\chi = \{x_m \in L^2(\mathbb{R}) : m = 1, ..., M\}$ can be defined by

$$\Gamma_{a,b}(\chi) \ := \ \frac{1}{M} \left| \sum_{m=1}^{M} e^i \text{arg}((W_\Psi x_m)(a, b)) \right|, \qquad (3.2.13)$$

where $(W_\Psi x_m)(a, b)$ is the continuous wavelet transform of the signal $x_m(t)$. $\Psi(a, b)$ indicates a wavelet with dilation–parameter a and translation–parameter b, derived from a mother wavelet Ψ [2]. This function yields a value in $[0, 1]$, where values close to 1 indicate phase locked activity, while values close to 0 indicate a uniform distribution of the instantaneous phases across all sweeps on the unit circle.
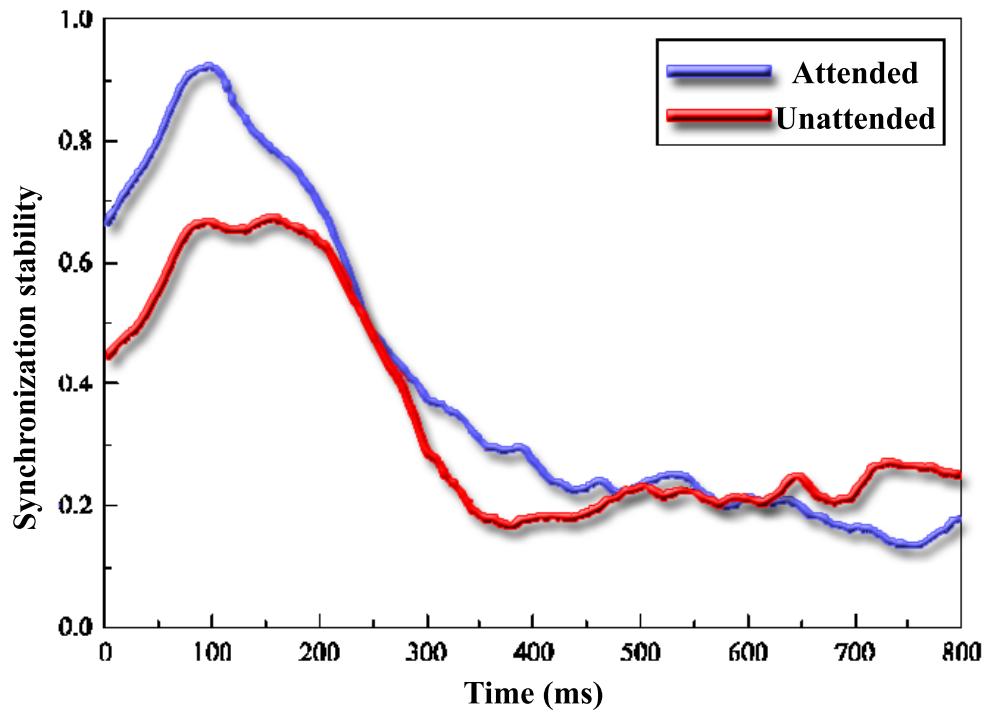
Figure 3.5: WPSS dynamics over the time–course of an ALR for focussed and non–focussed attention. The blue line depicts the attended, the red line the unattended condition. The maximum discriminability of attention correlates is given in the temporal range of the N1–P2 complex (up to 200 ms), where the attended condition features significantly reduced phase jittering.

Strauss et al could show that the phase stability in the range of the N1–P2 complex is a marker for attentional expenditure. Fig. 3.5 depicts the WPSS dynamics over the time–course of a series of single–sweep response for the attended and unattended case. Clearly visible is an amplitude shift in the temporal range of the N1–P2 complex. The phase data were extracted using the fourth derivative of a complex Gaussian as wavelet, limited to a scale parameter of 40 which corresponds to a pseudo–frequency of 6.4 Hz.

Habituation correlates: For the sake of simplicity we can define the attentional habituation as an involuntary transition from the attended state to the unattended state without changes in the stimulus properties. This transition must thus be reflected in the single–sweep dynamics. We can quantify this effect by utilizing a trial–specific coherence measure or by analyzing the von Mises concentration parameter over time. Both methods quantify the instantaneous phase inconsistencies in ERP responses over the number of successively presented stimuli:

- **Trial–to–trial wavelet coherence:** Let $(P^{\Psi,\delta}\alpha, \beta)$ be the wavelet cross spectrum between two signals α and β, where $\alpha, \beta \in L^2(\mathbb{R}), \delta \in \mathbb{R}_{>0}$. Here δ defines the window for the calculation of the wavelet coherence. For a fixed wavelet ψ with scale a and translation parameter b, the wavelet coherence $\Omega_\psi^\delta(\cdot, \cdot)$ of α and β is defined as:

$$(\Omega^{\psi,\delta}\alpha, \beta)(a,b) \;=\; \frac{|(P^{\psi,\delta}\alpha, \beta)(a,b)|}{\sqrt{(P^{\psi,\delta}\alpha, \alpha)(a,b) \; (P^{\psi,\delta}\beta, \beta)(a,b)}}. \qquad (3.2.14)$$

For a fixed wavelet ψ and smoothing parameter δ we define $(\Omega\alpha, \beta)(a,b) := (\Omega^{\psi,\delta})(a,b)$ in order to simplify the notation in the following.

Let $X = \{x_m \in L^2(\mathbb{R}) : m = 1, ..., M_0\}$ be a sequence of M_0 sweeps. We define the sweep—to–sweep time—scale coherence in X by

$$d_m^x(a,b) \;=\; (\Omega x_{m-1}, x_m)(a,b), \quad m = 2, ..., M_0 \qquad (3.2.15)$$

The coherence between single sweep in sequences is represented by a declining graph due to a decreasing coherence between two consecutive signals in the case of habituation. In order to visualize this sweep—to–sweep time–scale coherence (SSTC) decline, we make use of an analysis based on a moving average. Specifically, the moving average of the SSTC for a set X is given by the sequence

$$D_m^X(a,b) \;=\; \frac{1}{m}\sum_{n=1}^m d_n^X(a,b) \quad m = 2, ..., M_0 \qquad (3.2.16)$$

Drawback of this methodology compared to the later introduced von Mises concentration parameter is the sole comparison of neighboring single–sweeps, so there is only an oblique statement about the dynamic transition of single–sweeps over the entire duration of the experiment.

- **von Mises κ:** We extract the instantaneous phase angle θ from a narrow–band analytic signal $x_a(t) = x(t) + iH\{x(t)\}$, where $H\{x(t)\}$ is the Hilbert transform of $x(t)$, by $\theta = \arg(x_a(t))$. Here $x(t)$ is a bandpass–filtered single–sweep response to a specific stimulus.

The von Mises distribution is the cyclic pendant of the normal distribution on the unit circle and can be utilized to estimate the clustering of ERP instantaneous phase angles. The von Mises density is given by:

$$f(\theta|\mu, \kappa) = \frac{1}{2\pi I_0(\kappa)} \exp\left(\kappa \cos(\theta - \mu)\right) \qquad (3.2.17)$$

with $\theta \in [0, 2\pi)$. I_0 is the modified Bessel function of order 0. $\mu \in [0, 2\pi)$ is a measure of location, analogous to normal mean and $\kappa \geq 0$ is a measure of concentration, with $\frac{1}{\kappa}$ is analogous to the normal distributions variance σ^2. So κ values near zero indicate uniform distribution, whereas κ approaching 1 indicates perfect instantaneous phase alignment in subsequent single–sweeps $x(t)$

We can estimate the parameter κ of the von Mises distribution by utilizing an approximation to the maximum likelihood method. Let R be the resultant vector length from a set of N phase angles ϕ:

$$R = \frac{1}{N} \sum_{n=1}^{N} \exp(i\phi_n) \qquad (3.2.18)$$

The concentration parameter κ is now estimated based on R:

$$\kappa = \begin{cases} 2R + R^3 + 5R^{\frac{5}{6}} & \text{for } R < 0.53; \\ -0.4 + 1.39R + \frac{0.43}{(1-R)} & \text{for } R \geq 0.53 \text{ and } R < 0.85; \\ \frac{1}{(R^3 - 4R^2 + 3R)} & \text{for } R \geq 0.85 \end{cases} \qquad (3.2.19)$$

for a small number of N (< 15) the concentration parameter is adjusted by

$$\kappa = \begin{cases} \max(\kappa - \frac{2}{(N \kappa)}) & \text{for } \kappa < 2 \\ (N-1)^3 \frac{\kappa}{(N^3 + N)} & \text{else} \end{cases} \qquad (3.2.20)$$

For estimating the von Mises κ we use the *Circular Statistics Toolbox (Directional Statistics)* for Matlab (The MathWorks ®) by Philipp Berens [11].

Long–term habituation value h: We introduce a long–term habituation value h. Let $mx + y_0$ be a first order regression polynomial fit to resultant vector length over the number of stimuli in equation 3.2.13 or the concentration parameter κ over the number of stimuli in equation 3.2.20 . In quantitative terms, the long–term habituation value h is now defined by:

$$h = -\mu \; min\{0; \alpha\}, \tag{3.2.21}$$

where μ is a constant scaling factor. In other words, h is defined as the decrease of the WPSS or of the concentration parameter κ over the experiment and consecutive stimulation. This corresponds to a decline of selective auditory attention drawn to the stimuli.

3.2.2 Experimental study: Modality specificity of emotion–tinged stimuli

3.2.2.1 Visual domain:

Experimental setup: Subjects and stimulation: A total of 12 healthy volunteers (mean age: 25.33 y $\pm$ 4.78 y) with normal eyesight participated in our study. The volunteers were instructed to lie on a treatment couch with a horizontal 17–inch monitor at 60 cm above their heads.

Each subject was exposed to three experimental conditions in random order. The following items highlight the procedure exemplary:

- For the first condition, the subjects were told to relax and pay attention to the screen for 10 min. During this procedure, 20 different portrait–pictures of unknown people of European appearance (10 males, 10 females) with neutral face expression were presented to the volunteers in a random order. The pictures were taken from the database of Ekman & Friesen [33]. Every stimulus was presented for 750 ms; between two portraits, a fixation cross was displayed also for 750 ms (interstimulus interval (ISI)).

- After a short break, the subjects were instructed to relax and pay attention to the screen for the second condition: Again 20 different front–view portrait–pictures of unknown people with European appearance (10 males, 10 females) as of now with negative emotional face expressions (disgust, fear and/or anger) were presented to the volunteers. The procedure was the same as in the first condition, i.e., ISI=750 ms and the display of a fixation cross between successive stimuli.

- In a third condition we use a stimulus–exchange paradigm to exclude data distortion due to fatigue effects and to check for dishabituation. We presented a series of four front–view portrait–pictures of unknown people with European appearance (2 males, 2 females, Ekman & Friesen database) and neutral facial expression to the subjects. After 8 min the stimuli were exchanged for four similar looking portraits (again 2 males, 2 females). The subjects had no prior knowledge of the stimulus–exchange. The stimulus presentation followed the same setup as in the other conditions, i.e., ISI=750 ms and the display of a fixation cross between successive stimuli.

Data acquisition The visual event–related potentials were acquired by a commercially available biosignal–amplifier (g.tec USBamp, Guger Technologies Austria) for 600 s at a sampling frequency of 512 Hz. Single ERP–trials, i.e. the responses to the individual stimulus, were recorded from 5 scalp sites using Gold electrodes, placed according to the international 10–20 system (P3, PZ, P4, O1 & O2). All scalp electrodes were referenced to the vertex; the ground electrode was placed on the upper forehead. Impedances were balanced and maintained below 5 kΩ. Artifacts, defined by amplitudes over 50 μV, were removed by a threshold artefact filter.

The N170 VEP component is a member of the N1 family and ranges in latency between 156 ms and 189 ms. It is associated primarily with visual processing of human faces [84]. The topographic distribution of the N170 component for both familiar and unfamiliar faces is thus largest over the occipitotemporal regions. The N170 amplitude is significantly larger in response to faces than other natural or human–made objects [84]; reference–VEPs of the presented fixation cross did not show an N170 response.

Signal processing: Trial–to–trial wavelet coherence For signal processing we utilized the trial–to–trial wavelet coherence in this experiment. For a detailed description of the algorithm, please refer to the paragraph *"Trial–to–trial wavelet coherence"* in the methodological section 3.2.1.

3.2.2.2 Auditory domain

Subjects and stimulation ALR data were recorded from 10 voluntary, normal hearing subjects (4 female and 6 male; mean age: 30.92 y $\pm$ 3.75 y) with no history of hearing problems and a maximum hearing threshold below 15 dB(HL). Each subject was tested by an audiogram before and immediately after the experiment to foreclose post–experimental hearing impairment in response to the high–intensity stimulation. The auditory stimuli were 1kHz pure tones with a duration of 40ms and an interstimulus interval (ISI) of 1s. The auditory stimuli were presented monaurally via circumaural headphones (HDA–200, Sennheiser). The aversiveness grading of the stimulation was archieved by the presentation of two intensity levels. A 50 dB(SPL) tone was chosen as level reference, representing a neutral, irrelevant acoustic stimulation. A 100 dB(SPL) tone acts as aversive stimulus by crossing the individual discomfort level. Both stimuli were presented in a series of 800 events consecutively with 3 minutes break in between. The order of a series presentation was exchanged randomly to prevent data distortion by sensory fatigue. The intensity level was controlled by means of a programmable attenuator headphone buffer (g.PAH, g.Tec, Austria).

Data acquisition The electroencephalographic recordings were performed in a sound proof room. The EEG data activity was collected with a 24–bit biosignal amplifier (g.USBamp, g.Tec, Austria) using Ag/AgCl surface electrodes, placed at the left and right mastoid, the vertex and upper forehead. The EEG signal was sampled at 512 Hz and filtered using a digital filter (bandpass of 1 Hz–30 Hz). Trials that contained artifacts were rejected using threshold detection (amplitude ≥ 50 μV). 800 single sweep ALRs of each subject were obtained in this way.

Signal processing: Trial–to–trial wavelet coherence For signal processing we utilized the trial–to–trial wavelet coherence in this experiment. For a detailed description of the algorithm, please refer to the paragraph *"Trial–to–trial wavelet coherence"* in methodological section 3.2.1. We focus on the N1–P2 component of ALRs, due to its sensitivity to attention effects [64].

3.2.3 Numerical modeling of thalamo–cortical feedback interactions

For the simulation of attention in the processing of a simplified acoustic stimulus we adapted a neural–field model of thalamo–cortical interconnections by Rennie et al. [144; 83] to preliminary experimental results [183]. The primary model is set up of two basic modules, simulating the thalamic cores and the cortex, where the cortex is modeled as 2–dimensional surface.

The cortical module is build from excitatory pyramidal neurons (e), sprouting long range intracortical and cortico–thalamic axonal connections, and from short range inhibitory interneurons (i), indicating a Mexican hat connectivity.

The thalamic module is divided into two subdivisions, simulating the neural activity of specific sensory cores (medial geniculate body) (s) and the population activity of the thalamic reticular nucleus(r). The sensory relay nuclei project excitatory to the cortex, innervating the TRN by axon collaterals. The TRN projects inhibitory fibres to the MGB.

In modeling terms the projection paths are expressed as gain loops. The loop G1 is an inhibitory feedback loop. The MGB is conveying excitatory input to the cortex, while receiving inhibitory cortical input via a TRN relay on the back–projection. The G2 gain loop emphasizes the MGBs role as direct relay center of subthalamic information to the AC. Via G2 the MGB sends excitatory input to the cortex and receives excitatory input on the back–projection. The third gain loop G3 is an intrathalamic loop. The MGB projects excitatory to the TRN and receives inhibitory input on the back–projection.

The net effect P, as a function of range and time, of one or more neural populations (a) on the activity of a target population (b) is defined by the number of synapses

N_{ab} targeting population (b), where s_{ab} denotes the synaptic strength. ϕ_a is the activity rate of the source population (a):

$$P_{ab}(r,t) = \sum_a \nu_{ab}\ \phi_a(r,t), \quad \text{with}\quad \nu_{ab} \equiv N_{ab}\ s_{ab} \qquad (3.2.22)$$

As the dendritic passive electric properties impose a low–pass filtering on the signal, thus the membrane voltage $V(r,t)$ can be approximated by the convolution of the net activity effect $P(r,t)$ with a convolution kernel $L(t \geq 0)$, given by the neural rise and decay time constants ζ and ϖ:

$$L(t) = \frac{\zeta\ \varpi}{\varpi - \zeta}\ e^{-\zeta t}\ e^{-\varpi t} \qquad (3.2.23)$$

$$V(r,t) = (P(r,\cdot) * L)(t),\ t \in \mathbb{R} \qquad (3.2.24)$$

where $*$ is the symbol of the convolution integral. The response of a single neuron to a shift in the membrane voltage V can be approximated by the Heaviside function $\mathcal{H}$. Yet as the open state of a set of sodium channels follows a probability density function [65], the group–response function is sigmoidal. The change of the firing rate $Q(r,t)$ in response to a membrane voltage V shift is given by the maximum firing rate of the neural population Q_{max} and the mean of the threshold distribution relative to the resting potential θ. The constant $C = \pi/\sqrt{3}$ is chosen, so that the standard deviation of the derivative is equal to σ.

$$Q(r,t) = \frac{Q_{max}}{1 + e^{-C(V-\theta)/\sigma}}, \qquad (3.2.25)$$

As the change in membrane voltage δV is smaller than σ, Rennie and Robinson used a linear approximation to 3.2.25. $Q^{(0)}$ denotes the resting state activity, $V^{(0)}$ the resting potential. Thus the response function to small perturbations to the resting state becomes:

$$Q(r,t) \approx Q^{(0)} + \rho[V(r,t) - V^{(0)}], \qquad (3.2.26)$$

where

$$\rho \equiv \frac{dQ}{dV} = \frac{C\ Q}{\sigma}\left(1 - \frac{Q}{Q_{max}}\right), \qquad (3.2.27)$$

Using 3.2.27, the relation of activity changes of the target neuron population (b) in response to activity changes of the source population (a) can be described by defining the linear gain function G_{ab}:

$$G_{ab} = \frac{\Delta Q_a}{\Delta Q_b} = \rho_b N_{ab} s_a, \tag{3.2.28}$$

The serial connection of neural populations can be written as the product of their individual gain functions $G_{ab} G_{bc} = G_{abc}$.

The propagation of the firing rate Q can be approximated by a damped wave equation, where γ is the damping rate, given by the quotient of the axonal propagation velocity v and the mean axonal range r. Cortical inhibitory neurons (i), as well as intrathalamic projections (s,r) and sensory projections (n) have short–ranged axonal appendages, thus $r_{i,s,r,n} \approx 0$ and $D_{i,s,r,n} \approx 1$. It is

$$D = \frac{1}{\gamma^2} \left[\frac{\partial^2}{\partial t^2} + 2\gamma \frac{\partial}{\partial t} + \gamma^2 - v^2 \nabla^2 \right], \tag{3.2.29}$$

$$Q(r,t) = D \ \phi(r,t) \tag{3.2.30}$$

The ERP signal is dominantly generated by the postsynaptic potentials of cortical pyramidal cells [84] and thus directly dependent on ϕ_e. It is necessary to define a transfer function, relating the activity rate of the sensory neurons ϕ_n to the activity rate of the cortical pyramidal neurons ϕ_e. To obtain this transfer function the equations 3.2.22 to 3.2.30 are Fourier transformed. Assuming a delay of $t_0/2$ for a signal traveling from thalamus to cortex (or vice versa) we obtain for particular neural populations. Let k be the wavenumber $1/\lambda$ and ω is the angular frequency:

$$P_e(k,\omega) = \nu_{ee}\phi_e + \nu_{ei}\phi_i + \nu_{es}\phi_s e^{i\omega t_0/2}, \tag{3.2.31}$$

$$P_i(k,\omega) = \nu_{ie}\phi_e + \nu_{ii}\phi_i + \nu_{is}\phi_s e^{i\omega t_0/2}, \tag{3.2.32}$$

$$P_s(k,\omega) = \nu_{se}\phi_e e^{i\omega t_0/2} + \nu_{sr}\phi r + \nu_{sn}\phi n, \tag{3.2.33}$$

$$P_r(k,\omega) = \nu_{re}\phi_e e^{i\omega t_0/2} + \nu_{rs}\phi s, \tag{3.2.34}$$

$$L(\omega) = (1 - i\omega/\zeta)^{-1}(1 - i\omega/\varpi)^{-1}, \tag{3.2.35}$$

$$V(k,\omega) = L(\omega) \ P(k,\omega), \tag{3.2.36}$$

$$Q(k,\omega) = \rho \ V(k,\omega), \tag{3.2.37}$$

$$D(k,\omega) \ \phi(k,\omega) = Q(k,\omega), \tag{3.2.38}$$

$$D_e(k,\omega) = k^2 \ r^2 + (1 - i\omega/\gamma)^2 \tag{3.2.39}$$

$$D_i = D_s = D_r = D_n = 1, \tag{3.2.40}$$

Assuming an uniform all–to–all connectivity in the cortex, the impulse response for the model is given by:

$$I_{TC} = \frac{e^{i\omega t_0/2} \ L^2 \ G_{esn}}{1 - L^2 \ G_{srs}}, \tag{3.2.41}$$

modulated by cortical feedback loops

$$I_{CT} = D_e(1 - L \ G_{ei}) - L \ G_{ee}, \tag{3.2.42}$$

$$I_{CTC} = \frac{e^{i\omega t_0/2} \ (L^2 \ G_{ese} + L^3 \ G_{esre})}{1 - L^2 \ G_{srs}}. \tag{3.2.43}$$

Thus the transfer function $T(k,\omega)$ is

$$T(k,\omega) = \frac{\phi_e(k,\omega)}{\phi_n(k,\omega)} = \frac{I_{TC}}{I_{CT} + I_{CTC}}, \tag{3.2.44}$$

The stimulus for the simulation of evoked potentials can be approximated as Gaussian in space (thus in frequency) and time (see section 5.1); with t_s is the duration of the stimulus, t_{os} denotes the transmission delay from the subthalamic input to the auditory cortex; r_s is the spatial width of the stimulus at the cortex, r_{os} indicates the spatial distance of the stimulus center and the point of measurement. This simplification of the sensory input to the thalamus is also chosen to approximate the effects of a volume conduction for low frequencies [144]

$$\phi_n(r,t) = \frac{e^{-\frac{1}{2}\left(\frac{t-t_{os}}{t_s}\right)^2} \ e^{-\left(\frac{r-r_{os}}{r_s}\right)^2}}{t_s\sqrt{2\pi}} \frac{}{\pi r_s^2}, \tag{3.2.45}$$

respectively in the Fourier domain

$$\phi_n(k,\omega) = e^{\frac{1}{2}\omega^2 t_s^2} e^{i\omega t_{os}} e^{-\left(\frac{kr_s}{2}\right)^2} e^{ik\ r_{os}},\tag{3.2.46}$$

In consequence the simulated evoked response is generated by the inverse Fourier transform the product of the equations 3.2.44 and 3.2.46. In the spatial inverse Fourier transform we find:

$$R(r,\omega) \;=\; \frac{1}{2\pi}\ \int_0^\infty k\frac{\phi_e(k,\omega)}{\phi_n(k,\omega)} e^{-\frac{k\ r_s}{2}^2}\ J_0(k|r-r_{os}|)\ dk,\tag{3.2.47}$$

For a spatially delta–like stimulus with $r_s \to 0$ we find an analytic solution, where K_0 is a modified Bessel function of the second kind:

$$R(r,\omega) \;=\; \frac{I_{TC}K_0(q|r-r_{os}|)}{2\pi r_e^2(1\ -\ L\ G_{ei})}\tag{3.2.48}$$

q is given by:

$$q \;=\; \frac{1}{r_e}\ \sqrt{\left(1\ -\ \frac{i\omega}{\gamma}\right)^2\ -\ \frac{L\ G_{ee}+I_{CTC}}{1\ -\ L\ G_{ei}}}\tag{3.2.49}$$

The evoked response is now calculated by an inverse Fourier transform in the time domain, with N is a normalization factor to compensate for the unknown stimulus amplitude, for the ration of scalp to cortical voltages and for an unknown gain from peripheral neurons to cortical neurons:

$$R(r,t) \;=\; \frac{N}{2\pi}\int R(r,\omega)e^{-\frac{1}{2}(\omega t_s)^2}\ e^{i\omega t_{os}}\ e^{-i\omega t}d\omega\tag{3.2.50}$$

The simulated ERPs are processed with exactly the same methodologies as the experimentally acquired ERPs. A series of simulated ERPs can be topographically mapped in the same way as the segmented single sweep respones. Please refer to section 3.2.1 for a detailed description of the methodologies used to extract attention– and habituation correlates from simulated and measured ERPs.

3.2.4 Numerical modeling of a hippocampal comparator

Motivation: As described in section 3.2.3 a framework of traveling spike fields in a feedback model of thalamocortical projections is used to simulate auditory evoked responses. This model is able to simulate ERP single sweeps for a 2D–Gaussian simplified stimulus function and a given thalamocortical transfer function, representing gain and feedback properties [183]. In this model a state of focused attention can be described by an increase of the thalamocortical gain. Attention is considered to activate corticofugal projections, activating specific and unspecific thalamic cores in parallel, resulting in an increase of the thalamo–cortical gain G1 (Fig. 3.7, illustration on the right). Unspecific thalamic nuclei, in particular the TRN are considered to play an important role in the focusing of selective attention [25; 111; 199]. An increase in cortical neural reactivity, as implemented in the model by a raise in the thalamo–cortical gain function, predicts a higher regularity of subsequent evoked potentials. We hypothesize that this effect is a crucial measure for attention [103]. Experimental results on auditory ERPs in attentive and inattentive states already confirmed predictions of this in–silico model [180].

Unfortunately the model incorporates no mechanism for the simulation of attention dynamics. So the attention shift caused by habituation could not be modeled.

Physiologic background and structural simplification: The following proposal of a hippocampal comparator model is a modular expansion of the model for the simulation of evoked responses and is based on the physiological work of Vinogradova [186]. A reset of attention networks is likely to result in a shift in the neural firing phase of the systems involved, resulting in turn in a higher synchronization of neural activity in the attended stream in hierarchical higher stages of sensory processing. Yet in the hippocampus, synchronization of neural activity could result in habituation, in terms of a stimulus–repetition dependent reduction of the CA1 (Cornu Ammonis 1) activity. This habituation effect can be prevented or reverted by a disruption of the synchronicity in hippocampal input structures [186]. Our model of a hippocampal comparator function consists of four functional elements, each representing discrete anatomical structures. The medial septum diagonal band of broca (MSDB) and the Fascia Dentata (FD) subunits serve as modules for the formation and evolution of the neural stimulus representation by feature extraction methods. While MSDB activity represents the incoming perceptual stream,

yet stripped of higher content, FD activity can be seen to represent the degree of familiarity, i.e., preprocessed sensory information. MSDB and FD form two inputs to a hypothetical comparator unit CA3 (Cornu Ammonis 3), which on its part is controlling a valve–like element CA1. The primary input to the CA1 unit origins from a cortical element (entorhinal cortex) via the perforant pathway (PP). See Fig. 3.7 for a symbolic model representation. As long as the CA3 maintains its tonic activity, the integration of cortical signals in CA1 is impeded, as activity the Schaeffer's collaterals can block the integration of cortical signals from PP to CA1 neurons by affecting inhibitory neurons, or by shunting the signal propagation in apical dendrites. In this way CA3 controls the information transmission from cortical elements to the thalamus via CA1. A transient reduction of CA3 pyramidal activity (in response to a novel stimulus: see [186]), as well as the disconnection of the Schaeffer's collaterals results in disappearance of habituation in its CA1 target structures. Reinstating the tonic CA3 activity by synchronization of both input layers, causes a shunting of CA1 information transmission.

Well documented is the influence of the amygdala on the firing behaviour of the hippocampus, in particular on the dentate gyrus (FD) [70; 163], effectively disrupting the neural synchronisation processes. This limbic influence hints towards the assumption, that increased limbic influence causes an extended integration of cortical input in the CA1 and an accordingly prolonged boost of gains in the thalamo–cortical projections via the mammillothalamic tract.

Model implementation: To generate theta–nested gamma oscillations, as seen in [186], we set up a simple hippocampal unit network model, based on the work of Kopell et al. [89]. We used Izhikevic–type neuron models [71] to simulate Pyramidal cells (Pyr), fast spiking inhibitory interneurons (FS) and regular spiking interneurons (RS). $V \in \mathbb{R}$ and $u \in \mathbb{R}^+$ represent the membrane voltage and recovery variable respectively. Here u accounts for the pysiological repolarization by inhibitory feedback to v and $c \in \mathbb{R}$ represents the hyperpolarized afterspike potential. The parameters a,b and $d \in \mathbb{R}^+$ directly affect the spiking behaviour and can be utilized to adapt the simulation to a set of neuron subtypes. Parameter a describes the time–scale of the recovery variable u; b indicates the sensitivity of u to fluctuations in the membrane voltage V. Parameter d describes an after–spike reset of the recovery variable u. Izhikevich–type neurons are then given by:

$$\frac{dV}{dt} = 0.04V^2 + 5V + 140 - u + I \tag{3.2.51}$$

$$\frac{du}{dt} = a(bV - u) \tag{3.2.52}$$

$$if v \geq 30 \begin{cases} v \leftarrow c \\ u \leftarrow u + d \end{cases} \tag{3.2.53}$$

All parameters are adapted for the simulation of regular spiking principal cells (Pyr) and slow spiking inhibitory interneurons, as well as for the simulation of fast spiking cells of the stratum oriens–lacunosum moleculare (OLM). Table 3.2.4 summarizes the model parameters used in the simulation. The reciprocal influence is simulated, maintaining constant synaptic strengths at ratios given in [89].

Table 3.1: Simulation parameters for Izhikevich–type neurons, for different neuron types, taken from [71]

Neuron type	V	u	c	a	b	d
Principal neuron	-65	0.2	-65	0.02	0.2	8
Fast spiking interneuron	-65	0.2	-65	0.1	0.2	2
Regular spiking interneuron	-65	0.2	-65	0.02	0.2	8

The neuron subtypes form a complex feedback network with the following characteristics in the simulation. The principal neurons excert excitatory influence on both types of interneurons, receiving inhibitory feedback from fast and regular spiking interneurons in turn. Regular spiking interneurons additionally project to the fast spiking cells of the OLM and form a inhibitory feedback loop to neurons of its own type. The OLM neurons provide additional inhibitory input to regular spiking interneurons. Figure 3.6 illustrates the basic composition of the model:

See figure 4.19 for an illustration of the spiking activity of this unit model. To achieve a phase precession we utilized a decrease the simulated cholinergic input from the MSDB. Please see [131] and figure 4.19 for detailed information and modeling results on the influence of decremental cholinergic input across multiple scales. To reduce the model complexity we approximate the nested gamma–theta input streams into CA3 by two oscillating functions, expressing a theta–band potential U(t). Here T_0 is the base–period of the gamma–band oscillation and d is a constant in $\mathbb{R}^+$ describing the recruiting of CA3 neurons in time. Θ is a constant in $\mathbb{R}$ rep-
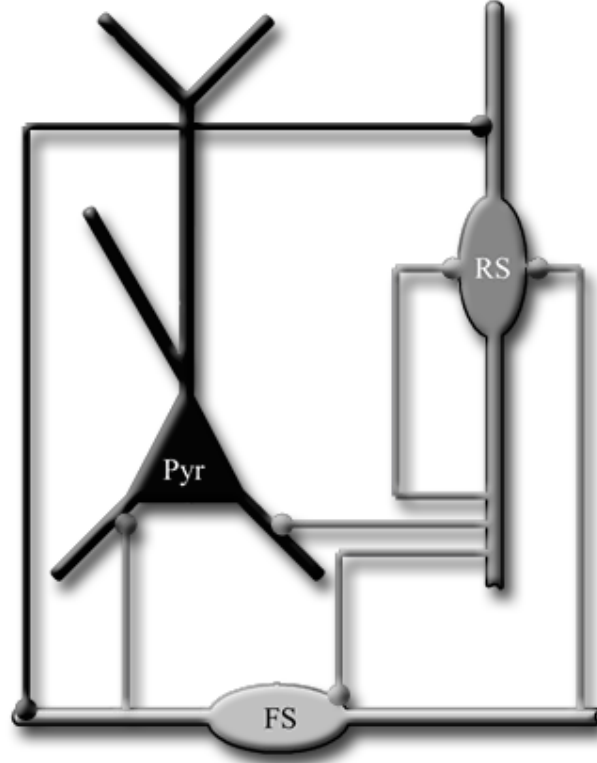
Figure 3.6: Conceptual circuitry of a functional hippocampal unit producing theta–nested gamma oscillations. Pyr indicates principal pyramidal cells, FS denotes fast spiking interneurons of the stratum oriens–lacunosum moleculare. RS represents regular spiking interneurons. Excitatory connections are illustrated in black, inhibitory projections in grey color.

resenting a bursting threshold. Let A_m, A_{burst} and A_l be constants in $\mathbb{R}^+$ denoting amplitudes, while ϕ_1 is a constant in $\mathbb{R}^+$ representing a phase displacement. Here $\varsigma(t)$ is a function in $\mathbb{R}$ acting as a slope–factor governing the evolving decrease in firing length due to sensory habituation on the cellular level [186].

$$U(t) \;=\; A_m \;+\; \frac{A_I}{1 + e^{t\varsigma(t)}} \sin(\omega t \;+\; \phi), \qquad (3.2.54)$$

merged with a superimposed high frequency burst spiking, aligned to theta–oscillation phase ϕ_1

$$O_{burst}(t) \;=\; \sum_{k=-\infty}^{\infty} A_{burst}\, e^{(-dt)(t-kT_0)}, \;\; \text{with } U_{burst}(t) = \begin{cases} O_{burst}(t) \;\geq\; \Theta \\ 0 \text{ else} \end{cases}.$$

$$(3.2.55)$$

Attentional long–term Habituation on the large scale level of ERPs is achieved by the synchronization of MSDB and FD bursting. As we describe the inputs to CA3 as coupled oscillators, the phasic behaviour of FD theta in relation to the MSDB oscillations can be approximated by Adler's equation, in which $\Delta\phi$ is a function in time, describing the phase difference of both input structures; $\Delta\omega$ is a constant in $\mathbb{R}$, denoting the difference in the respective angular velocities. The factor $\epsilon(n)$ indicates the coupling strength of both oscillators. $\epsilon(n)$ is simplified to be a linear function of n in $\mathbb{R}$, where n is the number of successively presented stimuli. In–vivo, ϵ might follow a non–linear function. For a series of stimuli and given physiological boundary conditions, the phase difference $\Delta\phi$ decreases with the number of presented stimuli, indicating a synchronization of the neural activity in CA3 [186].:

$$\frac{d\Delta\phi}{dt} \;=\; \Delta\omega \;+\; \epsilon(n)\;\sin(\Delta\phi), \tag{3.2.56}$$

As long as CA3 neurons are not prerecruited by FD projections, i.e. a synchronization of both input channels, they will react to MSDB input by a suppression of their tonic firing. In future this state is referred as reaction to novelty. In terms of modeling: The FD input imprints a response threshold on the CA3 subunit for a given timeframe defined by the decline of the potential d_{fd}. As long as the response threshold in CA3 is not higher than a given value it will react to MSDB input by a suppression of its tonic firing, putting the CA1 element into a receptive state. During this receptive state the CA1 subunit integrates the input from the EC. If a determined number of spikes $\Theta_{EC\to CA1}$ arrives in a theta-–band window the CA1 element reacts with a single action potential. The firing rate of CA1 $F_n^{CA1}(t)$ is given by

$$F_n^{CA1}(t) \;=\; \begin{cases} 1 \; if \xi_n(t) \\ 0 \; \text{otherwise} \end{cases}, \tag{3.2.57}$$

with d_{EC} denoting a single spike of a train of spikes originating from the EC. Let $\eta \in \{0, 1, 2, ..., \frac{2T}{\omega}\}$, where T denotes the duration of the CA3 reaction to novelty and $t \in \mathbb{R}_{\geq 0}$

$$\xi_n(t) \;=\; \sum_{\chi_n(t)}^{\chi_{n+1}(t)} \delta_{EC}(t). \tag{3.2.58}$$

We define a natural firing frequency of the CA1 neurons

$$f \;=\; \frac{\omega_{nat}}{2\pi} \tag{3.2.59}$$

with

$$W_{nat}(t) \;=\; A_i \, \sin(\omega_{nat}t \,+\, \phi_3) \tag{3.2.60}$$

in the theta band by by calculating a time-–window for the integration of incoming spikes. Upper and lower limit of every time window is given by the zeroes of a theta-–frequency oscillation

$$\chi_n(t) \;=\; \frac{\eta}{2\omega_i} \,-\, \phi_3 \tag{3.2.61}$$

Limbic activity, especially the modulation of the activity in the PP/FD pathway [98] can be modeled as additional driving force on the synchronizing oscillators, effectively preventing the synchronization and thus habituation. This is due to the limitation that the formation of stable steady states in three coupled oscillators strongly depends on small values of intrinsic frequency detuning [161].

In the case of habituation we gain an approximate sigmoidal function of spiking duration over the number of presented stimuli. We utilize this sigmoidal to modulate the gain loop G1 of the thalamo–cortical model, presented in section 3.2.3.
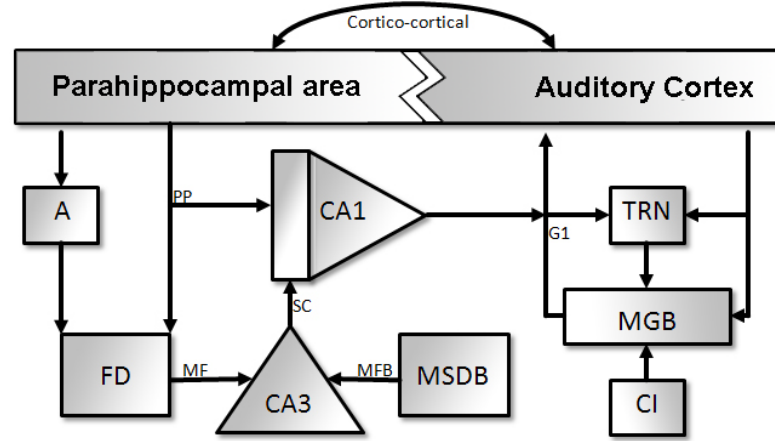
Figure 3.7: Descriptive illustration of the complete model. Left side depicts the functional modules of a hippocampal comparator: Medial septum and diagonal band of Broca (MSDB) projects via the medial forebrain bundle (MFB) to the Cornu Ammonis 3 (CA3). The dentate gyrus (FD) receives input from the parahippocampal area via the perforant pathway (PP) and from the amydgala (A). Its projections via mossy fibres (MF) form the second input to CA3. Via Schaeffer's collaterals (SC) the CA3 regulates a valve–like element CA1, which integrates PP activity and conveys information to the thalamus. The right side illustrates the thalamo–cortical attention module, and its subunits: The inferior colliculus (IC) is the input module to the specific thalamic relay module MGB. TRN is the thalamic reticular nucleus. Those subunits are interconnected by three feedback gain loops, from which only G1 is highlighted.

3.2.5 Experimental study: Habituation across different grades of severity in tinnitus

Experimental setup: Subjects and stimulation: ALR signals were recorded from patients of the MediClin Bosenberg Clinics (18 subjects, 5 female/13 male, mean–age 53.83 ± 5.68 y, and tinnitus tone average 5.11 ± 1.53 kHz) with a moderate to severe hearing loss. The grade of hearing impairment was defined by the pure tone average (PTA) of the frequencies 0.5 kHz, 1 kHz, 2 kHz, 4 kHz according to the recommendation of the British Society of Audiology (see mean PTA Fig. 4.16). According to the definition of the European Commission, a PTA of 20 dB Hearing Level (HL) or less is classified as normal hearing sensitivity, a mild hearing loss is defined with thresholds in the range of 21 to 39 dB(HL) and a moderate hearing loss is defined as a PTA from 40 to 69 dB(HL). Hearing ability was checked by an audiogram carried out before the experiments. After a detailed explanation of the

procedure, all subjects signed a consent form. The study protocol was approved by the Ethic Committee of the relevant Medical Association. The subjects were divided into two groups of tinnitus severity according to the mini–TQ12 tinnitus questionnaire by [63]. Decompensated group individually scored 16 or more points (grade IV); compensated group was defined by an individual score of less than 13 (grade I and II). The time for one complete experiment was approximately 40 min including time for preparation of the subject and electrodes placement. Ag/AgCl electrodes (Schwarzer GmbH, Germany) were attached as follows: ipsilateral to the stimulus at the corresponding mastoid (A1 or A2), common reference at the vertex (Cz), and ground at the upper forehead (Fpz). The electrode labels are according to the standard 10–20 system. Impedances were maintained below 5 kΩ in all measurements. The subjects were instructed to lie down in an acoustically insulated room trying to remain quiet, with the eyes closed. Subsequently, ALRs were obtained using a series of 750 1 kHz pure tone transients of 40 ms with an inter-stimulus interval (ISI) of 750 ms. A second set of ALRs was recorded with 40 ms transients (ISI 750 ms) in a frequency that fitted the tinnitus tone in each individual case. The stimuli were calibrated according to [37; 38; 142] by acquiring the peak equivalent (pe) sound pressure level (SPL). Each stimulation file was in parallel calculated with a trigger signal needed for further segmentation of the electroencephalographic (EEG) data. After calibration, the intensity level of all stimulation files was set to 65 dB pe SPL. A total of 600 sweeps, i.e., the response to an individual stimulus, free from amplitude artifacts (threshold detection of $> 50\ \mu$V) were considered for data processing

Experimental setup: Data acquisition: A computer controlled the presentation and intensity the level of the tone bursts and the acquisition of the EEG activity. The EEG data activity was collected with a 24–bit biosignal amplifier (g.USBamp, g.Tec, Austria), using a sampling frequency of 512 Hz, and a FIR bandpass filter with low and high cutoff frequencies of 1 and 30 Hz, respectively. The intensity level was controlled by means of a programmable attenuator headphone buffer (g.PAH, g.Tec, Austria). Each sound file was generated together with its respective trigger signal. The audio channel that corresponded to the stimuli was connected to the attenuator and afterwards delivered to the subject via circumaural headphones (HDA–200, Sennheiser). The trigger channel was connected to a trigger conditioner box (g.Trigbox, g.Tec) which adapted the voltage of the trigger signal in order to be acquired by the biosignal amplifier. The acquisition-processing program and

all further post–processing were achieved using tailor-made software for scientific computing (The MathWorks Inc., USA).

Signal processing: We use the von Mises concentration parameter κ as estimator for the habituation correlates. In this section we utilize κ to analyze the clustering of the instantaneous phase in the time interval of 87 ms to 127 ms (samples 45 to 65), corresponding to the ALR N1 component, for averaged ALR responses of 50 sweeps each. After data segmentation into single sweeps we obtain data matrices in which each row represents one averaged trial block and columns correspond to the time–sampling.

The methodology to estimate the von Mises κ is described in detail in section 3.2.1.

4 Results

4.1 Tinnitus in the peripheral hearing path

To ensure the proper functioning of our DCN model we started with the generation of response maps. In these illustrations the firing rate of the DCN principal cells is plotted over the stimulus intensity in dB(SPL) and the tonotopic best–frequency distribution of the DCN model. We started with the simulation of four pure tone stimulations in increasing frequencies of $2.5, 5, 7.5$ and 10 kHz in the range of 0 to 100 dB(SPL) each.
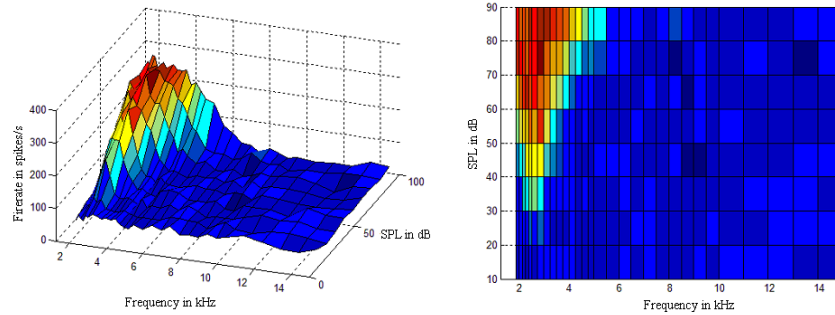
Figure 4.1: 3D and 2D illustration of a mean response map of the DCN model principal cells to a constant stimulus of 2.5 kHz over a range of 0 to 100 dB(SPL). Plotted is the average firing rate of the simulated DCN principal cells over stimulus intensity in dB(SPL) and over the principal neurons best–frequency. The number of neurons and the stepwise increase of the intensity level were reduced to enhance the illustrations intelligibleness.
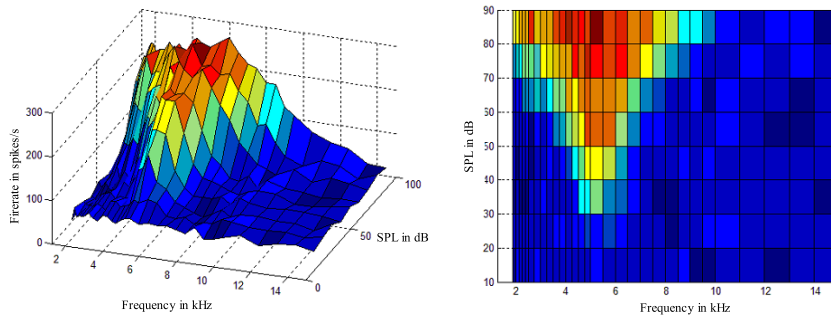
Figure 4.2: 3D and 2D illustration of a mean response map of the DCN model principal cells to a constant stimulus of 5 kHz over a range of 0 to 100 dB(SPL). Plotted is the average firing rate of the simulated DCN principal cells over stimulus intensity in dB(SPL) and over the principal neurons best–frequency. The number of neurons and the stepwise increase of the intensity level were reduced to enhance the illustrations intelligibleness.
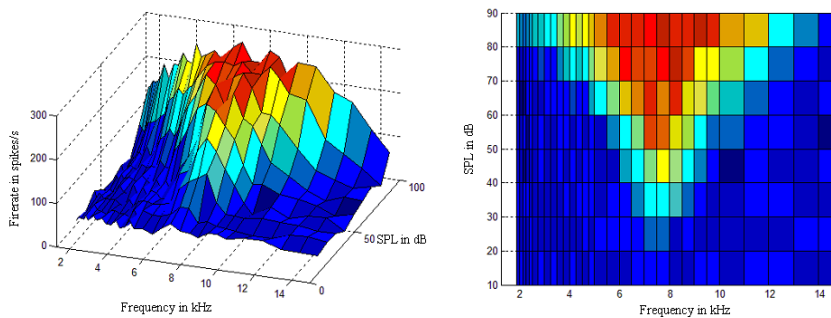
Figure 4.3: 3D and 2D illustration of a mean response map of the DCN model principal cells to a constant stimulus of 7.5 kHz over a range of 0 to 100 dB(SPL). Plotted is the average firing rate of the simulated DCN principal cells over stimulus intensity in dB(SPL) and over the principal neurons best–frequency. The number of neurons and the stepwise increase of the intensity level were reduced to enhance the illustrations intelligibleness.
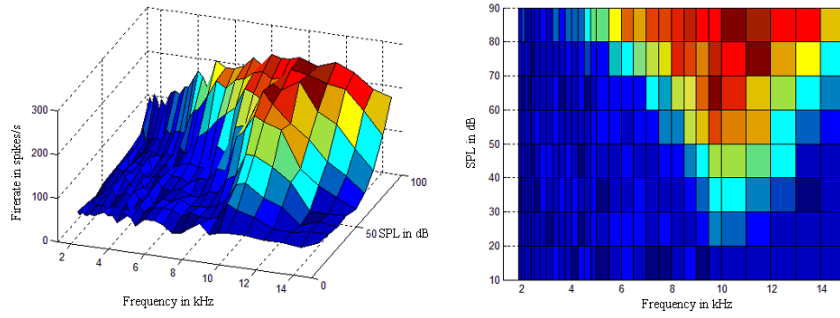
Figure 4.4: 3D and 2D illustration of a mean response map of the DCN model principal cells to a constant stimulus of 10 kHz over a range of 0 to 100 dB(SPL). Plotted is the average firing rate of the simulated DCN principal cells over stimulus intensity in dB(SPL) and over the principal neurons best–frequency. The number of neurons and the stepwise increase of the intensity level were reduced to enhance the illustrations intelligibleness.

For the sake of completeness an exemplary 2–dimensional illustration of the principal neuron firing rates across all 800 simulated neurons is inserted. The simulated stimulus was a 5 kHz pure tone. Fig. 4.5 illustrates the DCN principal cell responses for nine different stimulus intensities between 0 and 100 dB(SPL) in ascending order in spikes per second over a frequency range of 1–20 kHz. The bandwidth of characteristic responses broadens with rising stimulus intensity, hinting towards a reduction of frequency discrimination ability with increasing stimulus intensity.

The firing rate of neurons in response to a pure tone approximates a Gaussian across activated frequencies, with standard deviation σ increasing with the stimulus intensity. For high stimulus intensities this spatial Gaussian is distorted in the direction of high frequencies, giving rise to a positive skewness. We utilized a 2D–Gaussian (across frequency and time) as input into our model of thalamo–cortical interaction, see equation 3.2.45, assuming a moderate stimulus intensity.
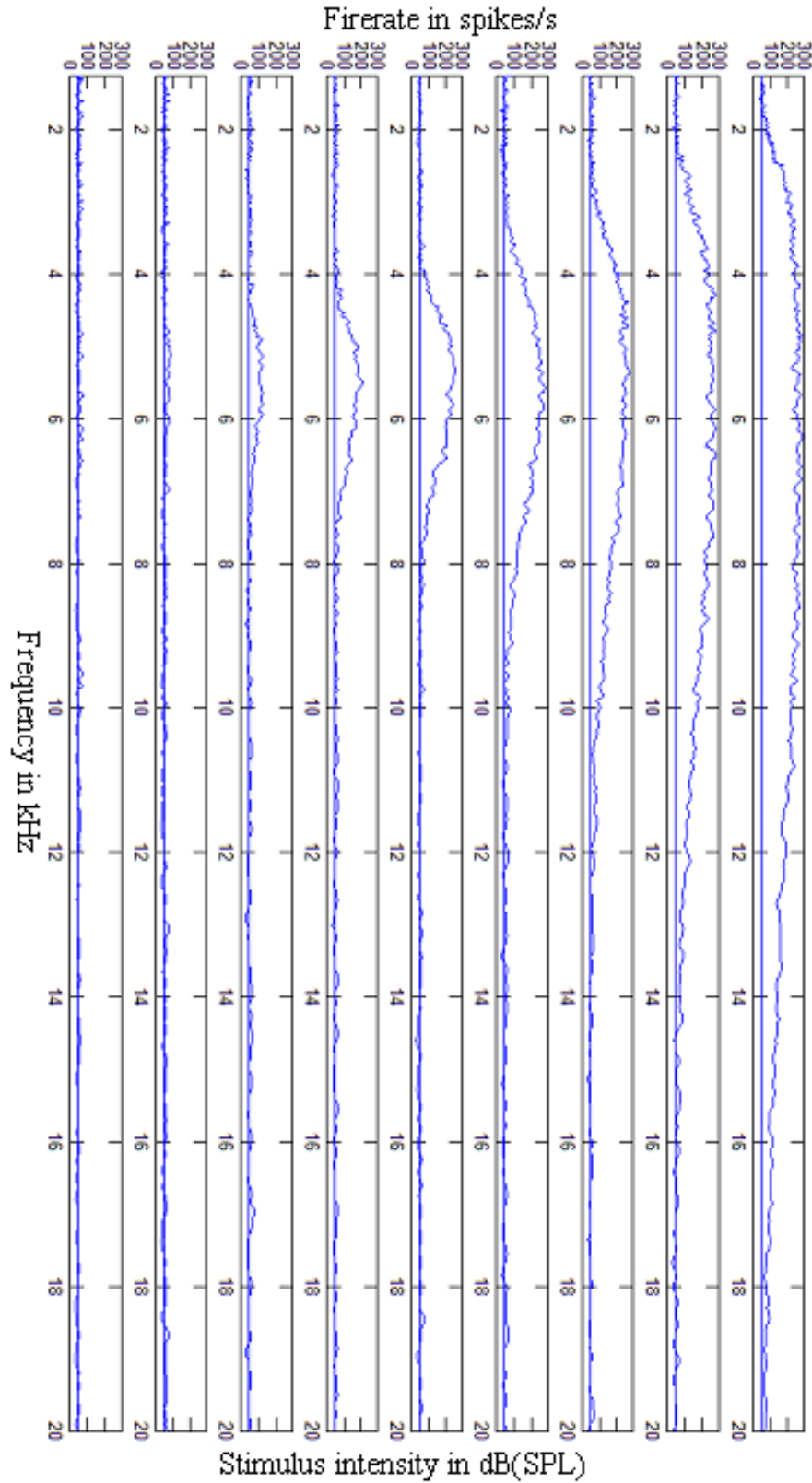
Figure 4.5: Mean response map of the DCN model principal cells to a stimulus of 5 kHz across 9 different stimulus intensities ranging from 0 to 100 dB(SPL) (bottom to top of illustration). Plotted for every intensity is the average firing rate of the simulated DCN the 800 principal neurons best–frequency.

We fed the output of the simulated AN and DCN model in the model of ascending lateral inhibitory networks as described in section 3.1.3 to estimate changes in the neural spiking response. The hyperactivity in the AN and DCN model, generated by the simulated tinnitus, has a direct influence on the neural response reliability (RR). We estimate the coefficient of variation (CoV), given by $\frac{1}{\lambda}$ with λ is the mean of the underlying Poisson distribution, to find a decrease with increasing spontaneous activity. This effect is additionally bolstered by the lateral information–transmission component in the ascending pathway.
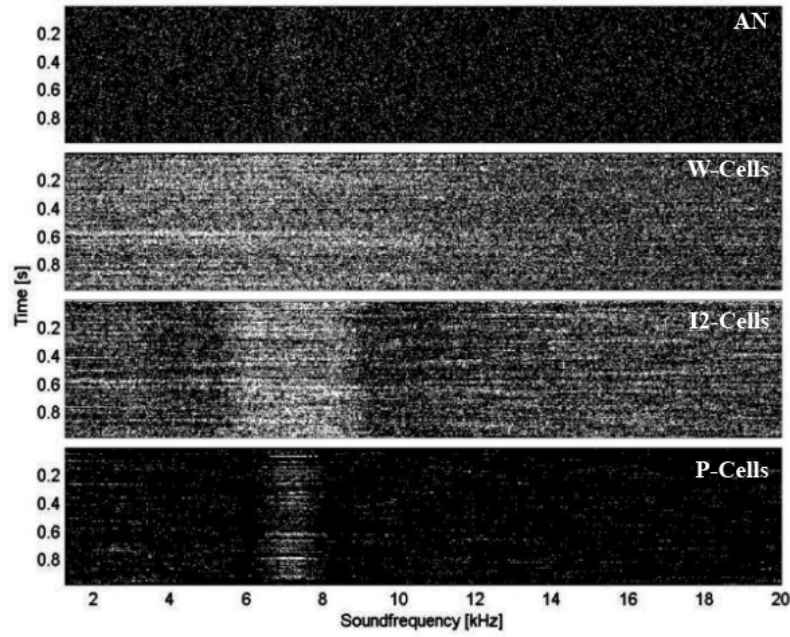
Figure 4.6: Spiking pattern of levels I (AN) to IV (P-Cells) in the DCN model. Depicted is the neural activity over time and a virtual tonotopy ranging from 1 to 20 kHz. Every dot represents a single AP. The highly regular and synchronized firing in the P-Cell layer is triggered by a hyperactivity in the AN in the range of 7 kHz. The effect of the wideband inhibitory cells (W-Cells) induces an increased contrast between hyperactive and spontaneous active areas by reducing the activity in frequency regions bordering the hyperactivity.

In the DCN model we can already identify an increase in the neural RR due to lateral inhibition effects. Fig. 4.6 illustrates exemplary the self–ordering of neural spiking in the DCN. Emanating from a hyperactivity in the AN in the frequency range of 7 kHz, the principal cells of the DCN react in a synchronized and regular

firing pattern. The tonotopy of hyperactivity and spontaneous firing is preserved across every level of the DCN model.

We conducted two experiments using a notched stimulus as described in [130] and in section 2.3.9. In the first experiment we document the function of CoV over a simulated tonotopy of 800 neurons, in response to pathologic peripheral hyperactivity and responding to a notched stimulus. Fig. 4.7 illustrates the neural RR in the pathologic case of peripheral hyperactivity (grey line) and for a Gaussian–shaped stimulus, with the notch bandwidth centered at the frequency range of the simulated tinnitus tone (black line). The pathologic case exhibits an increased neural RR, which can be perturbed by a tailor–made notched stimulus.
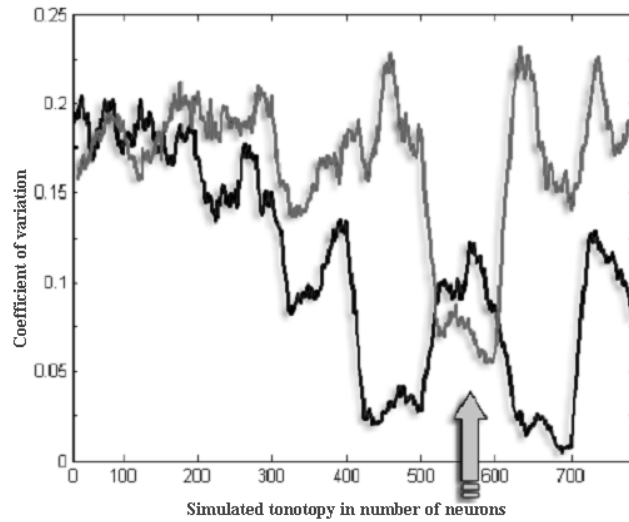
Figure 4.7: Neural RR, indicated by the CoV in the pathologic case of peripheral hyperactivity (grey line) and for a Gaussian–shaped stimulus, with a notch centered at the frequency range of the simulated tinnitus tone (black line). The pathologic case exhibits an increased neural RR, which can be perturbed by a tailor–made notched stimulus.

In the second experiment we analyze the effect of different notch bandwidths on the neural spontaneous activity. Additionally to emphasize the effect of lateral inhibitory projections we exaggerated the stimulus intensity in frequencies neighboring the simulated cochlear lesion. This edge effect would also occur if the total stimulus loudness is increased, but we chose this approach to minimize a potential patients overall noise exposure. Fig. 4.8 illustrates the effect of notch bandwidths

on the neural spontaneous activity in the tonotopic area of the simulated chochlear lesion. We used notch bandwidths of 0.7 to 1 octaves (1.4 kHz to 2 kHz) centered on a simulated tinnitus of 3 kHz and an edge frequency amplification factor of 1.3 and 1.6. We archived the best results, i.e., a reduction of neural hyperactivity to spontaneous firing, with narrow notches and high edge frequency intensities.
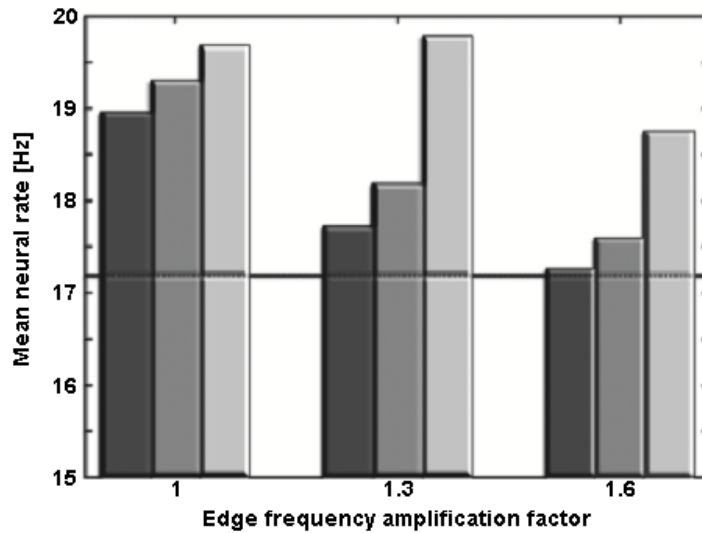

Figure 4.8: Mean neural activity in the tonotopic range of a simulated 3 kHz tinnitus tone in response to a notched acoustic stimulus. We utilized notch bandwidths of 1.4 kHz (dark grey bar), 1.6 kHz (medium grey bar) and 2 kHz (light grey bar) centered on a simulated tinnitus. The average level of spontaneous activity is indicated by a horizonal line at 17.2 Hz. The left group indicates a stimulation without edge amplification factor. In the middle and right group an amplification factor of 1.3 and 1.6 respectively was applied to frequencies neighboring the simulated lesion.

4.2 Tinnitus in prosencephalic structures

4.2.1 Intermodal effect of emotion tinged stimuli on habituation

Auditory domain: In this experiment we investigated the attention dynamics to a neutral stimulus for an aversive and for a neutral stimulus condition in "normal–hearing" subjects. A 50 dB(SPL), 1 kHz tone was chosen as level reference, representing a neutral, irrelevant acoustic stimulation. A 100 dB(SPL) tone acts as aversive stimulus by crossing the individual discomfort level. We applied the trial–to–trial wavelet coherence as measure of attention binding. This measure allows for a quantification of the drift from an attentive state to an inattentive state (habituation).
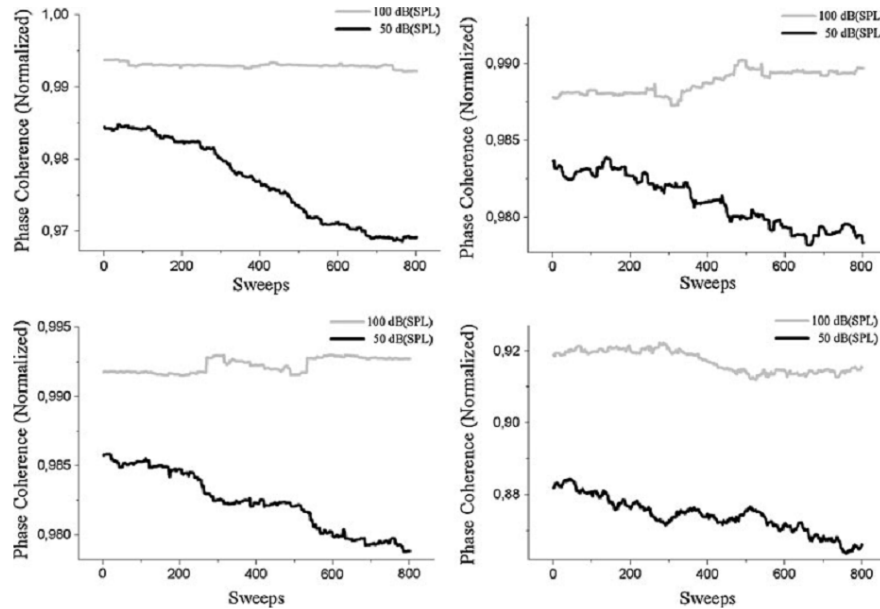
Figure 4.9: Four figures showing exemplary the results of the habituation experiments for four different subjects. The light grey curve depicts the normalized phase coherence over 800 stimuli for a stimulation level of 100 dB(SPL) (as described in section 3.2.2.2), the black curve indicates the normalized phase coherence for a stimulation level of 50 dB(SPL). Please compare these results to figure 4.21.

Images in 4.9 illustrate exemplary the dynamics of attention binding towards neutral and aversive acoustic stimuli in "normal–hearing" subjects. Depicted is the trial–

to–trial coherence (see methodology in section 3.2.1) over 800 successively presented stimuli. For the level reference stimulus of 50 dB(SPL) (black lines) we see in almost every subject a pronounced decrease of intertrial similarity over the duration of the experiment. The aversive stimulus generates high coherence values of single sweep responses (grey lines) over the entire experiment, indicating a high and invariant attention binding towards the high intensity tone.

Figs. 4.10 and 4.11 exemplary illustrate the intertrial coherence dynamics for a neutral and an aversive stimulus. Depicted is a contour plot of a 2D low–pass filtered topographic mapping of consecutive single sweep responses.
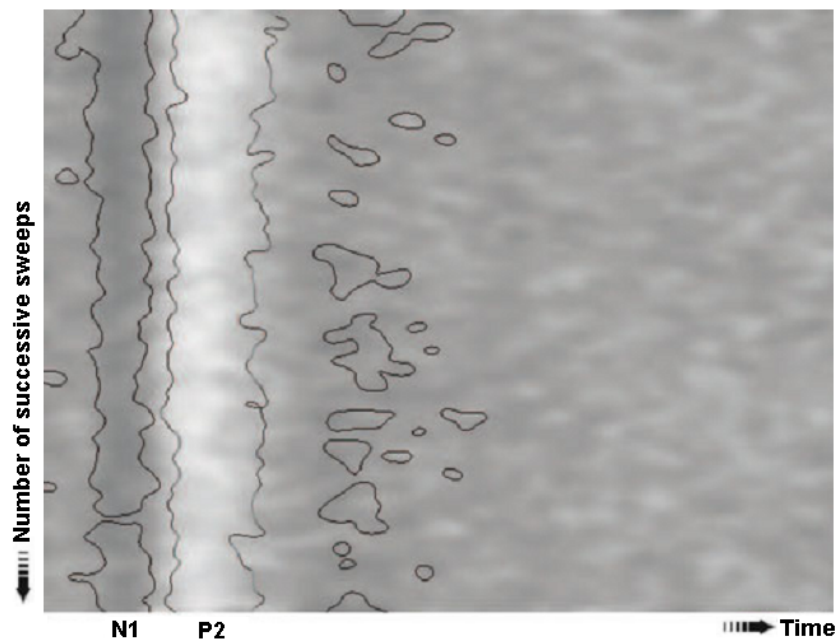
Figure 4.10: A stimulation with high intensity stimuli prevents the habituation to the stimulus. Depicted is a normalized contour–plot of a low–pass filtered, greyscale–coded single–sweep matrix of late auditory evoked potentials. Here light colours indicate high amplitudes, dark colours denote low amplitudes. Subsequent single–sweeps are displayed from top to bottom as horizontal lines. Notations N1 and P2 indicate the envelope of the N1 and P2 component of the evoked response.
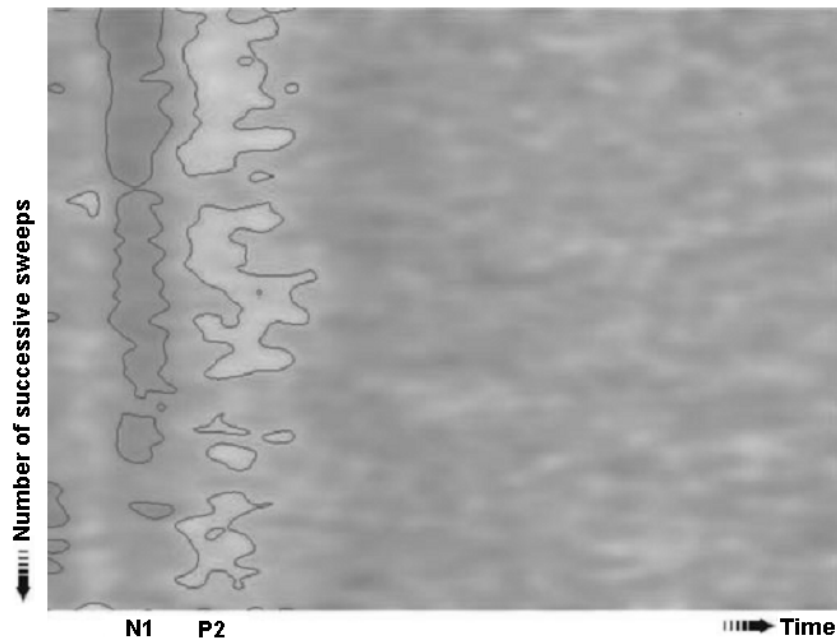
Figure 4.11: Low intensity stimulation leads to a habituation to the stimulus, indicated by a progressive fractionation of the N1–P2 trace contours. Depicted is a normalized contour–plot of a low–pass filtered, greyscale–coded single–sweep matrix of late auditory evoked potentials. Here light colours indicate high amplitudes, dark colours denote low amplitudes. Subsequent single–sweeps are displayed from top to bottom as horizontal lines. Notations N1 and P2 indicate the envelope of the N1 and P2 component of the evoked response.

Visual domain: In this experimental series we analyzed the intermodal effect of emotion tinged stimuli in the visual domain to gather additional experimental evidence for our working hypothesis of extra–sensory stimulus valence appraisal. It seems biologically plausible to assume a centralized mechanism for stimulus valence appraisal, rather than a redundant implementation of modality–specific valence evaluation structures. Yet we need experimental evidence to validate our model of a centralized hippocampal comparator. As literature already demonstrated the possibility of cross–modal distractors in attention paradigms, hinting towards a single limited capacity stage in attentive sensory processing [92; 93; 106], we aim to reproduce the habituation effects from the experiment in the auditory domain in this paradigm:

As in the auditory paradigm we evaluate the trial–to–trial coherence as a measure for habituation. Figs. 4.12 and 4.13 illustrate the habituation of our subjects towards neutral and emotionally aversive visual stimuli. Fig. 4.12 plots the trial–to–trial coherence over the number of subsequent stimuli for all four electrode positions. The light grey curves indicates the coherence dynamics towards neutral and aversive facial expressions. The colored lines illustrate the slope of a first order polynomial fit. We can see a more pronounced loss of intertrial coherence for neutral stimuli, compared to the aversive stimulus condition. These results mirror our findings from the auditory paradigm.
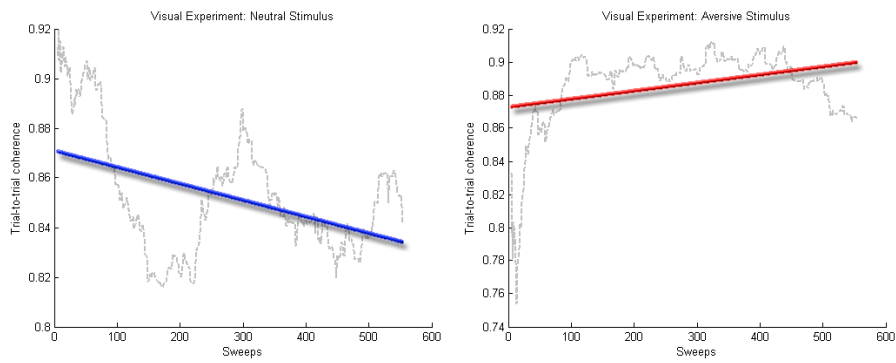
Figure 4.12: Exemplary illustration of trial–to–trial coherence as measure for habituation in the emotional and neutral face recognition task over the number of presented stimuli(sweeps). The images show the dynamic attention binding correlate from the electrode over right side fusiform area (P4 of the 10–20 system). The blue curve indicates the reaction towards neutral facial expressions; the red curve indicates the reaction to emotionally tinged faces.
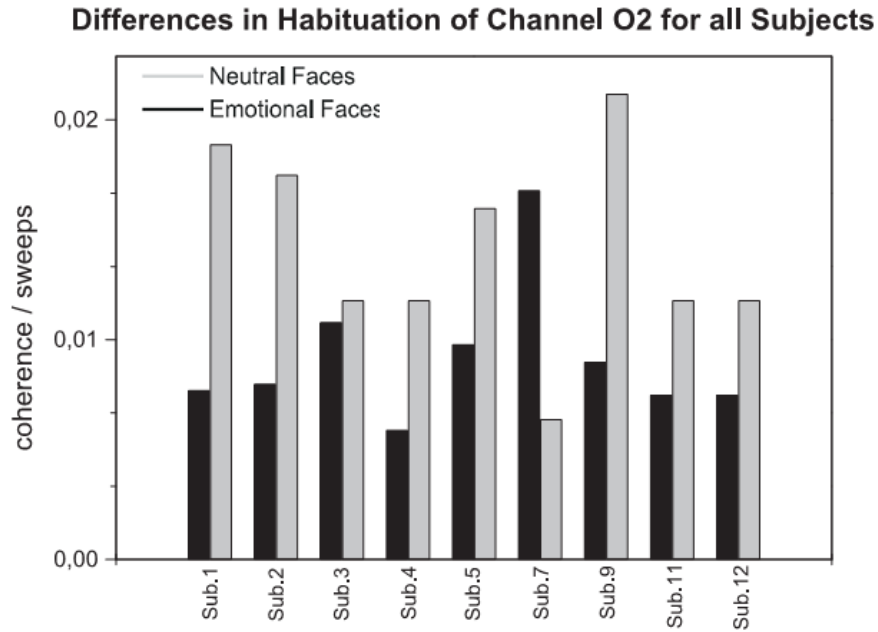
Differences in Habituation of Channel O2 for all Subjects

Figure 4.13: Differences in habituation in the emotional and neutral face recognition task for channel O2 over all considered subjects. The hight of a bar connotes a "habituation" value. The hight of a bar signifies the time–scale coherence over all sweeps, i.e., the higher a bar, the stronger is the habituation effect and vice versa.

Novelty effect triggers dishabituation: We conducted a visual stimulus–exchange paradigm as described in section 3.2.2.1 to discriminate attention habituation from fatigue and/or sensory adaptation effects. We expected a continuous decline in the trial–to–trial coherence, i.e. habituation, as the stimulus are of little subjective relevance. The novelty effect (in the sense of decreased familiarity) after the stimulus exchange results in a renewal of attention binding, indicated by an increase of the trial–to–trial coherence. Figs. 4.14 and 4.15 illustrate the dynamics of subsequent single responses to visual portrait stimuli in the range of the N140 component. As predicted the trial–to–trial coherence decreases until the stimulus exchange point, indicating a habituation towards the insignificant stimuli. After the exchange point the novelty of the unfamiliar stimuli involuntary captures attention. We interpret the data as proof of stimulus specificity of the attentional habituation.
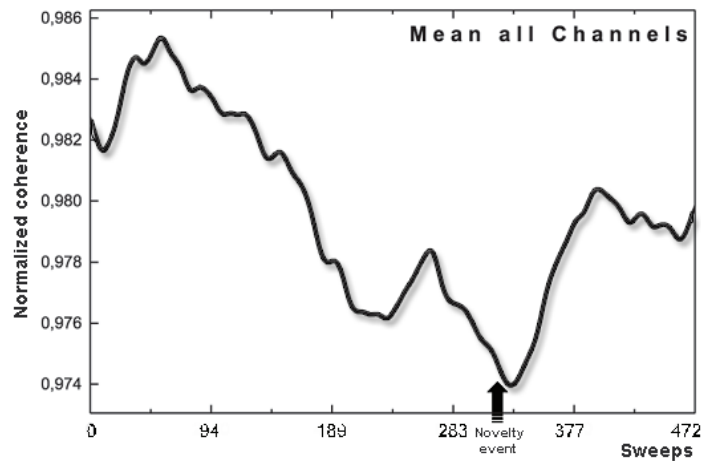
Figure 4.14: Grand average of the trial–to–trial coherence as measure for habit-
uation and dishabituation in the visual stimulus–exchange paradigm.
Depicted is the trial–to–trial coherence over the number of successively
presented stimuli (sweeps). The sudden stimulus exchange triggers a
renewal of attention resource allocation, indicated by increased trial–
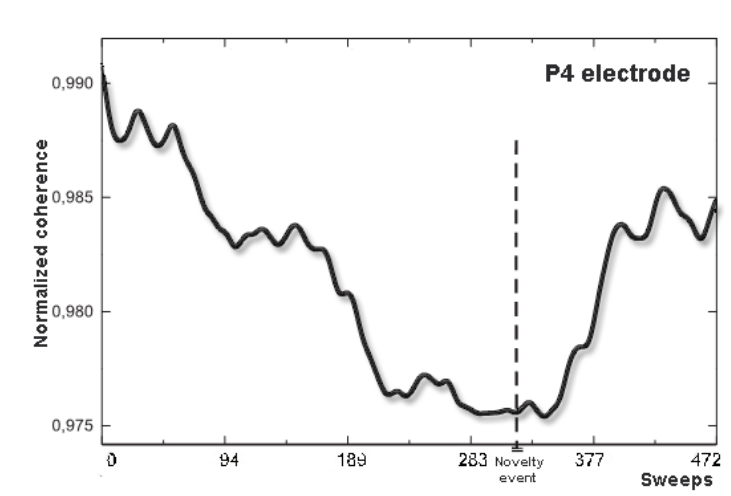to-trial coherence after the switching event.

Figure 4.15: Averaged trial–to–trial coherence at the P4 electrode position as
measure for habituation and dishabituation in the visual stimulus–
exchange paradigm. Depicted is the trial–to–trial coherence over the
number of successively presented stimuli (sweeps). The sudden stim-
ulus exchange triggers a renewal of attention resource allocation, in-
dicated by increased trial–to-trial coherence after the switching event.

4.2.2 Habituation across different grades of severity in tinnitus

Figure 4.16 illustrates the mean pure tone audiogram and standard deviation of 18 tinnitus patients, who took part in our habituation study. According to the definition of the European Commission, the subjects exhibit a mild to moderate hearing loss in the high–frequency region.
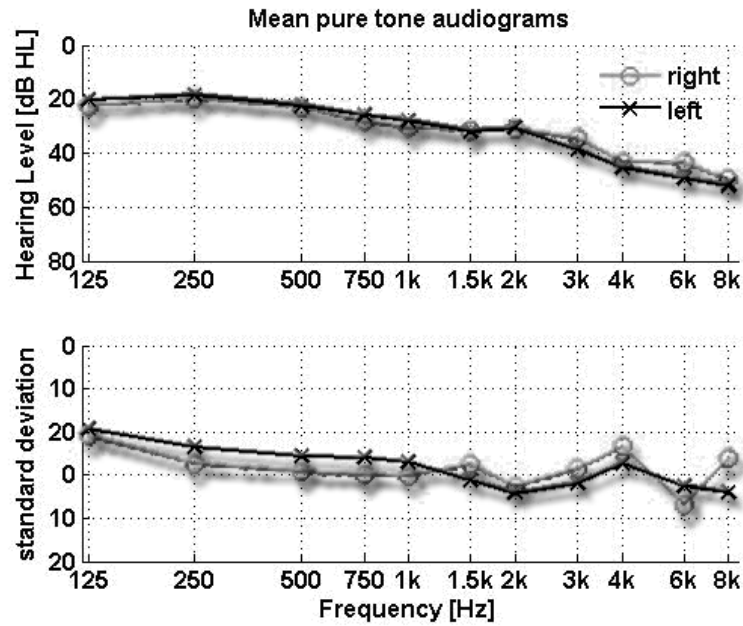

Figure 4.16: Mean pure tone audiogram of 18 tinnitus patients (upper illustration) and standard deviation (lower illustration). Depicted is the average hearing level in dB(HL) as spline over 6 octaves from 125 Hz to 8 kHz. The grey circles indicate a stimulation to the right ear; a stimulation to the left ear is indicated by black saltires. The patients exhibit a mild to moderate hearing loss in the high frequencies .

Fig. 4.17 illustrates our experimental findings in plots of mean von Mises kappa values over the number of sweeps packages. A polynomic fit was applied to illustrate the trend of attention deviation for the tinnitus tone (red line) and the 1 kHz tone (blue line) each.

In the compensated patients, the experimental results show a stronger habituation towards the neutral tone in comparison to the adaptation towards the tinnitus frequency. Surprisingly in the decompensated patients we can't see any habituation correlates, neither towards the tinnitus frequency nor to the 1 kHz target.
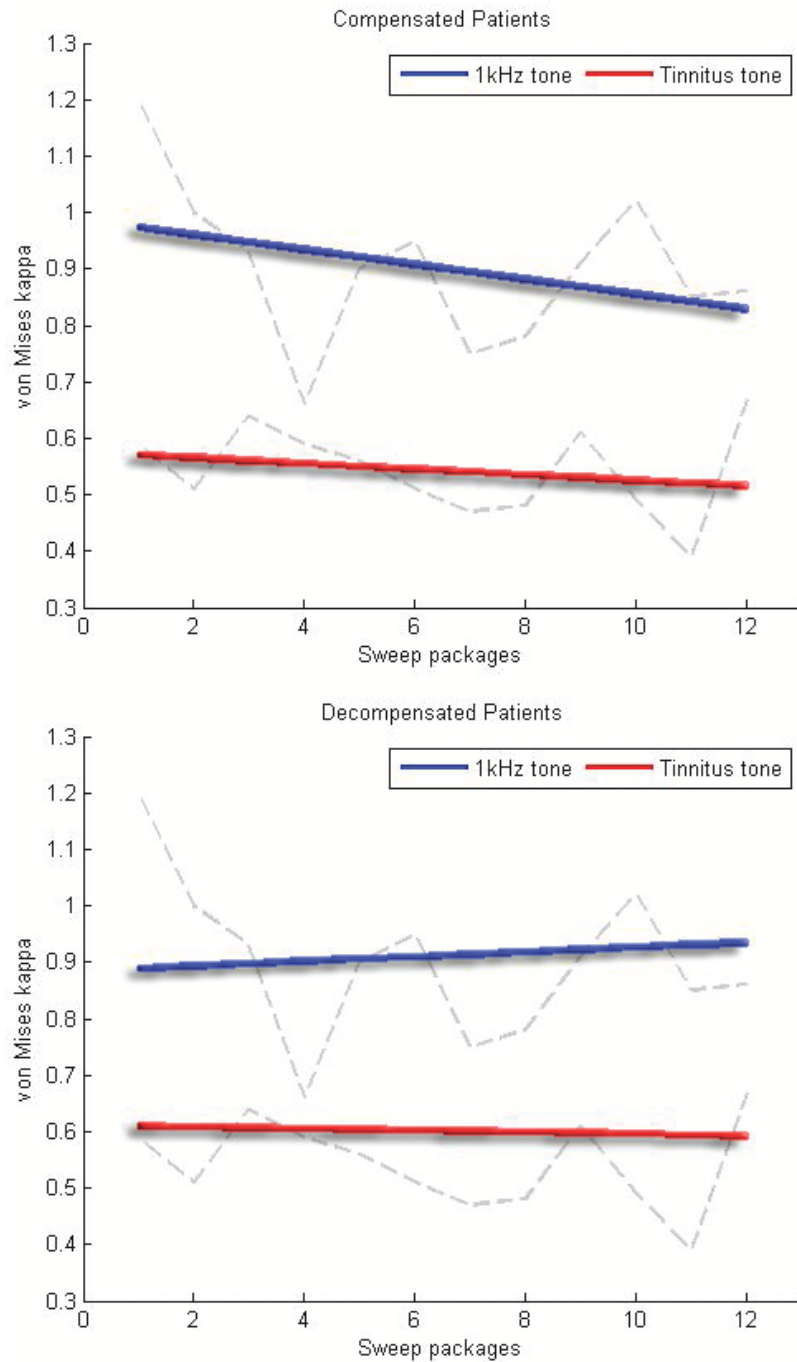
Figure 4.17: Measured mean ALR habituation correlates in terms of von Mises concentration parameter κ over the number of repetitive stimulations for compensated (upper graph) and decompensated (lower graph) tinnitus patients. The number of stimulus repetitions is indicated by sweep packages of 50 single–sweeps each. The red line indicates a polynomic fit of the habituation correlate to a stimulus in the patients tinnitus frequency, the blue line shows a polynomic fit of the habituation correlate to a stimulus of 1 kHz.
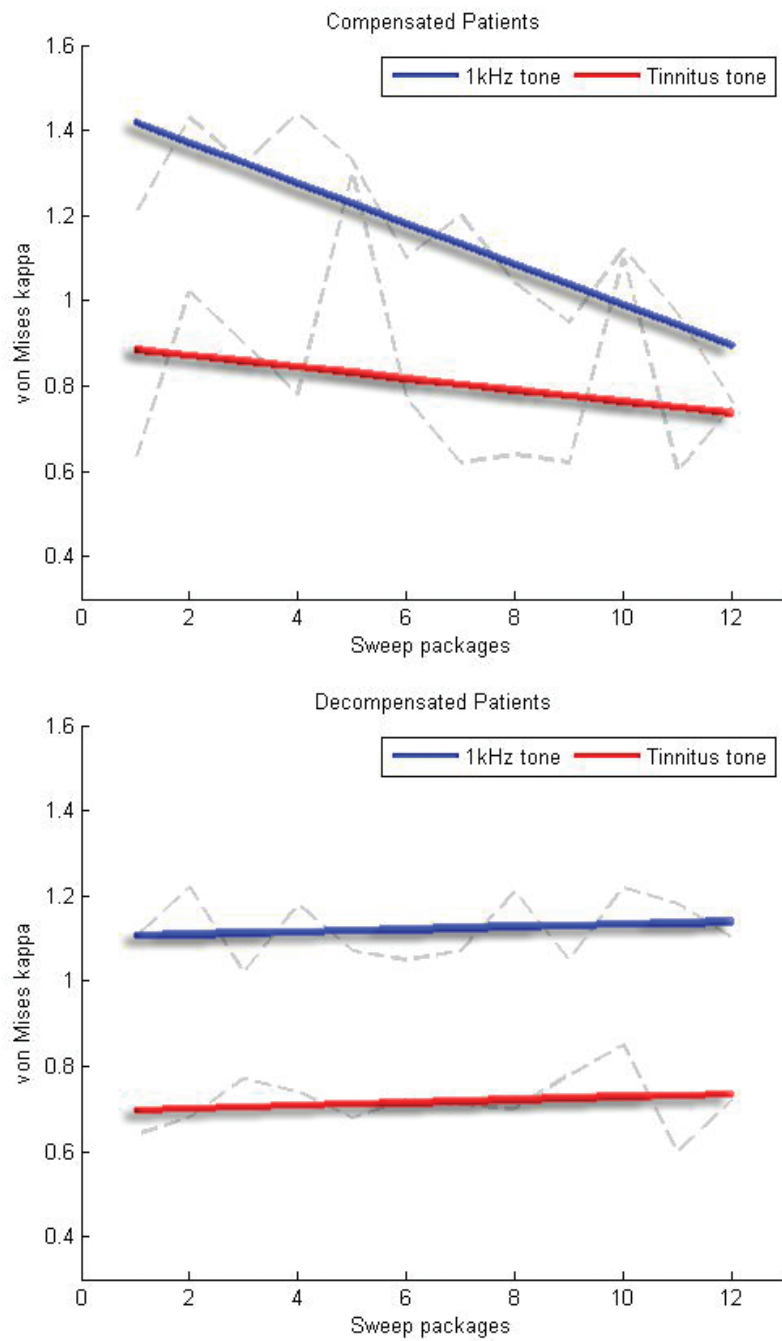
Figure 4.18: Simulated mean ALR habituation correlates in terms of von Mises concentration parameter κ over the number of repetitive stimulations for virtual compensated (upper graph) and decompensated (lower graph) tinnitus patients. The number of stimulus repetitions is indicated by sweep packages of 50 single–sweeps each. The red line indicates a polynomic fit of the habituation correlate to a stimulus in the patients tinnitus frequency, the blue line shows a polynomic fit of the habituation correlate to a stimulus of 1 kHz.

4.2.3 Modeling the role of a hippocampal comparator in attention and habituation

Fig. 4.19 illustrates the spiking behaviour of our hippocampal unit module. Plotted are spiking events as unit impulses (Kronecker's delta) over time. Based on anatomical routing of excitatory pyramidal cells, inhibitory basket cells and fast–spiking inhibitory OLM cells we were able to simulate a nested theta–gamma oscillation. A reduction of cholinergic input to the unit module resulted in a phase precession of the underlying theta oscillation. The figures show the spiking response for normal MSDB input (upper image) and for an attenuated MSDB cholinergic drive (lower image). The reduced MSDB cholinergic drive results in an envelope phase shift.
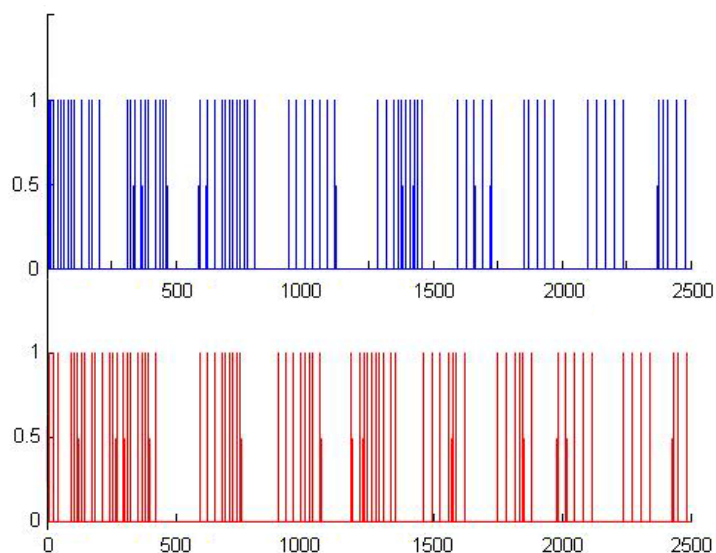

Figure 4.19: Exemplary simulation of a nested theta–gamma oscillation, expressed by spiking events (Kronecker's delta) over time. The phase precession of the underlying theta oscillation (gamma envelope) from upper to lower illustration results from a reduction of excitatory input to the unit module.

We initially modeled a set of 9 subjects (corresponding to the number of subjects tested) with varying model parameters randomly taken from a normal distribution within physiological limits. The parameters changed for modeling were axonal propagation velocity and range of thalamocortical axons to account for inter–individual variance.

The first modeling study comprised the simulation of available attention resources, represented by the phase synchronization measure briefly introduced in section 3.2.1. We compare the modeling prediction with experimental results gained from the experiment described in subsection 3.2.2.2. See fig. 4.20 for an illustration of measured and simulated phase stability over sweep–time for neutral and aversive stimuli. We can identify a significant difference of WPSS for the aversive and neutral condition in the range of the N1–P2 complex (50–200 ms). The simulated WPSS yielded higher values compared to the measured values. This effect is probably caused the fact that we do not simulate concurrent streams in the acoustic environment. Switching streams is likely to diminish the WPSS in human subjects. We address this topic briefly in section 5.2. In tinnitus patients we identify similar traces for mean phase stability values as attention measure for compensated (T1/T2) (neutral stimulus condition) and decompensated tinnitus patients (T3/T4) (aversive stimulus condition) [172].
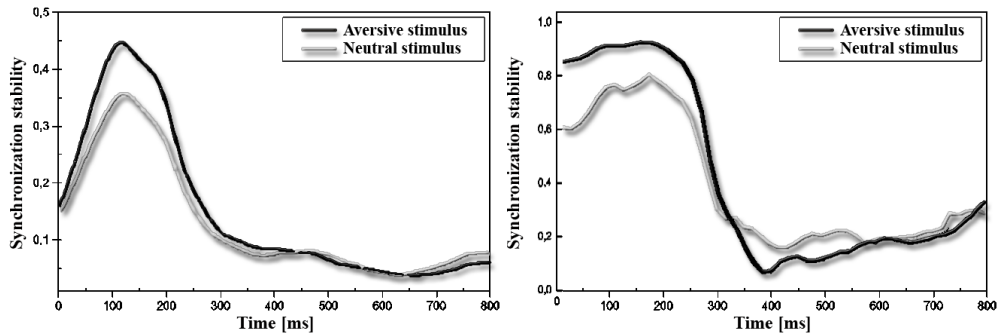

Figure 4.20: The figures show exemplary the measured and simulated mean WPSS over sweep–time for an aversive stimulus condition and for a neutral stimulus condition.

In a second experiment we modeled an attention drift as to be seen for habituation in tinnitus patients according to their subjective level of distress. By increasing the frequency detuning we could effectively prevent the increase of phase variance in the simulated ERP. Comparing these simulations with experimental the results from tinnitus patients, we can identify similar trends. Figs. 4.21 and 4.18 illustrate computational and experimental findings in plots of mean von Mises kappa values over the number of 12 sweep packages of 50 sweeps each.
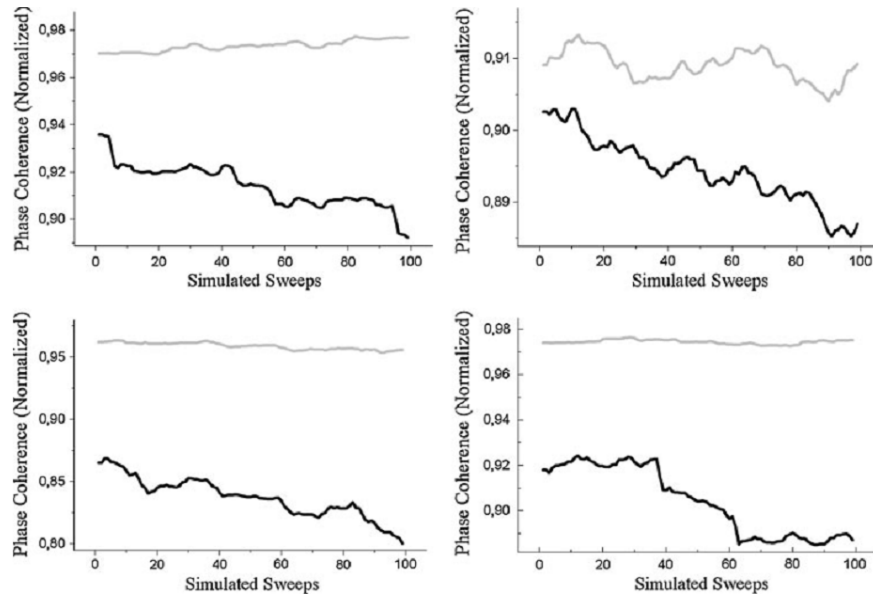
Figure 4.21: The figures show exemplary the results of four different simulations. The light grey curve depicts the trial–to–trial coherence over 100 ALR—-simulations (as described in section 3.2.1) for an unpleasant stimulation level, the black curve indicates normalized phase coherence for a comfortable stimulation level. Time scales are not adapted to to physiological habituation dynamics. Please compare these results to figure 4.9.

We calculated the habituation–value h, as presented in section 3.2.1, for the tinnitus tone stimulation and the 1 kHz control tone in compensated and decompensated patients each. In the following tables we compile the average h–values for the simulated data set and for the measured data set. The habituation towards the neutral control tone is exaggerated in the simulated data set. We can assume that this effect origins from the lack of concurrent streams in the simulation, which could affect the processing of the target tone in the measurement setting.

Table 4.1: Average habituation value h (see habituation value h in section 3.2.1) for the simulated data set

Compensated patients		Decompensated patients	
h–Value (1 kHz)	h–Value (tinnitus frequency)	h–Value (1 kHz)	h–Value (tinnitus frequency)
0.357	0.118	0	0

Table 4.2: Average habituation value h (see habituation value h in section 3.2.1) for the measured data set

Compensated patients		Decompensated patients	
h–Value (1 kHz)	h–Value (tinnitus frequency)	h–Value (1 kHz)	h–Value (tinnitus frequency)
0.118	0.121	0.028	0

5 Discussion

5.1 Peripheral mechanisms in tinnitus

Peripheral hyperactivity: The increase of the spontaneous firing rate can be considered as a physiological compensation process in response to a notch like hearing loss and the related deafferentiation of higher levels of sensory processing. This phenomenon is yet not sufficient to explain why and how the tinnitus percept arises and the mechanisms underlying tinnitus decompensation. Also the discrepancy of subjectively perceived tinnitus loudness and objective measures is not explicable on the base of the increased spontaneous firing rate.

We presented a computer simulation of self--organizing patterns of increased reliability and spiking coherence due lateral information flow in response to noisy impulse input (see figures 4.6 and 4.7). This increased spiking coherence can be considered as base for synchronous activity across a neural population which might be sufficient to activate cortical neurons, generating a percept. The factual generators of hyperactivity in the brainstem are yet not known beyond any doubt. Actual studies hint towards intrinsic neural properties of the DCN principal cells instead of additional top–down projections: In a rat model, Pál et al. demonstrated one major driving force of this DCN spontaneous activity in the HCN–channel (hyperpolarization–activated cyclic nucleotide–gated cation channel) configuration [137]. Also endogenous dynorphins within the olivo–cochlear system might play a role in the peripheral generation of tinnitus and hyperacusis. Dynorphin derivates play a role in the mediation of spontaneous neural activity and nerve sensitivity to Glutamate [151].

Above all, attentional top-–down mechanisms (e.g., thalamocortcial feedback loops) can further boost the synchronous activity of subcortical neuron populations in the sensory pathway, improving the competitive advantage of the stimulus in perceptual rivalry. Yet the mechanisms underlying decompensation remain to be addressed supplementary.

The model of peripheral hyperactivity and spiking regularity consequently led to an experimental study on the influence of sharp spectral edges on the neural self-–organizing patterns by means of subjective tinnitus loudness reduction. In extension of a short–term therapeutical intervention we fitted modified hearing aids to pure–tone tinnitus sufferers. These hearing aids have the optional feature of a band–notch adjusted to the individual tinnitus tone, as proposed by Okamoto et al.. (see 2.3.9 and [130]). The induction of sharp spectral edges to the environmental spectrum is likely to trigger lateral inhibition mechanisms. This supplemental technique for therapeutic intervention thus targets two possible generators of a stressful tinnitus percept: First, the amplification of sound for the wearer leads to a reduction of the listening effort and thus to a reduced stress level which is an important factor in tinnitus management [162]. Secondly the tailor–made notch suppresses the afore described neural hyperactivity and response reliability, leading to a loss of competitive advantage for the tinnitus tone. We named this approach ”notched environmental sound technology” (NEST). Our preliminary study included a group of 20 tinnitus patients from a hearing rehabilitation and tinnitus center. We matched the target and control group of patients according to their TQ–12 score and their hearing aid experience. The control group received the very same hearing aids as the target group, but without the NEST spectrum modification. We compared the therapy success by subjective and objective measures. For the subjective therapy evaluation we compared pre– and post therapeutic TQ–12 scores using Cohen's d–value. For the control group we see a small effect size, whereas the target group exhibits a large effect. For the objective analysis we utilized the habituation analysis explained in section 3.2.1. Both methodologies for therapy evaluation demonstrate an improvement of the therapeutic result using NEST to complement a three weeks inpatient intervention. The results of this study were submitted to the ”Clinical Otolaryngology” journal. (Please see List of Publications in the Appendix).

DCN model: The simulations of DCN neural reactions to a constant stimulus of given frequency and intensity is approximately Gaussian across the hearing path tonotopy (see 4.1). For high intensities the neural activity is distorted to a positive skewness, indicating an activation of neurons with larger distances in their characteristic frequencies in the direction of high frequency percepts. As demonstrated in [7] the on–sustained response (firing rate over time) to a neurons best frequency is approximate Gaussian for IC neurons with stimulus–specific adaptation. We thus can justify the use of a temporo–spatial Gaussian–like excitation (across time and frequencies) for the simulation of ALRs in our thalamo–cortical model (see section 3.2.3), as a valid approximation of a moderate intensity natural stimulus.

5.2 Expansion of the probabilistic attention model

Within the scope of this work, we propose an expansion to the probabilistic attention model, explained in section 2.3.2. The hierarchical information transfer is a serial shift of information content from a pre–attentive sensory register to a memory register fit for higher–level processing. The selection of streams is probabilistic, with the distribution following the exogenous weight in attention onset and orienting. Within the bandwidth of the transfer channel, the information content of a limited number of streams is conveyed to the high–level register and analyzed for semantic content. Following this transfer new streams are selected on the base of a re-assessed exogenous and endogenous weight total and again shifted to the high–level register. If the information content of one stream matches an engrammatic template its endogenous weight can be in– or decreased, resulting in a distortion of the existing probability distribution and thus in a more frequent recurrence of the stream's content in the high–level register. This serial processing of information streams is backed up by visual search experiments, where the time required for pattern matching increases with the number of equally weighted distractors [4] (see also probabilistic attention model in section 2.3.2).

This simplified model can address the problem of attentional load as expressed, e.g., by N. Lavie [92]. High attentional load can be described by a number of parallel sensory stream, akin to each other in terms of total weight. The cortical response to unattended stimuli is significantly reduced during tasks involving high perceptual load due to attention bandwidth limits [170]. The authors hypothesize

on the base of visual discrimination task that this reduction of cortical responses likely origins from reduced signal gains and a reduced tuning precision by a widening of the neural tuning. As we do not include perceptual rivalry into our model, but address cortical activity suppression by the transition of focussed to non–focussed attention (habituation, see section 2.3.4), we entirely focus on thalamocortical gain modulation.

The factors of vigilance and arousal could be addressed by a normalization of the probability distribution to the actual state of wakefulness, effectively limiting the bandwidth of conveyed information to hierarchically higher areas of semantic processing. Additionally, we could also hypothesize a distortion of the probability distribution by an increased variance (up to uniformity) in a state of reduced arousal. This effect would describe the increased distractibility, as every concurrent stream has almost the same probability of being selected for higher processing. Yet in modeling terms the variance of the probability distribution should be additionally a function of the stream's highest exogenous weight to take account for warning stimuli, activating the brainstem alerting network, as described, e.g., by Posner and Peterson [136]. In contrast, focussed attention and states of high arousal could be described by a reduced variance of the probability distribution. This indicates a high probability of a single stream being picked for semantic processing repetitively, with only small chances of interfering streams being conveyed to higher processing areas (reduced distractibility).

5.3 Testing the modality specificity of emotion–tinged stimuli

We decided to check for the effects of fatigue and sensory adaptation only in the visual domain, as the visual N170 is more robust to changes in the stimulus properties compared to the auditory N1. Changes in the stimulus tone frequency results in a distortion of the ALR morphology, and thus to a falsification of the extracted attention measure [126]. This is also the reason, we chose stimulus intensity as aversive factor in the auditory modality. In both tested modalities we could observe the very same effect of attention binding and habituation correlates in the N1–P2 component of ERPs. Aversive stimuli, be it high intensity stimuli or pictures displaying hor-

rifying content, lead to a high regularity of subsequent ERP instantaneous phases which we interpret as high attention binding (see section 3.2.1) as well as to a reduced ability to habituate to the presented stimuli, as shown by the increased trial–to–trial coherence over the duration of the experiment. These experiments also provide additional evidence that the observed attention drift is a behavioural habituation of the orienting response. We see both, the required stimulus specifity and the reaction specifity. In the visual domain we can clearly separate a dishabituation effect in response to stimulus novelty (see 4.2.1), as well as the attention regulating effects of emotional stimulus content.

By this implication we can assume an extrasensory mechanism of stimulus valence appraisal and attention control which influences at least two different modalities. We assume that this regulating effect targets the thalamocortical feedback system as key crossroad structure. The future analysis of olfactory information processing might shed additional light on this assumption as there is no direct thalamic relay between sensory neurons and the olfactory cortex. Yet these examinations might be impeded by coherent slow wave activity in the piriform cortex and the hippocampus, as well as in the piriform cortex and the mediodorsal thalamic nucleus in response to olfactory stimulation in the rat, as demonstrated by Courtiol et al. They propose that this increased coherence in parallel processing circuits is tightly linked to stimulus valence appraisal, attention and memory [24].

5.4 Habituation as measure to evaluate notched sound therapy in tinnitus

In section 2.3.9 we introduced the tailor–made notched music therapy approach of Okamoto et al [130]. Referring to their findings we conducted two experimental studies utilizing notched environmental sounds (NEST, see section 5.1) as a supplement to a stationary retraining therapy. We analyzed the patient's subjective self–assessment by the TQ12 questionnaire and objective EEG correlates of habituation before and after the inpatient intervention to evaluate the NEST. In the first study we show the patients's general acceptance of the notched hearing aid and the dependency of the ability to habituate on the subjective level of distress. The compensated patients exhibit a habituation deficit towards their individual tinnitus

tone, while the habituation towards a neutral 1 kHz tone is largely unhampered. Opposed to this, decompensated patients show a more general habituation deficit independent of the stimulus valence. We discuss this effect in section 5.6.

In our experimental setting we experienced large variances in estimating the habituation parameters towards neutral (1 kHz tone) and aversive (tinnitus tone) stimuli. These variances not only map interindividual variances in habituation, but are additionally generated by a morphological changes of the ALRs in response to the stimulus–frequency shift. We address this problem by collecting larger quantities of patient data. Furthermore, we prepare an experimental study to quantify the effect of stimulus–frequency shifts on the ALR morphology.

In the second study we evaluated the clinical effectiveness of the NEST therapy support in a pre– and post–therapy paradigm vs. a control group. The patients fitted with frequency notched hearing aids showed a significantly better therapy outcome compared to the patient group with out of the box hearing aids. Both, subjective self–assessment and objective habituation data provide evidence for an therapeutic use of NEST as a supplement to a stationary retraining therapy. Comparing our study outcome with the results of Okamoto et al. we demonstrate that we don't need to create a specific listening situation. The enjoyment of listening to music is no therapeutic necessity. In the TMNM therapy approach the patient is constrained to spend a considerable amount of time listening to their preferred music (7–21 h per week), whereas in the NEST approach the therapeutic effect of notched acoustic stimulation is integrated into the patient's daily routine. We could show that the unspecific triggering of limbic structures by emotional content conveyed by music is not required to achieve a therapeutic success. The core element of the psychotherapeutic intervention in the stationary retraining therapy is the patient's re–evaluation of the tinnitus tone. The intervention is designed to mitigate the fear reaction associated with the tinnitus tone [74] and thus is a more direct, tailor–made form to address the individual dysfunctional assessment of the tinnitus tone.

We did not directly compare the Patients improvement in subjective distress in TMNT and NEST, so we won't challenge any interventions effectiveness. Yet we can say, that tailor–made music is not required for a positive therapy outcome and that the methodology of NEST can be integrated in the patient's daily routine without the constraint of extended periods of active music listening. This integration of

tailored notch filters in hearing aids allow for a lengthy "treatment" period without the patient noticing any irritating effects.

5.5 Modeling habituation dynamics

We were able to simulate experimental data on attention and habituation using a model based on the hypothesis of the hippocampus working as a comparator and Vinogradova's theta–regulated attention theory. The effects of attention and habituation on the N1—P2 components of ALRs were reproduced.

Besides the Vinogradova model there exits a different model of CA1 working as a comparator by Lisman and Grace [101]. In this hypothesis the CA3 area predicts future events on the base of associative memory, while the CA1 is the factual comparator of incoming sensory information and predicted environmental changes. Lisman and Grace state, that the locus of novelty detection in the hippocampus is not known with certainty. Latest results however suggest that the CA3 area of the hippocampus is the factual comparator, e.g., Lee et al. and Hasselmo confirmed a potential role of the CA3 in novelty detection in 2005 [95; 62]. In our model the cortical input into the FD is set up from already preprocessed information and could be described as "degree of familiarity", thus being a neural representation of a memory engram. Yet we can not exclude that this cortical input is in–vivo a prediction of dynamic changes in the sensory environment. In the context of this work we assume a static sensory environment, to omit this undecidable dichotomy. In such an invariant environment a spatial memory representation is equivalent to a change prediction.

Crick stated 1984 a high importance of the thalamic reticular nucleus for the attentional spotlight [25]. Latest publications support this hypothesis. Animal models report from impairments in the attentional orienting after TRN lesions [189] and the result of C–Fos stains suggest a critical role of the TRN in attentional gating. Our results also support this hypothesis in–silico. Facing the problems of hippocampal models in comparison to experimental and behavioural data our model —in expanse— can provide satisfying results.

Along with the habituation there come a number of related claims and tasks like stimulus specificity, dishabituation (as shown in figure 4.14 in the results section)

or simply the inability to habituate towards annoying stimuli [90] as in the case of tinnitus. In all cases we assume a shift in at least the coding phase of either the sensory stream or of the memory trace respectively. Dishabituation occurs with changes in the signal parameters, thus in a change in the exogenous weight including spatial location. This can be considered as a break of the original stream grouping into an entirely new stream. In our model the continous signal stream is also interrupted and the encoding of a new stream results in a new signal phase and possibly a change in frequency and phase coding in the MSDB subunit. The specificity, i.e. the persistence of certain stimulus responses in the core system can be explained by a classical Hebbian approach and the resulting increase in the habituation rate.

In a number of cases subjects show an inability to habituate towards certain stimuli, often percepts of high subjective valence. A number of publications demonstrated the influence of the central amygdala on the dentate gyrus [70; 163]. An unpleasant stimulus thus might, by a co–activation of accompanying brain areas like the amygdala, prevent the habituation by a modification of the FD firing pattern. Comparable to this case of aversive stimulus processing, we hypothesize the possibility of voluntary attending insignificant stimuli. Planing areas are likely to influence the coded pattern in the FD as well.

Maintaining a simple and static sensory environment we did not model the appearance of concurrent auditory streams, so the feedback of the CA3 to the reticular formation (FR) via the Raphe nuclei (RN) is not included in the model yet. For further modeling purposes we consider the FR responsible for the selection of the attended stream by means of a probabilistic stream selection model presented in [183]. Thus the release from tonic inhibition during the reaction to novelty can be considered as method to stabilize the attended stream against concurrent stimuli [186]. Combining two independently developed neurofunctional models we were able to reproduce experimental results on attentional guidance due to stimulus novelty. We consider this approach as a promising method to gain deeper insights in the mechanisms underlying attentional habituation and the guidance of attention driven by stimulus novelty. Our experimental results as well as the in–silico reproduction of these results might lead to a better understanding of the effect of small neuronal groups on non–invasively measurable large–scale effects in humans, like, for example, the electroencephalogram. We neglected the detailed simulation of the

mechanisms involved in the formation of associative memory traces, but focussed entirely on the guidance of attention by a hippocampal comparator mechanism. As stated in the work of [13] a potentiation in both, STP and LTP, is associated with a (transient) facilitation of theta and gamma oscillations in the dentate gyrus. The subsequent steps in expanding our comparator–model will incorporate the detailed simulation of facilitation processes due to the increasing familiarity–level of repetitively presented stimuli.

5.6 Hypothesis of a general habituation deficit underlying the tinnitus decompensation grade

The experimental data provide insight in an interesting feature. We stimulated tinnitus patients with a control tone, deviant from their individual tinnitus frequency and with a stimulus tonally matched to their phantom perception. Based on our model we expected the ability to habituate better for the control tone than for the tinnitus matched tone. While this is true for the compensated patients the modeling prediction did not match exactly for decompensated patients. High distress patients generally show a reduced ability to habituate to both types of acoustic stimulation. This effect hints towards a general habituation deficit underlying the exacerbation in terms of subjective distress.

The heterogeneity of tinnitus severity cannot be explained purely on the base of neural reorganization limited to the sensory pathway. The attention binding to a sudden phantom noise, e.g., after an acoustic trauma is very quick [177] and thus cannot be correlated with long–term plastic changes in the thalamocortical pathway. Long–term plasticity might be responsible for the solidification of the pathologic tinnitus, but a more primitive mechanism must be responsible for the early attention binding [28]

The hippocampus is a structure known for the binding of perceptual elements into an egocentric representation, i.e., mapping of the sensory environment by a theta phase coding [82]. This map provides a dynamic prediction of the egocentric representation of the sensory environment and thus might serve as a detector of deviants, representing novel or vital events in the respective space.

5.6 Hypothesis of a general habituation deficit underlying the tinnitus decompensation grade

Honey et al. provided additional evidence that a spatial representation still exists in rats with hippocampal lesions, by showing spatial preference behaviour in lesioned animals [68]. These results indicate for a modulation of stimulus intensity or perceptual saliency deriving from changes in hippocampal activity. Anatomic evidence for strong interactions of a hippocampal comparator with limbic areas hints towards a context–dependent modulation of the interlinking processing of sensory information and memory engrams. Dysfunctional circuitries for evaluating the importance of a stimulus might in consequence lead to pathologic attentional binding as we observe in Tinnitus.

This pathologic deficit in the appraisal of sensory valence might form a neural base for the general emergence of tinnitus from neural hyperactivity in the auditory periphery [158; 119]. Moreover the co–activation of limbic and sensory areas can lead to a consolidation of sensory synapses. In the animal model the elicitation of Tinnitus leads to a significant increase in the IEGs arg3.1 and c–fos in the CeA and the AC. The C–Fos (protein) peak level is found in layer III and IV AC neurons, which are primary target of vMGB projections. This plastic reinforcement of thalamo–cortical circuitry might hint also towards a learned focal point of attentional resource allocation in the time–course of tinnitus chronification.

Future work encompasses the testing of this hypothesis by a multimodal ERP experiment. Should the patients exhibit similar habituation deficits in other sensory modalities, the hypothesis of a central dysfunction of the appraisal of the stimulus valence gains additional support.

6 Conclusion

Conclusion: Utilizing multiscale mathematical mapping and feature—reduction on available data we were able to simulate and predict large–scale neural dynamic behaviour and thus are able to set up a simplified functional model for a number of experimentally observable discrepancies in neural dynamics during tinnitus pathogenesis and chronification. This model comprises multiple hierarchical levels of auditory perception and processing (see also [124]). This implementation of computational methods for modeling and simulation allows for the integration of measurable physiological parameters across multiple scales into a single dynamic library of systemic interactions. Multiscale models moreover enable a selective alteration of neural functioning and thus a prediction of changes in network signaling behaviour by simulation. Making modeling predictions across multiple spatiotemporal scales regarding pathological changes in auditory processing from measurable but patient—specific large—scale effects (like, e.g., EEG) is a non—linear, ill-–posed inverse problem as it offers no unique solution and as slight perturbations in the initial conditions might lead to drastic alterations in the network signaling. Computational models across multiple spatiotemporal sales, with boundary conditions based on anatomical and electrophysiological data, can help to provide a reasonable answer to the question of tinnitus aetiopathology in patient-–centered care. We propose a model of multiple processing levels, in which primitive, intrinsic neural network mechanisms facilitate a self-–organized pattern of regular and synchronized activity after a peripheral trauma. Higher processing stages, e.g., for stimulus appraisal and attention guidance, further boost this increased orchestration of neural firing to the point of plastic changes in the auditory pathway, likely for the reduction of energy expenditure. In tinnitus these plastic changes likely mark the progressive centralization of hyperexcitability and the transition from the acute to chronic state.

Limitations of this work:

- The spread of coherent information in the auditory pathway due to lateral inhibition is a modeling parameter, that is still hard to access in the individual tinnitus patient. We thus cannot rely on absolute numbers for firing rates but have to analyze overall characteristic trends. Additionally we dealt with a symmetric lateral inhibition, which is a simplification of the asymmetric lateral inhibition in the physiological condition. This asymmetry causes a tonotopic shift of the compound action potential.

- The major limitation of this work, and of all other system–level neuronal models, is the simplification of neural signaling behaviour. As system–sized patches of neural tissues contain by far too many neurons for the modeling of individual cells (average neuron density in the primate cortex is approximately 100.000 neurons per cubic millimeter, with an average of $6 * 10^8$ synapses) the computation of group neurodynamics calls for a reduction of computational effort. In general the system models compute the mean activity of a neural population by the introduction of a neural step function (effectively reducing the individual neuron to a binary switch). Our model also suffers from simplifications. In the hippocampal comparator, for example, both inputs into the CA3 are described as stimulus dependent but stripped from higher stimulus properties [186]. We model both inputs as exemplary nested gamma–theta oscillations, as shown in literature, but we can't address the correlation of certain stimulus properties to the nested gamma–theta. The model thus can only approximate the in–vivo neurodynamics and is only efficient in the prediction of group behaviour.

- The experiments must be considered pilot studies, as we have only a limited number of subjects, leading to bigger variances due to interindividual variability. Increasing the number of subjects in follow–up studies, e.g., in the validation of the NEST approach in therapeutic intervention, will give us more reliable numbers and will minimize the error in predicting the typical response. Additional patient data will also provide us with finer boundary conditions to our numerical models, helping to adapt them to plastic changes in the course of the inpatient treatment.

Future work: The hypothesis of a generalized habituation deficit as catalyst for tinnitus decompensation has to be tested in additional sensory modalities. If other modalities are affected by the demonstrated habituation deficit, the model of extrasensory valence appraisal in attention allocation gains additional relevance in the analysis of neural mechanisms in the tinnitus decompensation. In loose connection with this neural mechanism it is necessary to clarify the meaning of increased neural response reliability in the subthalamic stages of the auditory pathway for attentional binding.

In the last year of my doctorate we began with a refinement of the thalamo–cortical feedback model by in–depth analysis of laminar neurodynamics in the rat animal model. We combine a 2D–surface mapping of stimulus dependent voltage fluctuations by voltage sensitive dye imaging with penetrating electrode arrays for additional laminar LFP data. Both data will be integrated into a multisource volume conduction model of the AC to: 1. clarify the temporal orchestration of bottom–up and top–down projections in the processing of auditory stimuli and 2. allow for additional constraints in the inverse analysis of EEG data. The results of this work are yet not sufficiently significant to be included in this thesis, but first pilot data is published in [50; 147].

Bibliography

[1] N. Adachi, T. Watanabe, H. Matsuda, and T. Onuma. Hyperperfusion in the lateral temporal cortex, the striatum and the thalamus during complex visual hallucinations: single photon emission computed tomography findings in patients with charles bonnet syndrome. *Psychiatry Clin Neurosci*, 54:157–162, 2000.

[2] L. Aguiar and M. Soares. The continuous wavelet transform: A primer. *NIPE Working Papers, NIPE – Universidade do Minho*, 16, 2011.

[3] H. Argstatter, M. Grapp, E. Hutter, P. Plinkert, and H. Bolay. Long–term effects of the "heidelberg model of music therapy" in patients with chronic tinnitus. *Int J Clin Exp Med.*, 5(4):273–288, 2012.

[4] S. Arun. Turning visual search time on its head. *Vision Research*, 74:86–92, 2012.

[5] Y. Atsumi and H. Nakao. Persistent fluctuations in synchronization rate in globally coupled oscillators with periodic external forcing. *Phys. Rev.*, 85:056207, 2012.

[6] A. Axelsson and A. Ringdahl. Tinnitus: a study of its prevalence and characteristics. *Br J Audiol*, 23:53–62, 1989.

[7] Y. Ayala, A. Udeh, K. Dutta, D. Bishop, M. Malmierca, and D. Oliver. Differences in the strength of cortical and brainstem inputs to SSA and non–SSA neurons in the inferior colliculus. *Nature Sci. Rep.*, 5:10383, 2015.

[8] D. Baguley, D. McFerran, and D. Hall. Tinnitus. *Lancet*, 382:1600–1607, 2013.

[9] J. Baizer, S. Manohar, N. Paolone, N. Weinstock, and R. Salvi. Understanding tinnitus: the dorsal cochlear nucleus, organization and plasticity. *Brain Res.*, 1485:40–53, 2012.

[10] G. Benshalom and E. White. Quantification of thalamocortical synapses with spiny stellate neurons in layer iv of mouse somatosensory cortex. *J Comp Neurol.*, 253(3):303–314, 1986.

Bibliography

[11] P. Berens. Circstat: A matlab toolbox for circular statistics. *Journal of Statistical Software*, 10, 2009.

[12] W. Bialek, F. Rieke, D. Warland, and R. de Ruyter. *Spikes – Exploring the Neural Code.* MIT Press, Cambridge, MA, USA, 1999.

[13] A. Bikbaev and D. Manahan-Vaughan. Hippocampal network activity is transiently altered by induction of long-term potentiation in the dentate gyrus of freely behaving rats. *Front Behav Neurosci.*, 1:7, 2007.

[14] A. Blood and R. Zatorre. Intensely pleasurable responses to music correlate with activity in brain regions implicated in reward and emotion. *Proc Natl Acad Sci. USA*, 98(20):11818–11823, 2001.

[15] A. S. Bregman. *Auditory Scene Analysis.* MIT Press, Cambridge, MA, USA, 1999.

[16] C. Börgers, S. Epstein, and N. Kopell. Background gamma rhythmicity and attention in cortical local circuits: a computational study. *Proc Natl Acad Sci. USA*, 102:7002–7007, 2005.

[17] C. Börgers and N. Kopell. Gamma oscillations and stimulus selection. *Neural Comput.*, 20:383–414, 2008.

[18] D. Broadbent. *Perception and Communication.* Pergamon Press, London, UK, 1958.

[19] R. Bruno and B. Sakmann. Cortex is driven by weak but synchronously active thalamocortical synapses. *Science*, 312:1622–1627, 2006.

[20] W. Burke. The neural basis of charles bonnet hallucinations: a hypothesis. *J Neurol Neurosurg Psychiatry*, 73:535–541, 2002.

[21] M. Busse, L. Haab, M. Mariam, C. Crick, T. Weis, W. Reith, and D. Strauss. Assessment of aversive stimuli dependent attentional binding by the n170 vep component. In *Conf Proc IEEE Eng Med Biol Soc.*, pages 3975–3978, Minneapolis, MN, USA, 2009.

[22] G. Buzsaki, C. Anastassiou, and C. Koch. The origin of extracellular fields and currents — eeg, ecog, lfp and spikes. *Nature Reviews*, 13:407–420, 2012.

[23] C. Cherry. Some experiments on the recognition of speech, with one and with two ears. *J Acoust Soc Am.*, 25:975–979, 1953.

[24] E. Courtiol and D. Wilson. Thalamic olfaction: Characterizing odor processing in the mediodorsal thalamus of the rat. *J Neurophysiol.*, 111(6):1274–1285, 2013.

[25] F. Crick. Function of the thalamic reticular nucleus: The searchlight hypothesis. *Proc Natl Acad Sci. USA*, 81:4586–4590, 1984.

[26] D. De Ridder, M. Congedo, and S. Vanneste. The neural correlates of subjectively perceived and passively matched loudness perception in auditory phantom perceptions. *Brain and Behavior*, 5(3), 1995.

[27] D. De Ridder, A. Elgoyhen, R. Romo, and B. Langguth. Phantom percepts: tinnitus and pain as persisting aversive memory networks. *Proc Natl Acad Sci USA*, 108:8075–8080, 2011.

[28] D. De Ridder, H. Fransen, O. Francois, S. Sunaert, S. Kovacs, and P. van de Heyning. Amygdalohippocampal involvement in tinnitus and auditory memory. *Acta Otolaryngol Suppl.*, 126:50–53, 2006.

[29] A. Destexhe and C. Bedard. Do neurons generate monopolar current sources? *J Neurophysiol*, 108:953–955, 2012.

[30] J. Deutsch and D. Deutsch. Attention: some theoretical considerations. *Psychological Review*, 70:80–90, 1963.

[31] K. Dohrmann, N. Weisz, W. Schlee, T. Hartmann, and T. Elbert. Neurofeedback for treating tinnitus. *Progress in brain research*, 166:473–485, 2007.

[32] R. Dolan. Emotion, cognition, and behavior. *Science*, 298:1191–1194, 2002.

[33] P. Ekman. Facial expression and emotion. *Am Psychol.*, 48:384–392, 1993.

[34] A. Elgoyhen and B. Langguth. Pharmacological approaches to the treatment of tinnitus. *Drug Discov Today*, 15:300–305, 2010.

[35] B. Epp, J. Hots, J. Verhey, and R. Schaette. Increased intensity discrimination thresholds in tinnitus subjects with a normal audiogram. *J Acoust Soc Am.*, 132:196–201, 2012.

[36] H. Flor, L. Nikolajsen, and T. Staehelin Jensen. Phantom limb pain: a case of maladaptive cns plasticity? *Nat Rev Neurosci.*, 7:873–881, 2006.

[37] E. for Standardization. Electroacustics-audiometric equipment. part 3: test signals of short duration. *The European Standard. EN 60645–3*, 2007.

[38] I. for Standardization. Acoustics–reference zero for the calibration of audiometric equipment. part 6: Reference threshold of hearing for test signals of short duration. *International Standards for Business. ISO 389-6*, 2007.

[39] W. Frank, B. Konta, and G. Seiler. Therapie desunspezifischen tinnitus ohne organische ursache. *DIMDI HTA—Bericht*, 43, 2060.

[40] P. Fries. A mechanism for cognitive dynamics: neuronal communication through neuronal coherence. *Trends Cogn Sci.*, 9:474–480, 2005.

[41] P. Fries, J. Schroeder, P. Roelfsema, W. Singer, and A. Engel. Oscillatory neuronal synchronization in primary visual cortex as a correlate of stimulus selection. *J. Neurosci.*, 22:3739–3754, 2002.

[42] E. Gao and N. Suga. Experience–dependent plasticity in the auditory cortex and the inferior colliculus of bats: role of the corticofugal system. *Proc Natl Acad Sci USA*, 97:8081–8086, 2000.

[43] S. Glickman, T. Higgins, and R. Isaacson. Some effects of hippocampal lesions on the behavior of mongolian gerbils. *Physiol Behav*, 5:931–938, 1970.

[44] G. Goebel and W. Hiller. Qualitätsmanagement inder therapie des chronischen tinnitus. *Otorhinolaryngol Nova*, 10:260–268, 2000.

[45] G. Goebel and H. W. *Tinnitus–Fragebogen TF – Ein Instrument zur Erfassung von Belastung und Schweregrad bei Tinnitus.* Hogrefe, Göttingen, 1998.

[46] S. Grossberg. How hallucinations may arise from brain mechanisms of learning, attention, and volition. *J Int Neuropsychol Soc.*, 6:583–592, 2000.

[47] S. Grossberg and J. Merrill. A neural network model of adaptively timed reinforcement learning and hippocampal dynamics. *Cogn Brain Res*, 1:3–38, 1992.

[48] J. Gu, B. Herrmann, R. Levine, and J. Melcher. Brainstem auditory evoked potentials suggest a role for the ventral cochlear nucleus in tinnitus. *J Assoc Res Otolaryngo*, 13:819–833, 2011.

[49] L. Haab, M. Busse, M. Mariam, T. Weis, and D. Strauss. Detection of a novelty event in the identification of faces in a passive VEP task. In *Conf Proc IEEE Conference on Neural Engineering*, pages 679–682, Cancun, Mexico, 2011.

[50] L. Haab, Z. Mortezapouraghdam, J. Schubert, J. Szczygielski, K. Schwerdtfeger, and D. Strauss. Modeling prediction of a generalized habituation deficit in decompensated tinnitus sufferers. In *Conf Proc IEEE Eng Med Biol Soc.*, San Diego, CA, USA, 2013.

[51] L. Haab, Z. Mortezapouraghdam, and D. Strauss. Modeling prediction of a generalized habituation deficit in decompensated tinnitus sufferers. In *Conf Proc IEEE Eng Med Biol Soc.*, Chicago, IL, USA, 2014.

[52] L. Haab, M. Scheerer, J. Ruckert, R. Hannemann, and D. Strauss. Support of a patient–specific therapeutical acoustic stimulation in tinnitus by numerical modeling. In *Conf Proc IEEE Eng Med Biol Soc.*, pages 5578–5581, San Diego, CA, USA, 2012.

[53] L. Haab, C. Trenado, M. Mariam, and D. Strauss. Neurofunctional model of large–scale correlates of selective attention governed by stimulus–novelty. *Cognitive Neurodynamics*, 5:103–111, 2011.

[54] L. Haab, C. Trenado, and D. Strauss. Neurofunctional model of limbic influences on electroencephalographic correlates of selective attention governed by stimulus–novelty. In *Conf Proc IEEE Conference on Neural Engineering*, pages 710–713, Antalya, Turkey, 2009.

[55] L. Haab, C. Trenado, and D. Strauss. Modeling the influence of the hippocampal comparator function on selective attention according to stimulus novelty. In *IFMBE Proceedings*, volume 25(4), pages 1720–1723, 2010.

[56] L. Haab, E. Wallhäusser-Franke, and D. Strauss. Event–related potentials as correlates of attentional binding in tinnitus: Some insight from neurodynamical multiscale modeling. In *4th International TRI Conference: Frontiers in Tinnitus Research*, Dallas, TX, USA, 2010.

[57] L. Haab, E. Wallhäusser-Franke, C. Trenado, and D. Strauss. Modeling limbic influences on habituation deficits in chronic tinnitus aurium. In *Conf Proc IEEE Eng Med Biol Soc.*, pages 4234–4237, Minneapolis, MN, USA, 2009.

[58] J. Hall. *Handbook of Auditory Evoked Responses.* Allyn & Bacon, Boston, MA, USA, 1992.

[59] R. Hallam. *Manual of the Tinnitus Questionnaire.* The Psychological Corporation Harcourt Brace, 1996.

[60] S. Haller, N. Birbaumer, and R. Veit. Real–time fmri feedback training may improve chronic tinnitus. *Eur Radiol.*, 20:696–703, 2010.

[61] K. Hancock and H. Voigt. Wideband inhibition of dorsal cochlear nucleus type IV units in cat: A computational model. *Annals of Biomedical Engineering*, 27:73–87, 1999.

[62] M. Hasselmo. The role of hippocampal regions CA3 and CA1 in matching entorhinal input with retrieval of associations between objects and context: theoretical comment on lee et al. *Behav Neurosci.*, 119:342–345, 2005.

[63] W. Hiller and G. Goebel. Rapid assessment of tinnitus–related psychological distress using the mini–TQ. *Int J Audiol.*, 43(10):600–604, 2004.

[64] S. A. Hillyard, R. F. Hink, V. L. Schwent, and T. Picton. Electrical signs of selective attention in the human brain. *Science*, 182:177–180, 1973.

[65] A. Hodgkin and A. Huxley. A quantitative description of membrane current and its application to conduction and excitation in nerve. *J. Physiol.*, 117:500–544, 1952.

[66] H. Hoffman and G. Reed. *Epidemiology of tinnitus*, pages 16–41. BC Decker, Lewiston, NY, USA, 2004.

[67] H. Hoffman and G. Reed. *Prevalence of Chronic Tinnitus.* NIH, National Insitute on Deafness and other Communication Disorders (NIDCD), 2012.

[68] R. Honey, V. Marshall, A. McGregor, J. Futter, and M. Good. Revisiting places passed: sensitization of exploratory activity in rats with hippocampal lesions. *Q J Exp Psychol (Hove)*, 60:625–634, 2007.

[69] J. House and D. Brackmann. Tinnitus: surgical treatment. *Ciba Found Symp*, 85:204–216, 1981.

[70] Y. Ikegaya, H. Saito, and K. Abe. Dentate gyrus field potentials evoked by stimulation of the basolateral amygdaloid nucleus in anesthetized rats. *Brain Res Bull.*, 718:53–60, 1996.

[71] E. Izhikevich. Simple model of spiking neurons. *IEEE Transactions on Neural Networks*, 14:1569–1572, 2003.

[72] E. Izhikevich and R. FitzHugh. Fitzhugh-nagumo model. *Scholarpedia*, 1(9):1349, 2006.

[73] J. Jang, Y. Youn, J. Seok, S. Ha, H. Shin, S. Ahan, K. Park, and O. Kwon. Hypermetabolism in the left thalamus and right inferior temporal area on positron emission tomography–statistical parametric mapping (pet-spm) in a patient with charles bonnet syndrome resolving after treatment with valproic acid. *J Clin Neurosci*, 18:1130–1132, 2011.

[74] P. Jastreboff and M. Jastreboff. Tinnitus retraining therapy (TRT) as a method for treatment of tinnitus and hyperacusis patients. *J Am Acad Audiol.*, 11:162–177, 2000.

[75] N. Kahlbrock and N. Weisz. Transient reduction of tinnitus intensity is marked by concomitant reductions of delta band power. *BMC Biol.*, 6, 2008.

[76] D. Kahneman. *Attention And Effort.* Prentice–Hall, Englewood Cliffs, NJ, USA, 1973.

[77] J. Kaltenbach. The dorsal cochlear nucleus as a participant in the auditory, attentional and emotional components of tinnitus. *Hear Res*, 216–217:224–234, 2006.

[78] J. Kaltenbach, J. Rachel, T. Mathog, J. Zhang, P. Falzarano, and M. Lewandowski. Cisplatin–induced hyperactivity in the dorsal cochlear nucleus and its relation to outer hair cell loss: relevance to tinnitus. *J. Neurophysiol.*, 88:699–714, 2002.

[79] J. Kaltenbach, J. Zhang, and C. Afman. Plasticity of spontaneous neural activity in the dorsal cochlear nucleus after intense sound exposure. *Hear Res*, 147:282–292, 2000.

[80] P. Kanold and E. Young. Proprioceptive information from the pinna provides somatosensory input to cat dorsal cochlear nucleus. *J Neurosci.*, 21:7848–7858, 2001.

[81] B. Kapp, W. Supple, and P. Whalen. Effects of electrical stimulation of the amygdaloid central nucleus on neocortical arousal in the rabbit. *Behav.Neurosci.*, 108:81–93, 1994.

[82] R. Kempter, C. Leibold, G. Buzsáki, K. Diba, and R. Schmidt. Quantifying circular–linear associations: hippocampal phase precession. *J Neurosci Methods.*, 207(1), 2012.

[83] C. Kerr, C. Rennie, and P. Robinson. Physiology–based modeling of cortical auditory evoked potentials. *Biol Cybern.*, 98(2):171–184, 2008.

[84] A. Key, G. Dove, and M. Maguir. Linking brainwaves to the brain: an ERP primer. *Dev Neuropsychol.*, 27:183–215, 2005.

[85] C. Kim, H. Choi, J. Kim, H. Chang, R. Park, and I. Kang. General behavioral activity and its component patterns in hippocampectomized rats. *Brain Res*, 19:379–394, 1970.

[86] A. Kimura, I. Yokoi, H. Imbe, T. Donishi, and Y. Kaneoke. Auditory thalamic reticular nucleus of the rat: anatomical nodes for modulation of auditory and cross–modal sensory processing in the loop connectivity between the cortex and thalamus. *J Comp Neurol.*, 520:1457–1480, 2012.

[87] W. Kistler and W. Gerstner. Reduction of the hodgkin–huxley equations to a single–variable threshold model. *Neural Computation*, 5:1015–1045, 1997.

[88] K. Koerber, R. Pfeiffer, W. Warr, and N. Kiang. Spontaneous spike discharges from single units in the cochlear nucleus after destruction of the cochlea. *Exp Neurol.*, 16(2):119–130, 1966.

[89] N. Kopell, C. Börgers, D. Pervouchine, P. Malerba, and A. Tort. *Gamma and Theta Rhythms in Biophysical Models of Hippocampal Circuits.*, pages 423–457. Springer Series in Computational Neuroscience 5, 2010.

[90] V. Kryukov. The role of the hippocampus in long–term memory: is it memory store or comparator? *J Integr Neurosci.*, 7(1):117–184, 2008.

[91] N. Lavie. Perceptual load as a necessary condition for selective attention. *Journal Of Experimental Psychology Human Perception And Performance*, 21:451–468, 1995.

[92] N. Lavie. *Selective attention and cognitive control: Dissociating attentional functions through different types of load.* MIT–Press, Cambridge, MA, USA, 2000.

[93] N. Lavie. Attention, distraction, and cognitive control under load. *Current Directions in Psychological Science*, 19:143–148, 2010.

[94] A. Leaver, L. Renier, M. Chevillet, S. Morgan, H. Kim, and J. Rauschecker. Dysregulation of limbic and auditory networks in tinnitus. *Neuron*, 69:33–43, 2011.

[95] I. Lee, M. Hunsaker, and R. Kesner. The role of hippocampal subregions in detecting spatial novelty. *J Neurosci.*, 25:145–153, 2005.

[96] K. Lee, H. Buxton, and J. Feng. Cue–guided search: A computational model of selective attention. *IEEE Transactions on Neural Networks*, 16:910–924, 2005.

[97] L. Levy, U. Ziemann, R. Chen, and L. Cohen. Rapid modulation of gaba in sensorimotor cortex induced by acute deafferentation. *Ann. Neurol*, 52:755–761, 2002.

[98] Z. Li and G. Richter-Levin. Priming stimulation of basal but not lateral amygdala affects long-term potentiation in the rat dentate gyrus in vivo. *Neuroscience*, 246:13–21, 2013.

[99] B. Liddell, K. Brown, A. Kemp, M. Barton, P. Das, A. Peduto, E. Gordon, and L. Williams. A direct brainstem–amygdala–cortical "alarm" system for subliminal signals of fear. *Neuroimage*, 24:235–243, 2005.

[100] W. Link, U. Konietzko, G. Kauselmann, M. Krug, B. Schwanke, U. Frey, and D. Kuhl. Somatodendritic expression of an immediate early gene is regulated by synaptic activity. *Proc Natl Acad Sci. USA*, 92:5734–5738, 1995.

[101] J. Lisman and A. Grace. The hippocampal–VTA loop: controlling the entry of information into long–term memory. *Neuron.*, 46(5):703–713, 2005.

[102] Y. Low and D. Strauss. EEG phase reset due to auditory attention: an inverse time–scale approach. *J Physiol Measurement*, 30:821–832, 2009.

[103] Y. Low and D. Strauss. A performance study of the wavelet–phase stability (WPS) in auditory selective attention. *Brain Res Bull.*, 86:110–117, 2011.

[104] S. Luck, editor. *An Introduction to the Event–Related Potential Technique.* MIT Press, Cambridge, USA, London, UK, 2005.

[105] J. Luebke, V. Egger, B. Sakmann, and D. Feldmeyer. Columnar organization of dendrites and axons of single and synaptically coupled excitatory spiny neurons in layer 4 of the rat barrel cortex. *J. Neurosci.*, 20:5300–5311, 2000.

[106] J. Macdonald and N. Lavie. Visual perceptual load induces inattentional deafness. *Attention, Perception & Psychophysics*, 73:1780–1789, 2011.

[107] R. MacGregor. *Neural and Brain Modeling.* CA: Academic, San Diego, CA, USA, 1987.

[108] C. Mahlke and E. Wallhäusser-Franke. Evidence for tinnitus-related plasticity in the auditory and limbic system, demonstrated by arg3.1 and c–fos immunocytochemistry. *Hear Res.*, 195:17–34, 2004.

[109] T. Makovski, B. Hommel, and G. Humphreys. Early and late selection: effects of load, dilution and salience. *Front Psychol.*, 5:248, 2014.

[110] M. Mariam, W. Delb, F. Corona-Strauss, M. Bloching, and D. Strauss. Comparing the habituation of late auditory evoked potentials to loud and soft sounds. *Physiol. Meas.*, 30(2):141–153, 2009.

[111] K. McAlonan, V. Brown, and E. Bowman. Thalamic reticular nucleus activation reflects attentional gating during classical conditioning. *J Neurosci.*, 20:8897–8901, 2000.

[112] M. Meikle and T. Walsh. Characteristics of tinnitus and related observations in over 1800 tinnitus clinic patients. *J Laryngol Otol Suppl*, 9:17–21, 1984.

[113] J. Melcher, R. Levine, C. Bergevin, and B. Norris. The auditory midbrain of people with tinnitus: Abnormal sound–evoked activity revisited. *Hear Res*, 257:63–74, 2009.

[114] J. Mellott, N. Foster, A. Ohl, and B. Schofield. Excitatory and inhibitory projections in parallel path from the inferior colliculus to the auditory thalamus. *Front Neuroanat.*, 5(124), 2014.

[115] R. Miller and R. Matzel. *The comparator hypothesis: a response rule for the expression of associations.*, pages 51–92. Academic Press, NY, USA, 1988.

[116] A. Møller, B. Langguth, D. DeRidder, and T. E. Kleinjung, editors. *Textbook of Tinnitus.* Springer Science and Business Media, New York, USA, 2011.

[117] N. Moray. Attention in dichotic listening: Affective cues and the influence of instructions. *Quarterly Journal of Experimental Psychology*, 11:56–60, 1959.

[118] W. Mulders, D. Ding, R. Salvi, and D. Robertson. Relationship between auditory thresholds, central spontaneous activity, and hair cell loss after acoustic trauma. *J Comp Neurol.*, 519:2637–2647, 2011.

[119] W. Mulders and D. Robertson. Hyperactivity in the auditory midbrain after acoustic trauma: dependence on cochlear activity. *Neuroscience*, 164:733–746, 2009.

[120] W. Mulders and D. Robertson. Progressive centralization of midbrain hyperactivity after acoustic trauma. *Neuroscience*, 192:753–760, 2011.

[121] I. Mutschler, B. Wieckhorst, O. Speck, A. Schulze-Bonhage, J. Hennig, E. Seifritz, and T. Ball. Time scales of auditory habituation in the amygdala and cerebral cortex. *Cereb. Cortex*, 20(11):2531–2539, 2010.

[122] C. Newman, G. Jacobson, and J. Spitzer. Development of the tinnitus handicap inventory. *Arch Otolaryngol Head Neck Surg.*, 122:143–148, 1996.

[123] C. Nicolas-Puel, T. Akbaraly, R. Lloyd, C. Berr, A. Uziel, G. Rebillard, and J. Puel. Characteristics of tinnitus in a population of 555 patients: specificities of tinnitus induced by noise trauma. *Int Tinnitus J*, 12:64–70, 2006.

Bibliography

[124] A. Norena and B. Farley. Tinnitus–related neural activity: theories of generation, propagation, and centralization. *Hear Res*, 295:161–171, 2013.

[125] A. Norena, C. Micheyl, S. Chery-Croze, and L. Collet. Psychoacoustic characterization of the tinnitus spectrum: implications for the underlying mechanisms of tinnitus. *Audiol Neurootol*, 7:358–369, 2002.

[126] R. Näätänen, P. Paavilainen, T. Rinne, and K. Alho. The mismatch negativity (MMN) in basic research of central auditory processing: a review. *Clin Neurophysiol.*, 118:2544–2590, 2007.

[127] A. Nunez and E. Malmierca. *Corticofugal Modulation of Sensory Information.* Springer, Berlin, Heidelberg, New York, 2006.

[128] P. Nunez and R. Srinivasan, editors. *Electric Fields of the Brain: The Neurophysics of EEG, 2nd Edition.* Oxford University Press, New York, USA, 2005.

[129] D. Oertel and E. Young. What's a cerebellar circuit doing in the auditory system? *Trends Neurosci.*, 27:104–110, 2004.

[130] H. Okamoto, H. Stracke, W. Stoll, and C. Pantev. Listening to tailor–made notched music reduces tinnitus loudness and tinnitus-related auditory cortex activity. *Proc Natl Acad Sci. USA*, 107:1207–1210, 2010.

[131] N. Oros, A. Chiba, D. Nitz, and J. Krichmar. Learning to ignore: A modeling study of a decremental cholinergic pathway and its influence on attention and learning. *Learn. Mem.*, 21:105–118, 2014.

[132] C. Pantev, A. Wollbrink, L. Roberts, A. Engelien, and B. Lütkenhöner. Short-term plasticity of the human auditory cortex. *Brain Research*, 842:192–199, 1999.

[133] M. Penner. Magnitude estimation and the "paradoxical" loudness of tinnitus. *J Speech Hear Res.*, 29:407–412, 1986.

[134] D. Perkel, G. Gerstein, and G. Moore. Neuronal spike trains and stochastic point processes. I. the single spike train. *Biophys J.*, 7(4):391–418, 1967.

[135] X. Perrot, P. Ryvlin, J. Isnard, and L. Collet. Evidence for corticofugal modulation of peripheral auditory activity in humans. *Cereb Cortex.*, 16:941–948, 2006.

[136] S. Peterson and M. Posner. The attention system of the human brain: 20 years after. *Annu Rev Neurosci.*, 35:73–89, 2012.

[137] B. Pál, A. Pór, G. Szucs, I. Kovács, and Z. Rusznák. HCN channels contribute to the intrinsic activity of cochlear pyramidal cells. *Cell Mol Life Sci.*, 60(10):2189–2199, 2003.

Bibliography

[138] D. Purves, G. Augustine, D. Fitzpatrick, L. Katz, A. LaMantia, J. O McNamara, and S. Williams, editors. *Neuroscience, 2nd edition.* Sinauer Associates Inc., Sunderland, USA, 2001.

[139] R. Rajan. Plasticity of excitation and inhibition in the receptive field of primary auditory cortical neurons after limited receptor organ damage. *Cerebral Cortex*, 11:171–182, 2001.

[140] J. Rauschecker. *Auditory processing and plasticity.*, pages 202–214. MIT–Press, Cambridge, MA, USA, 2011.

[141] J. Rauschecker, A. Leaver, and M. Mühlau. Tuning out the noise: limbic–auditory interactions in tinnitus. *Neuron*, 66:819–826, 2010.

[142] U. Richter and T. Fedtke. Reference zero for the calibration of audiometric equipment using clicks as test signal. *Int J Audiol.*, 44:478–487, 2005.

[143] W. Roberts, W. Dember, and M. Brodwick. Alternation and exploration in rats with hippocampal lesions. *J Comp Physiol Psychol*, 55:695–700, 1962.

[144] P. Robinson, C. Rennie, D. Rowe, S. O'Connor, and E. Gordon. Multiscale brain modelling. *Philos Trans R Soc Lond B Biol Sci.*, 360(1457):1043–1050, 2005.

[145] S. Robinson, J. McQuaid, E. Viirre, L. Betzig, D. Miller, K. Bailey, J. Harris, and W. Perry. Relationship of tinnitus questionnaires to depressive symptoms, quality of well–being and internal focus. *Int Tinnitus J.*, 9:97–103, 2003.

[146] J. Roederer. *The Physics and Psychophysics of Music 4th ed.* Springer Science and Business Media, New York, USA, 2009.

[147] A. Romero Santiago, K. Schwerdtfeger, J. Szczygielski, P. Flotho, J. Schubert, M. Hmila, L. Haab, and D. Strauss. Motion reduction and multidimensional denoising in voltage–sensitive dye imaging. In *Conf Proc IEEE Eng Med Biol Soc.*, Milano, Italy, 2015.

[148] A. Roye, T. Jacobsen, and E. Schröger. Personal significance is encoded automatically by the human brain: an event-related potential study with ringtones. *Eur J Neurosci.*, 26(3):784–790, 2007.

[149] M. Rubio, K. Gudsnuk, Y. Smith, and D. Ryugo. Revealing the molecular layer of the primate dorsal cochlear nucleus. *Neuroscience*, 154:99–113, 2008.

[150] J. Ruckert, L. Haab, R. Hannemann, and D. Strauss. Suppression of spontaneous activity in a computational tinnitus DCN model depends on notched stimulation bandwith. In *Conf Proc IEEE Conference on Neural Engineering*, pages 1406–1409, San Diego, CA, USA, 2013.

[151] T. Sahley, R. Nodar, and F. Musiek. Endogenous dynorphins: Possible role in peripheral tinnitus. *Int Tinn J.*, 5(2):76–91, 1999.

[152] E. Salzmann. Importance of the hippocampus and parahippocampus with reference to normal and disordered memory function. *Fortschr Neurol Psychiatr.*, 60:163–176, 1992. [in German].

[153] D. Sanderson, S. McHugh, M. Good, R. Sprengel, P. Seeburg, J. Rawlins, and D. Bannerman. Spatial working memory deficits in glua1 ampa receptor subunit knockout mice reflect impaired short-term habituation: evidence for wagner's dual–process memory model. *Neuropsychologia*, 48:2303–2315, 2010.

[154] N. Sato and Y. Yamaguchi. Online formation of a hierarchical cognitive map for object-place association by theta phase coding. *Hippocampus*, 15:963–978, 2005.

[155] N. Sato and Y. Yamaguchi. Theta synchronization networks emerge during human object-place memory encoding. *Neuroreport*, 18:419–424, 2007.

[156] M. Savastano. Tinnitus with or without hearing loss: are its characteristics different? *Eur Arch Otorhinolaryngol*, 265:1295–1300, 2008.

[157] R. Schaette. *Tinnitus–Related Hyperactivity through Homeostatic Plasticity in the Auditory Pathway.* PhD thesis, Humboldt–Universität, Berlin, Germany, September 2007.

[158] R. Schaette and R. Kempter. Development of tinnitus–related neuronal hyperactivity through homeostatic plasticity after hearing loss: a computational model. *Eur J Neurosci*, 23:3124–3138, 2006.

[159] R. Schaette and D. McAlpine. Tinnitus with a normal audiogram: physiological evidence for hidden hearing loss and computational model. *J Neurosci.*, 31:13452–13457, 2011.

[160] N. Schinkel-Bielefeld. *Contour Integration Models Predicting Human Behavior.* PhD thesis, Universität Bremen, Bremen, Germany, July 2007.

[161] J. Schwarz, G. Dangelmayr, A. Stevens, and K. Bräuer. Burst and spike synchronization of coupled neural oscillators. *Dynamical Systems*, 16(2):125–156, 2001.

[162] G. Searchfield, M. Kaur, and W. Martin. Hearing aids as an adjunct to counseling: Tinnitus patients who choose amplification do better than those who don't. *Int J Audiol.*, 49:574–579, 2010.

[163] A. Sheth, S. Berretta, N. Lange, and H. Eichenbaum. The amygdala modulates neuronal activation in the hippocampus in response to spatial novelty. *Hippocampus*, 18:169–181, 2007.

[164] D. Simons and C. Chabris. Gorillas in our midst: sustained inattentional blindness for dynamic events. *Perception*, 28:1059–1074, 1999.

[165] D. Simons and D. Levin. Failure to detect changes to people during a real–world interaction. *Psychonomic Bulletin & Review*, 5:644–649, 1998.

[166] W. Singer and C. Gray. Visual feature integration and the temporal correlation hypothesis. *Annu Rev Neurosci.*, 18:555–586, 1995.

[167] N. Singh and F. Theunissen. Modulation spectra of natural sounds and ethological theories of auditory processing. *J Acoust Soc Am.*, 114:3394–3411, 2003.

[168] F. Skinner. Conductance–based models. *Scholarpedia*, 1(11):1408, 2006.

[169] L. Squire, A. Shimamura, and D. Amaral. *Memory and the hippocampus.*, pages 208–239. Academic Press, NY, USA, 1988.

[170] M. Stolte, B. Bahrami, and N. Lavie. High perceptual load leads to both reduced gain and broader orientation tuning. *Journal of Vision*, 197:55–64, 2004.

[171] D. Strauss, W. Delb, R. D'Amelio, Y. Low, and P. Falkai. Objective quantification of the tinnitus decompensation by synchronization measures of auditory evoked single sweeps. *IEEE Trans. on Neural Systems & Rehabilitation Engineering*, 16:74–81, 2008.

[172] D. Strauss, W. Delb, R. D'Amelio, Y. Low, and P. Falkai. Objective quantification of the tinnitus decompensation by synchronization measures of auditory evoked single sweeps. *IEEE Trans. on Neural Systems & Rehabilitation Engineering*, 16:74–81, 2008.

[173] N. Suga. Role of corticofugal feedback in hearing. *J Comp Physiol A Neuroethol Sens Neural Behav Physiol.*, 194(2):169–183, 2008.

[174] N. Suga, Z. Xiao, X. Ma, and W. Ji. Plasticity and corticofugal modulation for hearing in adult animals. *Neuron*, 36:9–18, 2002.

[175] A. Takesian, V. Kotak, and D. Sanes. Developmental hearing loss disrupts synaptic inhibition: implications for auditory processing. *Future Neurol*, 4:331–349, 2009.

[176] W. Thorpe. Some problems of animal learning. *Proceedings of the Linnaean Society of London*, 156:70–83, 1944.

[177] J. Touma. Controversies in noise–induced hearing loss (NIHL). *Ann.Occup.Hyg.*, 36:199–209, 1992.

[178] A. Treisman. Contextual cues in selective listening. *Quarterly Journal of Experimental Psychology*, 12(4):242–248, 1960.

[179] C. Trenado. *A Neural Field Model for Auditory Selective Attention Neural Correlates and its Possible Application in the Study of the Tinnitus Decompensation.* PhD thesis, Universität des Saarlandes, Homurg, Germany, September 2009.

[180] C. Trenado, L. Haab, W. Reith, and D. Strauss. Biocybernetics of attention and habituation neural correlates in the tinnitus decompensation. *J Neurosci Methods*, 178:237–247, 2009.

[181] C. Trenado, L. Haab, W. Reith, and D. Strauss. Toward a realistic simulation framework for large–scale neural correlates in clinical applications. In *Conf Proc IEEE Conference on Neural Engineering*, pages 199–202, Antalya, Turkey, 2009.

[182] C. Trenado, L. Haab, and D. Strauss. Integrative multiscale modeling approach to the study of tinnitus decompensation neural correlates. In *Conf Proc IEEE Eng Med Biol Soc.*, pages 3975–3978, Vancouver, Canada, 2008.

[183] C. Trenado, L. Haab, and D. Strauss. Corticothalamic feedback dynamics for neural correlates of auditory selective attention. *IEEE transactions on neural systems and rehabilitation engineering*, 17:46–52, 2009.

[184] C. Trenado, Y. Low, L. Haab, W. Delb, and D. Strauss. Large scale modeling of attention in tinnitus decompensation. In *9th International Tinnitus Seminars*, Göteborg, Sweden, 2008.

[185] V. Vielsmeier, J. Strutz, T. Kleinjung, M. Schecklmann, P. Kreuzer, M. Landgrebe, and B. Langguth. Temporomandibular joint disorder complaints in tinnitus: further hints for a putative tinnitus subtype. *PLoS One*, 7(6):1–5, 2012.

[186] O. Vinogradova. Hippocampus as comparator: role of the two input and two output systems of the hippocampus in selection and registration of information. *Hippocampus*, 11:578–598, 2001.

[187] I. Vogel, P. van de Looij-Jansen, C. Mieloo, A. Burdorf, and F. de Waart. Risky music listening, permanent tinnitus and depression, anxiety, thoughts about suicide and adverse general health. *PLoS One*, 9(6):1–8, 2014.

[188] E. Wallhäusser-Franke, C. Mahlke, R. Oliva, S. Braun, G. Wenz, and G. Langner. Expression of c–fos in auditory and non–auditory brain regions of the gerbil after manipulations that induce tinnitus. *Exp.Brain Res.*, 153:649–654, 2003.

[189] G. Weese, J. Phillips, and V. Brown. Attentional orienting is impaired by unilateral lesions of the thalamic reticular nucleus in the rat. *J Neurosci.*, 19(22):10135–10139, 1999.

[190] N. Weisz, T. Hartmann, K. Dohrmann, W. Schlee, and A. Norena. High–frequency tinnitus without hearing loss does not mean absence of deafferentation. *Hear Res.*, 222:108–114, 2006.

[191] J. Wolfe. Guided search 2.0: A revised model of visual search. *Psychonomic Bulletin & Review*, 1(2):202–238, 1994.

[192] N. Wood and N. Cowan. The cocktail party phenomenon revisited: attention and memory in the classic selective listening procedure of cherry (1953). *J Exp Psychol Gen.*, 124:243–262, 1995.

[193] Z. Xiao and N. Suga. Reorganization of the cochleotopic map in the bat's auditory system by inhibition. *Proc.Natl.Acad.Sci.USA*, 99:15743–15748, 2002.

[194] Y. Yamaguchi, N. Sato, H. Wagatsuma, Z. Wu, C. Molter, and Y. Aota. A unified view of theta–phase coding in the entorhinal–hippocampal system. *Curr Opin Neurobiol*, 17:197–204, 2007.

[195] S. Yang, B. Weiner, L. Zhang, S. Cho, and S. Bao. Homeostatic plasticity drives tinnitus perception in an animal model. *Proc Natl Acad Sci USA*, 108:14974–14979, 2011.

[196] D. Yi and M. Chun. Attentional modulation of learning-related repetition attenuation effects in human parahippocampal cortex. *J Neurosci.*, 25:3593–3600, 2005.

[197] R. Zatorre. Music, the food of neuroscience? *Nature*, 434:312–315, 2005.

[198] X. Zheng and H. Voigt. A modeling study of notch noise response of type III units in the gerbil dorsal cochlear nucleus. *Annals of Biomedical Engineering*, 34:1935–1946, 2006.

[199] B. Zikopoulos and H. Barbas. Prefrontal projections to the thalamic reticular nucleus form a unique circuit for attentional mechanisms. *J Neurosci.*, 26:7348–7361, 2006.

[200] B. Zikopoulos and H. Barbas. Pathways for emotions and attention converge on the thalamic reticular nucleus in primates. *J Neurosci*, 32:5338–5350, 2012.

[201] K. Zilles and G. Rehkämper. *Funktionelle Neuroanatomie: Lehrbuch und Atlas (Springer–Lehrbuch).* Springer, Berlin, Heidelberg, 1998.

List of Publications

Peer–Reviewed Journals

2015 L. Haab and F.I. Corona–Strauss and C. Bernarding and R. Hannemann and H. Seidler and D.J.Strauss: Quantification and Modeling Prediction of a Habituation Deficit in Tinnitus. *Submitted to J. Neuroscience* 2015

2015 D.J. Strauss and F.I. Corona—Strauss and H. Seidler and L. Haab and R. Hannemann: Notched Environmental Sounds: A New Hearing Aid Supported Tinnitus Treatment Evaluated in 20 Patients. *Submitted to Clinical Otolaryngology* 2015

2014 Z. Mortezapouraghdam and L. Haab and F.I. Corona-Strauss and G. Steidl and D.J. Strauss: Assessment of Long-Term Habituation Correlates in Event–Related Potentials Using a von Mises Model. *IEEE Trans Neural Syst Rehabil Eng.* DOI:10.1109/TNSRE.2014.2361614 2014

2011 L. Haab, C. Trenado, M. Mariam and D.J. Strauss: Neurofunctional Model of Large–Scale Correlates of Selective Attention Governed by Stimulus-Novelty. *Cognitive Neurodynamics* 5(1):103–111 2011

2009 C. Trenado, L. Haab and D.J. Strauss: Corticothalamic Feedback Dynamics for Neural Correlates of Auditory Selective Attention. *IEEE Trans. on Neural Systems & Rehabilitation Engineering* 17:46–52 2009

2009 C. Trenado, L. Haab, W. Reith and D.J. Strauss: Biocybernetics of Attention and Habituation Neural Correlates in the Tinnitus Decompensation. *J Neurosci Methods* 178(1):237–247 2009

2008 C. Trenado, L. Haab, W. Reith and D.J. Strauss: Biocybernetics of Attention in the Tinnitus Decompensation: An Integrative Multiscale Modeling Approach. *J Neurosci Methods* 78:237–247 2008

Conference Publications

MEDLINE listed:

2015 A.E. Romero Santiago and K. Schwerdtfeger and J. Szczygielski and P. Flotho and J.K. Schubert and M. Hmila and L. Haab and D.J. Strauss: Motion Reduction and Multidimensional Denoising in Voltage–sensitive Dye Imaging. *Proceedings of the 37th International IEEE EMBS Conference* Milano, Italy

2015 C. Lehser and R. Hannemann and F.I. Corona–Strauss and D.J. Strauss and L. Haab and B. Seidler–Fallbhöhmer and H.Seidler: Dysfunctional Long Term Habituation to Exogeneous Tinnitus-Matched Sounds in Patients with High Tinnitus Distress. *Proceedings of the 37th International IEEE EMBS Conference* Milano, Italy

2014 Z. Mortezapouraghdam and L. Haab and G. Steidl and D.J. Strauss: Detection of change points in phase data: A Bayesian analysis of habituation processes. *Proceedings of the 36th International IEEE EMBS Conference* Chicago, IL, USA

2014 L. Haab and Z. Mortezapouraghdam and D.J. Strauss: Modeling prediction of a generalized habituation deficit in decompensated tinnitus sufferers. *Proceedings of the 36th International IEEE EMBS Conference* Chicago, IL, USA

2012 L. Haab, M. Scheerer, J. Ruckert, R. Hannemann, and D.J. Strauss: Support of a patient–specific therapeutical acoustic stimulation in tinnitus by numerical modeling. *Proceedings of the 34th International IEEE EMBS Conference* San Diego, CA, USA

2010 L. Haab, C. Trenado and D.J. Strauss: Modeling the Influence of the Hippocampal Comparator Function on Selective Attention according to Stimulus Novelty. *IFMBE Proceedings* 25(4):1720–1723

2009 L. Haab, E. Wallhäusser–Franke, C. Trenado, D.J. Strauss: Modeling Limbic Influences on Habituation Deficits in Chronic Tinnitus Aurium. *Proceedings of the 31th International IEEE EMBS Conference* Minneapolis, MN, USA

2009 M. Busse, L. Haab, M. Mariam, C. Crick, T. Weis, W. Reith, and D.J. Strauss: Assessment of Aversive Stimuli Dependent Attentional Binding by the N170 VEP Component. *Proceedings of the 31th International IEEE EMBS Conference* Minneapolis, MN, USA

2008 C. Trenado, L. Haab and D.J. Strauss: An Integrative Multiscale Modeling Approach to the Study of Tinnitus Decompensation Neural Correlates. *Proceedings of the 30th International IEEE EMBS Conference* Vancouver, Canada

2007 C. Trenado, L. Haab and D.J. Strauss: Modeling Neural Correlates of Auditory Attention in Evoked Potentials Using Corticothalamic Feedback Dynamics. *Proceedings of the 29th International IEEE EMBS Conference* Lyons, France

IEEE listed:

2013 J. Ruckert, L. Haab, R. Hannemann and D.J. Strauss: Suppression of Spontaneous Activity in a Computational Tinnitus DCN Model depends on Notched Stimulation Bandwith. *Proceedings of the 6th International IEEE EMBS Conference on Neural Engineering* San Diego, CA, USA

2013 L. Haab, Z. Mortezapouraghdam, J.K. Schubert, J. Szczygielski, K. Schwerdtfeger and D.J. Strauss: Analysis of Dominant Neural Activity Clustering in Laminar Cortical Processing of Acoustic Stimuli in Rat Utilizing Von Mises–Fisher Distribution. *Proceedings of the 6th International IEEE EMBS Conference on Neural Engineering* San Diego, CA, USA

2011 L. Haab, M. Busse, M. Mariam, T. Weis and D.J. Strauss: Detection of a novelty event in the identification of faces in a passive VEP task. *Proceedings of the 5th International IEEE EMBS Conference on Neural Engineering* Cancun, Mexico

2010 L. Haab, E. Wallhäusser–Franke and D.J. Strauss: Event-Related Potentials as Correlates of Attentional Binding in Tinnitus: Some Insight from Neurodynamical Multiscale Modeling. *4th International TRI Conference: Frontiers in Tinnitus Research* Dallas, TX, USA

2009 C. Trenado, L. Haab, W. Reith and D.J. Strauss: Toward a Realistic Simulation Framework for Large–Scale Neural Correlates in Clinical Applications. *Proceedings of the 4th International IEEE EMBS Conference on Neural Engineering* Antalya, Turkey

2009 L. Haab, C. Trenado and D.J. Strauss: Neurofunctional Model of Limbic Influences on Electroencephalographic Correlates of Selective Attention Governed by Stimulus–Novelty. *Proceedings of the 4th International IEEE EMBS Conference on Neural Engineering* Antalya, Turkey

2008 C. Trenado, Y. F. Low, L. Haab, W. Delb and D.J. Strauss: Multiscale modeling of attention and habituation effects in the tinnitus decompensation. *Frontiers in Human Neuroscience: 10th International Conference on Cognitive Neuroscience* Bodrum, Turkey

2008 C. Trenado, Y. F. Low, L. Haab, W. Delb, D.J. Strauss: Large scale modeling of attention in tinnitus decompensation. *9th International Tinnitus Seminars* Göteborg, Sweden

Diploma and Master Thesis

2008 L. Haab: Neurofunctional Multi–Scale Modeling of Selective Auditory Attention. Cummulative Master–Thesis University of Applied Sciences Saarbrücken

2004 L. Haab: Sichere Grenzen der funktionellen Elektrostimulation. Fraunhofer Institute for Biomedical Engineering, IBMT St. Ingbert

Danksagung:

Eine wissenschaftliche Arbeit ist nie das Werk einer einzelnen Person, deshalb ist es jetzt an der Zeit, mich bei allen Menschen zu bedanken, die mir die Erstellung meiner Dissertation ermöglicht haben. Mein besonderer Dank gilt meinem Doktorvater,

Prof. Dr. Dr. Daniel J. Strauss, der mir die Anfertigung dieser interdisziplinären Arbeit erst ermöglicht hat. Speziell danke ich ihm für die Überlassung dieses faszinierenden Themas und für die herzliche Aufnahme in seine Arbeitsgruppe. Als Student habe ich Prof. Strauss als exzellenten Lehrer kennen gelernt, der mich erstmals an die Biosignalverarbeitung und die numerische Modellierung komplexer biologischer Systeme herangeführt hat. Besonders bedanken will ich mich auch für die Freiheit, die er mir während der gesamten Promotionszeit gewährte. Sein kompetenter Rat und seine Hilfe trugen maßgeblich zum Gelingen dieser Arbeit bei.

Weiterhin möchte ich mich bedanken bei **Prof. Dr. Karsten Schwerdtfeger** und **Dr. Jacek Szczygielski** für fachliche Diskussionen, die großartige Kooperation und ihre uneingeschränkte und geduldige Bereitschaft mir ihr fundiertes neuroanatomisches Wissen weiterzugeben.

Viele großartige Menschen haben mich auf dem Weg zur Promotion begleitet. Mein großer Dank gilt meinen Mitdoktoranden, allen voran meinem langjährigen Studiengefährten **Dr. Michael Busse**. In allen Hochs und Tiefs der Doktorandenzeit warst Du mir der beste Mitstreiter, den man sich nur wünschen kann. Danke für Deine fachkundige Unterstützung und für die visionären und kreativen Diskussionen zu allem Sinn und Unsinn des Wissenschaftlerlebens. Das Gartenzwergimperium ist noch nicht abgeschrieben.

Ich könnte mir keine besseren Arbeitskollegen vorstellen, als ich sie in der Systems Neuroscience & Neurotechnology Unit gefunden habe. **Corinna Bernarding:** Danke für die vielen hilfreichen und motivierenden Gespräche und die herzliche Atmosphäre in den Kaffeepausen und auch in den langen Nachtschichten beim Schreiben von Drittmittelanträgen. Du warst mir eine echte Stütze in den trüben Tagen. **Farah Corona-Strauss**, **Ernesto Gonzalez-Trejo**, **Manuel Kohl**, **Yin Fen Low**, **Zeinab Motezapouraghdam**, **Novaf Özgün**, **Alejan-**